DESIGN OF MINIMAL ION CHANNELS

By

Zhiguang Yuchi

A Thesis

Submitted to the School of Graduate Studies

In Partial Fulfillment of the Requirement

For the Degree

Doctor of Philosophy

McMaster University

DOCTOR OF PHILOSOPHY (2009) McMaster University

(Biochemistry and Biomedical Sciences) Hamilton, Ontario

TITLE: Design of minimal ion channels

AUTHOR: Zhiguang Yuchi, B. Sc. (Fudan University)

SUPERVISOR: Dr. Daniel S. C. Yang

NUMBER OF PAGE: 123

Dedicated to my beautiful wife Yutu Shen,

who has been a constant inspiration and support for me.

Also dedicated to my parents Jun Yuchi and Zhuoran Cai,

my grandparents Jing Yuchi, Huilun Wang and Lu Pang,

my aunts Min Yuchi, Zhuoya Cai and Wangping Li,

my uncles Xuexun Tang, Jinhu Xu and Fan Jiang,

I could not have come so far without all of you.

Acknowledgements

I would like to thank the following individuals for their extraordinary support during my Ph.D. study and thesis pursuit.

My supervisor Dr.Daniel Yang, for allowing me to pursue my doctoral work in his laboratory, for all manner of valuable advice and direction, for listening to hundreds of my dumb ideas, but most importantly, for encouraging me thousands times when I facing frustration. I feel truly lucky to have worked in his laboratory.

My committee members, Dr. Richard Epand and Dr. Murray Junop, who provided me invaluable guidance during my Ph.D. study. Many scientific lessons they taught will be beneficial for all the remaining of my career.

Dr. James Britten, who introduced me to and apprenticed me in the world of X-ray crystallography.

Dr. Victor Pau, for patiently answering my endless scientific questions.

Finally, all the colleagues in Yang's laboratory, Yongfang Zhu, Bridget Lu, Chand Mangat, Pardie Hamboyan, Helen He, Jeremy Yang, Marcos Haikalis, Tian Ma, Ben Huang, Carrie Hong, Wen He and Raymond Xu, for providing an pleasant and educational laboratory environment. I have shared many enjoyable moments with them.

Abstract

We developed some universal platforms to overexpress the minimal functional entities of ion channels. The modular property of ion channels have been demonstrated from many aspects, such as crystal structures, chimeric channel experiments and discovery of similar modules in distantly related protein families. Thus it should be feasible to express each module independent of other channel modules. The pore-forming module of ion channels has multiple important properties as selectivity, conductivity and drug-binding. If it can be overexpressed, it will provide valuable information about channel selectivity to different ions and structural bases for drug binding as well as important application in drug screening and rational drug design.

To test this, we first used the model channel KcsA to identify the minimal requirements for a pore-forming domain to functionally exist independently. Chapter 2 of this thesis explains in detail how the wild type C-terminal cytoplasmic domain of KcsA functions. We found that this domain has dual function as pH-sensor and tetramerization domain, and it is essential for the expression of the pore-forming domain of KcsA. Once we knew the physiological role of the cytoplasmic domain, the scenario was set to answer the question of how to make it better for the application of structural and functional studies.

In chapter 3 and chapter 4, we replaced the wild type C-terminal domain with non-native tetramerization domains. We identified the direct correlation between protein expression level and overall thermostability of pore-forming domains. The C-terminal tetramerization domains stabilize channels in a cooperative way and play a critical way in *in vivo* channel assembly. The selection of the linker between pore-forming domain and

tetramerization domain, the splicing motif, and the handedness of C-terminal tetrameric coiled coils all affect channel expression level and stability.

We applied our finding in KcsA to a wide range of ion channels in chapter 5, including voltage-gated potassium channels, Ca^{2+}-gated potassium channels, inward-rectifying potassium channels, cyclic nucleotide-gated potassium channels and voltage-gated sodium channels. We managed to express similar minimal structural modules from these more structurally complicated channels with the assistance of different cytoplasmic tetramerization domains. Several minimal channels expressed well and showed similar biophysical and functional property as the wild type channels.

These studies demonstrate that the pore-forming modules of ion channels can be expressed independently while retaining the proper structure and drug-binding properties as their wild type predecessors when using our universal expression platform. The potential application in structural studies and drug-screening is promising.

Table of Contents

List of Figures and Tables

Figures:

Tables:

List of Abbreviations:

Å	Angstrom
BICINE	N,N-Bis(2-hydroxyethyl)glycine
Ca^{2+}	Calcium Ion
Ci-VSP	Ciona voltage-sensor containing Phosphatase
CHAPS	3-((3-cholamidopropyl)dimethylammonio)-1-propanesulfonic acid
CTD	C-terminal Domain
E.coli	Escherichia coli Bacteria
EPR	Electron Paramagnetic Resonance
FPLC	Fast Protein Liquid Chromatography
HEPES	2-[4-(2-Hydroxyethyl)-1-piperazinyl]ethanesulfonic acid
His	Histidine
His-tag	Polyhistidine sequence for Ni^{2+}-chelate Affinity Chromatography
IPTG	Isopropyl β- D -1-thiogalactopyranoside
K^+	Potassium Ion
LB	Luria-Bertani Media
LDAO	Lauryldimethylamine-oxide
mg	milligram
mM	millimolar
MWCO	Molecular Weight Cut Off
Na^+	Sodium Ion
OD	Optical Density
PCR	Polymerase Chain Reaction
PDB	Protein Data Bank
PMSF	Phenylmethanesulfonyl Fluoride
POPE	1-Palmitoyl-2-Oleoyl-sn-Glycero-3-Phosphoethanolamine
POPG	1-Palmitoyl-2-Oleoyl-sn-Glycero-3-[Phospho-rac-(1-glycerol)]
rCTD	Recombinant C-terminal Domain of KcsA
RMSD	Root Mean Square Deviation

SDS	Sodium Dodecyl Sulfate
SDS PAGE	Sodium Dodecyl Sulfate Polyacrylamide Gel Electrophoresis
TEV protease	Tobbaco Etch Virus Protease
Tm	Tetramer-monomer Dissociation Temperature
TM	Transmembrane Helix
TRIS	Trishydroxymethylaminomethane

Chapter 1.

Introduction

1.1 Ion channels

Ion channels are pore-forming proteins that allow the movement of ions across cell membranes down their electrochemical gradient (1). Ion channels play indispensable roles for all life, from viruses to humans. Their most well-known function is to control the nervous system by sensing neurotransmitter at synapse and propagating impulse along the nerve cell. In human, they are also involved in a wide variety of other biological processes, such as muscle contraction, epithelial transport of nutrients and ions, T-cell activation and pancreatic beta-cell insulin release (2-4). Ion channels are equally important for simple organisms. In bacteria, ion channels carry the function of mechanosensation and chemotaxis as well as pH homeostasis (5-7). And viruses use them to regulate virion assembly and disassembly in host cells (8). The fast response property of ion channels makes them key components in many biological processes that involve rapid changes in cells, and one of the most versatile proteins in nature.

Despite the very diverse functions of ion channels, they all share similar biophysical characters. Most ion channels have selectivity for specific ions. For example, potassium channels can distinguish potassium ions from sodium ions by a selectivity of nearly one thousand fold. Surprisingly, while fulfilling such a restrictive selection requirement, they can still conduct over 10^7 ions per second, almost reaching the diffusion limit (1). Gating of channels is another wonder. Although different channels can sense a diverse range of stimuli, including voltage changes, mechanical force and to many different chemical

compounds, they can transmit all the signal-induced sensor movements to the gates and allow the transient opening of channels for fractions of seconds (9).

When I started my research, Dr. Roderick MacKinnon just won the Nobel Prize for his groundbreaking work on solving the first few crystal structures of ion channels, including KcsA, MthK and KvAP (10-12). From these structures, for the first time, people can have the chance to appreciate perhaps the most exquisite design in nature.

KcsA is the first channel that has a known crystal structure and has been used widely as the model for ion channels (Figure 1.1). It is a truncated form of KcsA (lacking C-terminal end) that was crystallized at 3.2 Å resolution, but it is sufficient to elucidate the molecular arrangement of the pore-forming domain in the closed state. Four identical subunits assembled to form a pore with four-fold symmetry. The ion conducting passage lies in the centre of the tetramer along the symmetry axis. Each subunit contains two major transmembrane α-helices, TM1 which is located at the periphery of the channel and TM2 which is facing the central permeation pathway. One crucial structural component called selectivity filter is located at near the extracellular part of the channel. The selective function of the filter is contributed by the carbonyl groups of four stretched fragments of amino acids, one from each subunit, pointing at the permeation pathway. These carbonyl groups form a perfectly coordinated cage for potassium ions so that it can mimic the water molecules in the hydrated form of potassium (Figure 1.2). When potassium ions move between the solution and the selectivity filter, there is no energy penalty for desolvation. But when smaller ions like sodium ions pass through, there

would be a huge energy penalty for dehydration. That explains why the channel can possess accurate selectivity and at the same time keep the extremely high conductivity (10,13-15). Below the selective filter is a cavity filled with water. This polar cavity counteracts the dielectric barrier formed by cell membrane and facilitates ion permeation (14).

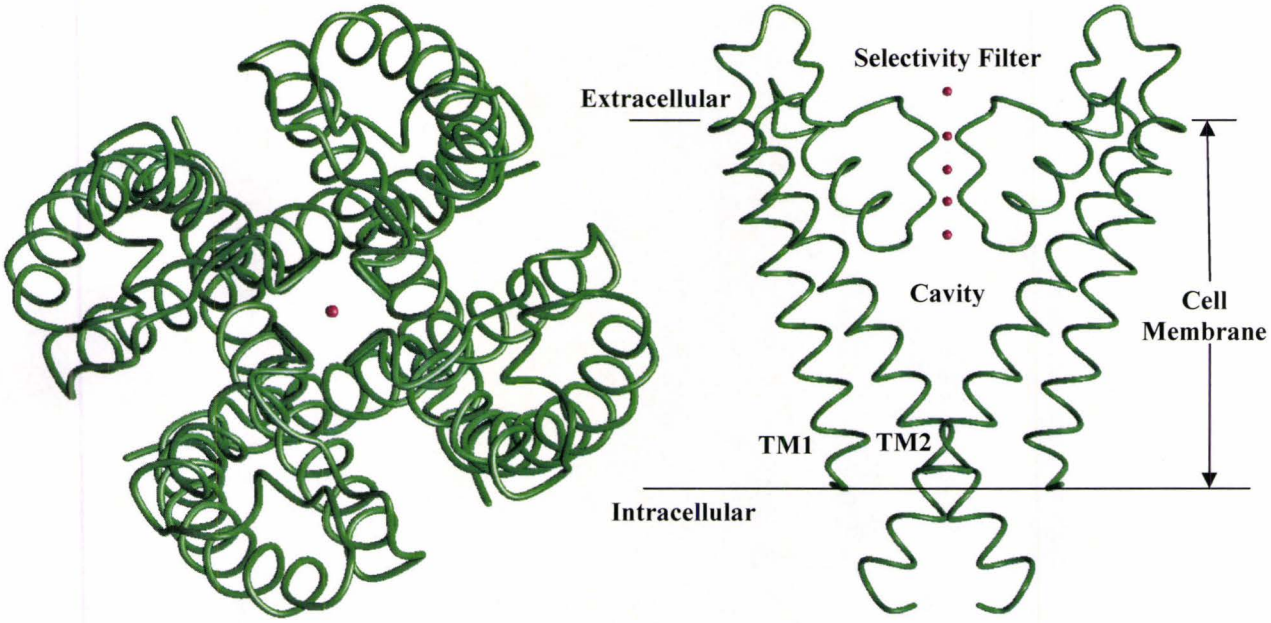

Figure 1.1 Structure of KcsA channel (10). The top view on the left panel shows an overall four-fold symmetry of KcsA. The right panel is a side view of the channel. Only two opposite subunits are shown for clarity. The structural elements of transmembrane helix 1 (TM1), transmembrane helix 2 (TM2), selectivity filter and cavity are labelled. The purple dots represent the potassium ions observed in the crystal structure.

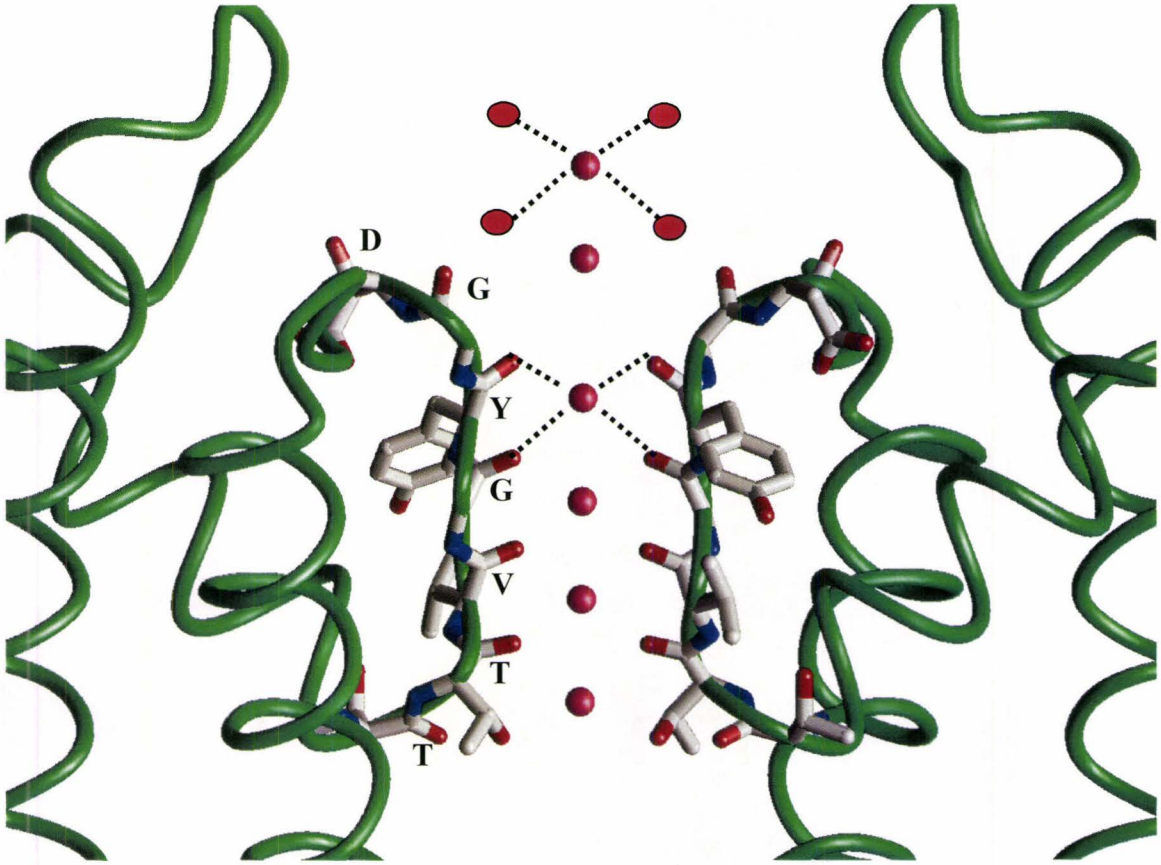

Figure 1.2 A close look at the selectivity filter region of KcsA. The selectivity filter of two subunits is shown in stick representation with several signature sequence residues labeled. Purple dots represent the potassium ions and the red dots represent the water molecules in the hydration shell of one potassium ion in solution.

Since this pioneering work, a few other channel structures have emerged, including MthK (the first structure showing a channel in the open state) (16), KvAP (the first structure of a voltage-gated channel) (12), Kir (the first structure of an inward-rectifier channel) (17), rKv1.2 (the first structure of an eukaryotic channel) (18), NaK (the first structure of a non-selective channel) and etc. However, there remain a large number of ions channels to be characterized crystallographically for understanding the relationship between diverse stimuli and gating of channels as well as important application in rational drug designs. These are especially true for the Na^+ and Ca^{2+} channels since there is not a single structure been determined. With the current efficiency of structure

determination of ion channels, it will take a long time before we can get a reasonable understanding of ion channels. For this reason, I started to search for some universal platforms for easy overexpression and crystallization of a wide range of cation channels.

We classified cation channels into three major families according to their topologies: type I, exemplified by KcsA, has four-fold symmetry and each subunit has two transmembrane helices (2-TM) with small cytoplasmic domains; type II is ligand-gated channel, exemplified by MthK, similar to type I but with a large C-terminal cytoplasmic ligand-sensing domain; type III, exemplified by voltage-gated potassium channels, has the same four-fold symmetry but six transmembrane helices (6-TM) in each subunit (Figure 1.3). The four extra TMs (S1-S4) play the role as a voltage-sensor (19). Other families are in the adapted forms based on these three major topologies. Sodium channels and calcium channels are made up of single polypeptides with 24 transmembrane helices arranged in 4 repeating 6-TMs subunits and exhibiting pseudo-four-fold symmetry, similar to the third class. Two-pore-domain potassium channels are made up of dimers of polypeptides that contain two consecutively linked Type I 2-TMs subunits.

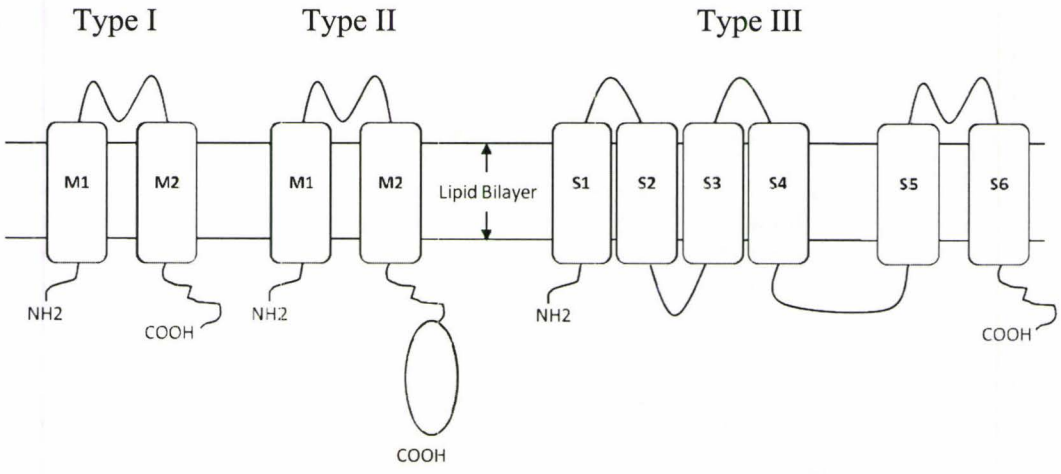

Figure 1.3 The three main classes of cation channels. Left panel shows type I, which consists of 2-TM with small cytoplasmic domain; middle panel shows type II with 2-TM and big cytoplasmic ligand-binding domain; right panel shows type III, which consists of 6-TM.

1.2 Modular property

Although the three types of cation channels differ in structure and function, they all have similar modular properties. From the known crystal structures, cation channels from different families all have a pore-forming domain composed of 2 TMs and the structural contacts between ligand-binding domains or voltage-sensing domains with pore-forming domains are minimal (12,16-18). The modular property has also been proven by a number of chimera experiments. A voltage-gate potassium (Kv) channel chimera was generated by replacing its pore-forming region (S5-S6) with the counterpart of KcsA (M1-M2). The chimeric channel successfully functions as a voltage-gated potassium channel (20). Similar experiments were also done between an inward-rectifying potassium channel (IRK1) and KcsA (20) as well as between a cyclic nuleotide-gated (CNG) channel and KcsA (21), which proves the functional and structural conservation of pore-forming domain among all the three types of cation channels. The discovery of voltage-sensor domain in Ci-VSP (Ciona voltage-sensor containing phosphatase), a distantly related protein as a phosphatase, further demonstrated the evolutionary modular property of ion channels (22-25).

The ion channels are a very important family of drug targets, which is related to a number of diseases such as diabetes, epilepsy, migraine, and etc (26-28). The fifteen ion channel modulators currently on market generate worldwide sales over $15 billion, including anti-hypertensive amlodipine besylate (Norvasc; Pfizer) and anti-insomnia zolpidem tartrate (Ambien; Sanofi Aventis) (29). There are two major drug-binding sites in ion channels. First is at the entrance of selectivity filter (outer pore), which binds drugs like tetraethylammonium and kaliotoxin. The other is at the central cavity of the ion-

conducting pore (inner pore), which binds drugs like tetrabutylammonium and bupivacaine (30-32). Both of these two sites lie in the pore-forming module. There are some drugs that bind to the sensing modules or intracellular regulatory modules (32-34), but most drugs directly interact with the pore-forming module and affect the channel function by blocking.

The aim of my project is to study structural and functional properties of individual channel modules by utilizing their modular property. The focus is on the pore-forming modules because this part of channel is in charge of the conductivity, selectivity and drug-binding property of the channel. Structural information about this part of channel is very valuable for understanding how drugs interact with specific channels and thus guiding rational drug design.

Recently there were three reported attempts to express the pore-forming modules of different ion channels independently. First attempt was on the skeletal muscle sodium channels (35,36). Given that the eukaryotic sodium channel has 24–TM in a single protein molecule, it is very difficult to express the whole channel and get enough protein for crystallization studies. Chen *et al.* (34) expressed the eight pore-forming helices, four sets of S5-S6, as linked concatemer. This minimal construct formed a toxin-activable ionophore but did not reconstitute the Na^+ channel permeation pathway with full fidelity. Similar engineering work was also done on some homotetrameric ion channels, such as Ryanodine receptor calcium channel RyR1 (37) and prokaryotic voltage-gated potassium channel KvLM (38). Their pore-forming domains together with C-terminal cytoplasmic domains following S6 helices were cloned and expressed independently. The expression of these minimal channels can be detected at Western-blot and the minimal KvLM also

displayed conduction and selection properties as wild type potassium channels. These prior studies on minimal channels are encouraging. They provided experimental evidence for the feasibility of functionally expressing ion channels in their minimal form. The details of characterization of the minimal channels as well as strategies used for generating the minimal constructs were different in each of these studies, therefore it is not immediately apparent which is a better strategy to be applied to other channels. We aim to systematically address the problem of minimal channel design and to develop a platform that is robust and easily applicable to a diverse range of ion channels. This will facilitate structural characterization of the most conserved but valuable structural module, the pore-forming domain.

1.3 Tetramerization domains of ion channels

In chapter 2 and 3 of this thesis, we use model channel KcsA to study the minimal size requirement for the pore-forming domain to be expressed independently. We found that the C-terminal cytoplasmic domain can self-associate into tetrameric form in solution and it is essential for the expression and stability of the pore-forming domain of KcsA. The function of C-terminal domain can be replaced by an artificial tetramerization coiled coil structure, proving a tetramerization interaction in cytoplasmic domain is necessary for the expression of the pore-forming domain.

Tetramerization domains have been identified in many different ion channel families. In voltage-gated potassium channel family, there is an N-terminal cytoplasmic domain, called T1 (tetramerization domain 1), which was shown to self-associate into tetrameric form when isolated from the channel (39-41). T1 is important for the functional assembly

of Kv channel *in vivo* and its function can also be replaced by non-native tetramerization domain (42). Tetramerization domains were also found in other families of ion channels such as ether-a-go-go channels, potassium inwardly-rectifying channels, calcium activated channels and cyclic nucleotide-gated (CNG) channels (43-48).

Another interesting finding is that these tetramerization domains often carry more than the single function as tetramerization interaction in channel assembly. Our study in chapter 2 demonstrated that the C-terminal domain of KcsA also plays the role as a pH-sensor which modulates the channel gating. A similar phenomenon has also been found in other channels: tetramerization domain of calcium activated channels serves as a Ca^{2+}-sensing modulator (16,45,49); tetramerization domain of CNG channels serves as a cyclic nucleotide-sensing modulator (50,51); T1 domain of Kv channel is also in charge of interacting with intracellular regulatory proteins (52-59). The combination of multi-function in a single domain reflects the high efficiency of energy consumption in cells.

There are still many channels without a known tetramerization domain. The reason could be: 1) they exist but are yet to be identified; 2) they do not exist. If the later is true, it could be one of the reasons to account for the low expression level of some particular channels. Through the findings on the tetramerization domains of KcsA and other ion channels, we speculate that the expression yields of some of the hardly expressed ion channels can be significantly improved by incorporating a non-native tetramerization domain at an appropriate site.

1.4 Coiled coils

We thoroughly investigated the effect of different tetramerization domains on model channel KcsA in chapter 3 and 4. In the recent crystal structure on full length KcsA channel, the C-terminal domain of KcsA presents as a parallel coiled coil structure (60) (Figure 1.4A). In order to mimic this native C-terminal structure as well as fine-tune its tetramerization effect, many different tetramerization coiled coils structures were selected to test by replacing the native tetramerization domain of KcsA with them (Figure 1.4B).

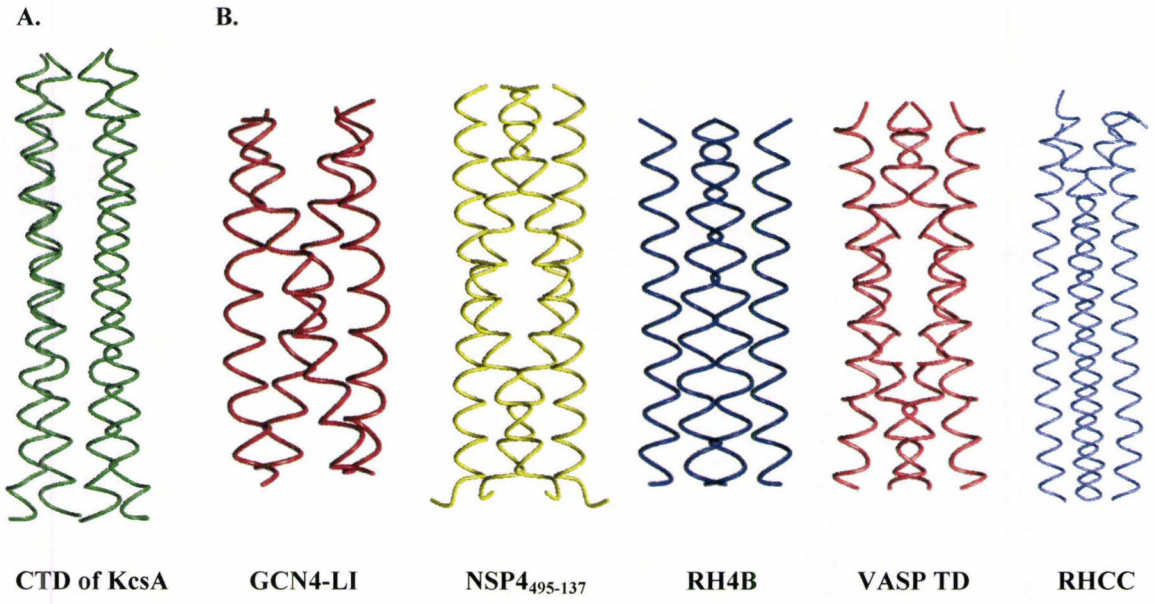

Figure 1.4 Structure of different coiled coils. (A) Crystal structure of C-terminal domain (CTD) of KcsA (pdb code: 3EFF). (B) Crystal structures of different coiled coils: GCN4-LI (pdb code: 1GCL), $NSP_{495-137}$ (pdb code: 1G1I), RH4B (pdb code: 2O6N), VASP TD (pdb code: 1USE) and RHCC (pdb code: 1FE6).

Coiled coil structure is a ubiquitous motif present in many protein families, which represents about 5-10% of all protein sequences from genomic analysis (61). The versatility of coiled coil motif has been shown by discovery of them in many different proteins, many of which have known crystal structures (62,63). Coiled coils form the major structural unit of the cytoskeleton and cytoskeletal "motor proteins", including keratin and tropomyosin. These filament structures form an interconnected network,

which is involved in maintaining cell shape, enabling cellular motion and cellular division (64-66). One special feature of coiled coils is their pH-sensitive conformational change caused by the protonation and deprotonation of interface polar residues. Cells make use of this property of coiled coils in many proteins. The function of ATP synthase is regulated by a natural inhibitory protein, IF1, which has a C-terminal coiled coil domain providing pH sensitivity. When pH is lower than 6.5, the histidine residues on the surface of coiled coil structure will be protonated, which causes the dimerization of IF1 and turn the protein into the active form. At higher pH, the dissociation of dimer protein will turn it off to the inactive form (67). Similar function is also found in coiled coil domains from the virus envelop glycoproteins. They mediate the fusion of viral and host membranes, which is triggered by acidic pH condition (68,69). The C-terminal domain of KcsA channel is another good example of natural utilization of pH-sensitive coiled coil domain (70). Using pH-sensing property of coiled coils to control the channel gating can simplify the gating system of ion channels and facilitate the functional analysis as well as drug screening process. In the study of chapter 4, we demonstrate that the non-native pH-sensing coiled coil is able to open the KcsA in a similar adjustable manner, which opens the potential application of using it as a universal signal sensor for other ion channels.

More complicated coiled coils, the asymmetric ones, have also been identified, which is represented by the SNARE protein complex. In this heterotetrameric complex, one of them is located in vesicle and the other three are in cell membrane. The specific recognition and formation of coiled coil structure will mediate the membrane fusion and facilitate the exocytic process (71-73). Since many of Na^+ and Ca^{2+} channels are

asymmetric, the addition of these asymmetric coiled coil structures may be a good scaffold for the expression of this class of ion channels.

The handedness of coiled coils is an important factor that affects their contribution to the pore-forming domain of ion channels. In chapter 3 and 4, we chose five coiled coils with different handedness (left, parallel, slight right and right) (Figure 1.4B) and compare their effects on pore-forming domain of KcsA both *in silico* and *in vivo*. Based on the crystal structure, we know that the C-terminal half of inner helices of KcsA transmembrane domain form a right-handed coiled coil structure. We added six candidate coiled coils after this inner helix either with a flexible linker as spacer or by directly splicing them together. We found that the linker will impair the expression and stability of the pore-forming domain when compared to the non-linker ones. Among directly spliced constructs, there is a correlation between the handedness of C-terminal coiled coil and the overall stability of the pore-forming domain. The right-handed coiled coil at C-terminal end can form a continuous coiled coil structure with the inner helix, which shows a much higher stability than the chimera with two coiled coils with contradictory handedness. Out of the right-handed coiled coils, RHCC shows the least RMS in the structural alignment with inner helix of KcsA. As a consequence, the chimeric channel KcsA-RHCC displays a high expression level and extreme thermostability.

1.5 Universality of the ion channel expression platform

Based on the knowledge we gained from KcsA studies, in chapter 5, we broaden our targets to diverse ion channels from five different categories, including voltage-gated potassium channels, Ca^{2+}-gated potassium channels, inward-rectifying potassium

channels, cyclic nucleotide-gated potassium channels and prokaryotic voltage-gated sodium channels.

From the known crystal structures of cation channels, all of their inner helices in pore-forming domains form right-handed coiled coil structure (10,12,16-18,74,75). Theoretically, it should be possible to use a similar platform for the expression of all their pore-forming domains by using a strong C-terminal cytoplasmic tetrameric coiled coil. In practice, there are a few problems complicating this platform. First, most ion channels have no known crystal structures. Designing the chimeric channels based on computer modeling like we did for KcsA is impossible. Second, although some channels have been crystallized, they were crystallized in open conformation. The close structures can hardly be predicted accurately by modeling to guide the design of chimeric channels. Therefore, we resorted to the screening method.

In our trials, we tried to use our best candidate RHCC to assist the expression of the pore-forming domains of different ion channels. We built many constructs by splicing RHCC to different positions of their pore-forming domains and screened the better candidates by measuring their induction level with Western-blot. Those with higher expression level were further purified and characterized biophysically and functionally. A number of them showed relatively high expression levels and similar biophysical properties as well as normal function as wild type channels.

Ion channels are important drug targets and their pore-forming domains are the cores for drug interaction. The development of this platform may open a new way to facilitate structural and functional studies for a wide range of ion channels.

1.6 References

1. Hille, B. (2001) *Ion Channels of Excitable Membrane*, Sinauer Associates, Inc, Sunderland, MA
2. Camerino, D. C., Desaphy, J. F., Tricarico, D., Pierno, S., and Liantonio, A. (2008) *Adv Genet* **64**, 81-145
3. Camerino, D. C., Tricarico, D., and Desaphy, J. F. (2007) *Neurotherapeutics* **4**, 184-198
4. Verkman, A. S., and Galietta, L. J. (2009) *Nat Rev Drug Discov* **8**, 153-171
5. Ito, M., Xu, H., Guffanti, A. A., Wei, Y., Zvi, L., Clapham, D. E., and Krulwich, T. A. (2004) *Proc Natl Acad Sci U S A* **101**, 10566-10571
6. Eckert, R. (1972) *Science* **176**, 473-481
7. Oakley, A. J., Martinac, B., and Wilce, M. C. (1999) *Protein Sci* **8**, 1915-1921
8. Pinto, L. H., Dieckmann, G. R., Gandhi, C. S., Papworth, C. G., Braman, J., Shaughnessy, M. A., Lear, J. D., Lamb, R. A., and DeGrado, W. F. (1997) *Proc Natl Acad Sci U S A* **94**, 11301-11306
9. Jan, L. Y., and Jan, Y. N. (1994) *Nature* **371**, 119-122
10. Doyle, D. A., Morais Cabral, J., Pfuetzner, R. A., Kuo, A., Gulbis, J. M., Cohen, S. L., Chait, B. T., and MacKinnon, R. (1998) *Science* **280**, 69-77
11. Jiang, Y., Lee, A., Chen, J., Cadene, M., Chait, B. T., and MacKinnon, R. (2002) *Nature* **417**, 523-526
12. Jiang, Y., Lee, A., Chen, J., Ruta, V., Cadene, M., Chait, B. T., and MacKinnon, R. (2003) *Nature* **423**, 33-41

13. Zhou, Y., Morais-Cabral, J. H., Kaufman, A., and MacKinnon, R. (2001) *Nature* **414**, 43-48

14. Roux, B., and MacKinnon, R. (1999) *Science* **285**, 100-102

15. Morais-Cabral, J. H., Zhou, Y., and MacKinnon, R. (2001) *Nature* **414**, 37-42

16. Jiang, Y., Lee, A., Chen, J., Cadene, M., Chait, B. T., and MacKinnon, R. (2002) *Nature* **417**, 515-522

17. Kuo, A., Gulbis, J. M., Antcliff, J. F., Rahman, T., Lowe, E. D., Zimmer, J., Cuthbertson, J., Ashcroft, F. M., Ezaki, T., and Doyle, D. A. (2003) *Science* **300**, 1922-1926

18. Long, S. B., Campbell, E. B., and Mackinnon, R. (2005) *Science* **309**, 897-903

19. Choe, S. (2002) *Nat Rev Neurosci* **3**, 115-121

20. Lu, Z., Klem, A. M., and Ramu, Y. (2001) *Nature* **413**, 809-813

21. Ohndorf, U. M., and MacKinnon, R. (2005) *J Mol Biol* **350**, 857-865

22. Iwasaki, H., Murata, Y., Kim, Y., Hossain, M. I., Worby, C. A., Dixon, J. E., McCormack, T., Sasaki, T., and Okamura, Y. (2008) *Proc Natl Acad Sci U S A* **105**, 7970-7975

23. Kohout, S. C., Ulbrich, M. H., Bell, S. C., and Isacoff, E. Y. (2008) *Nat Struct Mol Biol* **15**, 106-108

24. Murata, Y., Iwasaki, H., Sasaki, M., Inaba, K., and Okamura, Y. (2005) *Nature* **435**, 1239-1243

25. Murata, Y., and Okamura, Y. (2007) *J Physiol* **583**, 875-889

26. Cooper, E. C., and Jan, L. Y. (1999) *Proc Natl Acad Sci U S A* **96**, 4759-4766

27. Sobey, C. G. (2001) *Arterioscler Thromb Vasc Biol* **21**, 28-38

28. Shieh, C. C., Coghlan, M., Sullivan, J. P., and Gopalakrishnan, M. (2000) *Pharmacol Rev* **52**, 557-594

29. Molokanova, E., and Savchenko, A. (2008) *Drug Discov Today* **13**, 14-22

30. Fernandez, D., Ghanta, A., Kauffman, G. W., and Sanguinetti, M. C. (2004) *J Biol Chem* **279**, 10120-10127

31. Myokai, T., Ryu, S., Shimizu, H., and Oiki, S. (2008) *Mol Pharmacol* **73**, 1643-1651

32. Colatsky, T. J. (1996) *Circ Res* **78**, 1115-1116

33. Birch, P. J., Dekker, L. V., James, I. F., Southan, A., and Cronk, D. (2004) *Drug Discov Today* **9**, 410-418

34. Ruta, V., and MacKinnon, R. (2004) *Biochemistry* **43**, 10071-10079

35. Chen, Z., Alcayaga, C., Suarez-Isla, B. A., O'Rourke, B., Tomaselli, G., and Marban, E. (2002) *J Biol Chem* **277**, 24653-24658

36. Pincin, C., Ferrera, L., and Moran, O. (2005) *Biochem Biophys Res Commun* **334**, 140-144

37. Kang, G. B., Song, H. E., Song, D. W., Kim, M. K., Rho, S. H., Kim do, H., and Eom, S. H. (2007) *Protein Pept Lett* **14**, 742-746

38. Santos, J. S., Grigoriev, S. M., and Montal, M. (2008) *J Gen Physiol* **132**, 651-666

39. Li, M., Jan, Y. N., and Jan, L. Y. (1992) *Science* **257**, 1225-1230

40. Shen, N. V., Chen, X., Boyer, M. M., and Pfaffinger, P. J. (1993) *Neuron* **11**, 67-76

41. Kreusch, A., Pfaffinger, P. J., Stevens, C. F., and Choe, S. (1998) *Nature* **392**, 945-948

42. Zerangue, N., Jan, Y. N., and Jan, L. Y. (2000) *Proc Natl Acad Sci U S A* **97**, 3591-3595

43. Jenke, M., Sanchez, A., Monje, F., Stuhmer, W., Weseloh, R. M., and Pardo, L. A. (2003) *EMBO J* **22**, 395-403

44. Tinker, A., Jan, Y. N., and Jan, L. Y. (1996) *Cell* **87**, 857-868

45. Jiang, Y., Pico, A., Cadene, M., Chait, B. T., and MacKinnon, R. (2001) *Neuron* **29**, 593-601

46. Quirk, J. C., and Reinhart, P. H. (2001) *Neuron* **32**, 13-23

47. Schmalhofer, W. A., Sanchez, M., Dai, G., Dewan, A., Secades, L., Hanner, M., Knaus, H. G., McManus, O. B., Kohler, M., Kaczorowski, G. J., and Garcia, M. L. (2005) *Biochemistry* **44**, 10135-10144

48. Zhou, L., Olivier, N. B., Yao, H., Young, E. C., and Siegelbaum, S. A. (2004) *Neuron* **44**, 823-834

49. Ptak, C. P., Cuello, L. G., and Perozo, E. (2005) *Biochemistry* **44**, 62-71

50. Trudeau, M. C., and Zagotta, W. N. (2002) *Proc Natl Acad Sci U S A* **99**, 8424-8429

51. Young, E. C., and Krougliak, N. (2004) *J Biol Chem* **279**, 3553-3562

52. Deutsch, C. (2002) *Annu Rev Physiol* **64**, 19-46

53. Shi, G., Nakahira, K., Hammond, S., Rhodes, K. J., Schechter, L. E., and Trimmer, J. S. (1996) *Neuron* **16**, 843-852

54. Yu, W., Xu, J., and Li, M. (1996) *Neuron* **16**, 441-453

55. Gulbis, J. M., Zhou, M., Mann, S., and MacKinnon, R. (2000) *Science* **289**, 123-127

56. Gu, C., Jan, Y. N., and Jan, L. Y. (2003) *Science* **301**, 646-649

57. Cushman, S. J., Nanao, M. H., Jahng, A. W., DeRubeis, D., Choe, S., and Pfaffinger, P. J. (2000) *Nat Struct Biol* **7**, 403-407

58. Minor, D. L., Lin, Y. F., Mobley, B. C., Avelar, A., Jan, Y. N., Jan, L. Y., and Berger, J. M. (2000) *Cell* **102**, 657-670

59. Kurata, H. T., Soon, G. S., Eldstrom, J. R., Lu, G. W., Steele, D. F., and Fedida, D. (2002) *J Biol Chem* **277**, 29045-29053

60. Uysal, S., Vasquez, V., Tereshko, V., Esaki, K., Fellouse, F. A., Sidhu, S. S., Koide, S., Perozo, E., and Kossiakoff, A. (2009) *Proc Natl Acad Sci U S A* **106**, 6644-6649

61. Mewes, H. W., Frishman, D., Gruber, C., Geier, B., Haase, D., Kaps, A., Lemcke, K., Mannhaupt, G., Pfeiffer, F., Schuller, C., Stocker, S., and Weil, B. (2000) *Nucleic Acids Res* **28**, 37-40

62. Cohen, C., Reinhardt, B., Parry, D. A., Roelants, G. E., Hirsch, W., and Kanwe, B. (1984) *Nature* **311**, 169-171

63. Lupas, A. (1996) *Trends Biochem Sci* **21**, 375-382

64. Kreplak, L., Doucet, J., and Briki, F. (2001) *Biopolymers* **58**, 526-533

65. Hodges, R. S., Saund, A. K., Chong, P. C., St-Pierre, S. A., and Reid, R. E. (1981) *J Biol Chem* **256**, 1214-1224

66. Holtzer, M. E., Breiner, T., and Holtzer, A. (1984) *Biopolymers* **23**, 1811-1833

67. Gordon-Smith, D. J., Carbajo, R. J., Yang, J. C., Videler, H., Runswick, M. J., Walker, J. E., and Neuhaus, D. (2001) *J Mol Biol* **308**, 325-339

68. Carr, C. M., and Kim, P. S. (1993) *Cell* **73**, 823-832

69. Bullough, P. A., Hughson, F. M., Skehel, J. J., and Wiley, D. C. (1994) *Nature* **371**, 37-43

70. Pau, V. P., Zhu, Y., Yuchi, Z., Hoang, Q. Q., and Yang, D. S. (2007) *J Biol Chem* **282**, 29163-29169

71. Banfield, D. K. (2001) *Trends Biochem Sci* **26**, 67-68

72. Chen, Y. A., and Scheller, R. H. (2001) *Nat Rev Mol Cell Biol* **2**, 98-106

73. Rice, L. M., Brennwald, P., and Brunger, A. T. (1997) *FEBS Lett* **415**, 49-55

74. Shi, N., Ye, S., Alam, A., Chen, L., and Jiang, Y. (2006) *Nature* **440**, 570-574

75. Nishida, M., Cadene, M., Chait, B. T., and MacKinnon, R. (2007) *Embo J* **26**, 4005-4015

Chapter 2.

Characterization of the C-terminal domain of a potassium channel from *Streptomyces lividans* (KcsA)

Reproduced in part with permission from [Victor P. T. Pau, Yongfang Zhu, Zhiguang Yuchi, Quyen Q. Hoang and Daniel S. C. Yang (2007). Characterization of the C-terminal domain of a potassium channel from Streptomyces lividans (KcsA) *J Biol Chem* **282**, 29163-29169.] Copyright © ASBMB.

I generated of C-terminal deleted KcsA construct, prepared the liposome containing this construct and characterized its thermostability; Pau wrote the manuscipt and did the majority of the experiments; Zhu did the electrophysiological experiments; Hoang assisted in the writing of the manuscript; Daniel supervised the project.

2.1 ABSTRACT

KcsA, a potassium channel from *Streptomyces lividans*, is a good model for probing the general working mechanism of potassium channels. To date, KcsA's physiological activator is still unknown but *in vitro* studies showed that it could be opened by lowering the pH of the cytoplasmic compartment to 4. The C-terminal domain (CTD, residues 112 - 160) was proposed to be the modulator for this pH responsive event. Here, we support this proposal by examining the pH profiles of: a) thermal stability of KcsA with and without its CTD; and b) aggregation properties of a recombinant fragment of CTD. We found that the presence of the CTD weakened and enhanced the stability of KcsA at acidic and basic pHs respectively. In addition, the CTD fragment oligomerized at basic pHs with a transition profile close to that of channel opening. Our results are consistent with the CTD being a pH modulator. We propose herein a mechanism on how this domain may contribute to the pH-dependent opening of KcsA.

2.2 INTRODUCTION

Permeation of ions across cellular membranes is essential to life but it is energetically unfavorable due to the dielectric barrier formed by the lipidic components of the membrane. Ions channels provide means to overcome this barrier. These channels allow high flux of ions across the membrane while maintaining high selectivity in a well-regulated manner (1,75). The mechanisms of efficiency, selectivity and open-closed switching of channels have been the focus of many scientists in the field (10,11,17,33,76,77). Towards these goals, studies on the potassium channel KcsA from *Streptomyces lividans* have provided a wealth of information.

KcsA exists as a homo-tetramer with each subunit consisting of 160 residues (78,79). Crystal structure of a truncated KcsA (consisting of residues 23-124 without the N and C terminal domains) showed two transmembrane α-helices separated by a P loop in each subunit (9,12). The tetrameric structure resembles an inverted teepee with the base facing the extracellular side. The wall of the teepee is made up of eight helices (two from each monomer) and the body of the teepee is filled with four P loops (one from each monomer) forming a narrow passage that is selective for K^+ ions. Mechanism for efficiency and selectivity was proposed based on this structure (9,80). The mechanism for open-closed switching of KcsA, however was not immediately evident from the structure of the truncated molecule in the crystal.

KcsA has been demonstrated to be a pH-dependent channel *in vitro* that its opening probability increases as the intracellular pH decreases (81,82). The gating site is located at the narrow opening of the teepee that faces the intracellular space (10). While the N-terminal and C-terminal domains (CTD) are absent in the crystal structure, they are

predicted to face towards the cytosol (81,83). The N-terminal domain was proposed to be a membrane anchor (81,83). When it was truncated the activity of the channel was not altered (22). The CTD was proposed to be a modulator for open-closed switching (81,84). Its partial removal (last 35 residues) destabilized the tetramer and increased ion flux through the channel at neutral pH, suggesting that it stabilized the closed state (81). In addition, the deletion mutant was still able to open in a pH-dependent manner but with an altered transition profile indicating that the primary pH sensor is not located in the last 35 residues (81). Recent study suggested that the "pH-sensor" is located at the N-terminus end of the first transmembrane helix (H25;(85). To date, the detailed mechanism of gate opening remains elusive and requires further investigation. We investigated the role of CTD in gate opening by examining a) its contribution to the thermal stability of KcsA tetramer and b) its oligomerization, at various pHs. We also proposed a mechanism to relate our findings to the open-closed switching of KcsA.

2.3 RESULTS

Overexpression, purification and characterization of rKcsA and chKcsA.

*r*KcsA was expressed in E. coli. and purified to homogeneity as analysed on SDS-PAGE (Figure 2.2 A & C). CTD-truncated KcsA (KcsA-CTD) and rctKcsA were generated by limited chymotrypsin digestion as it was previously reported that KcsA can be cleaved specifically after residue 125 by chymotrypsin (86). The activities of rKcsA and rctKcsA were confirmed by cell-attached patch-clamp technique (Figure 2.1 A to C). The pH profiles of rKcsA and rctKcsA were similar to that reported by Cortes et al by Rb^+ flux assay (81).

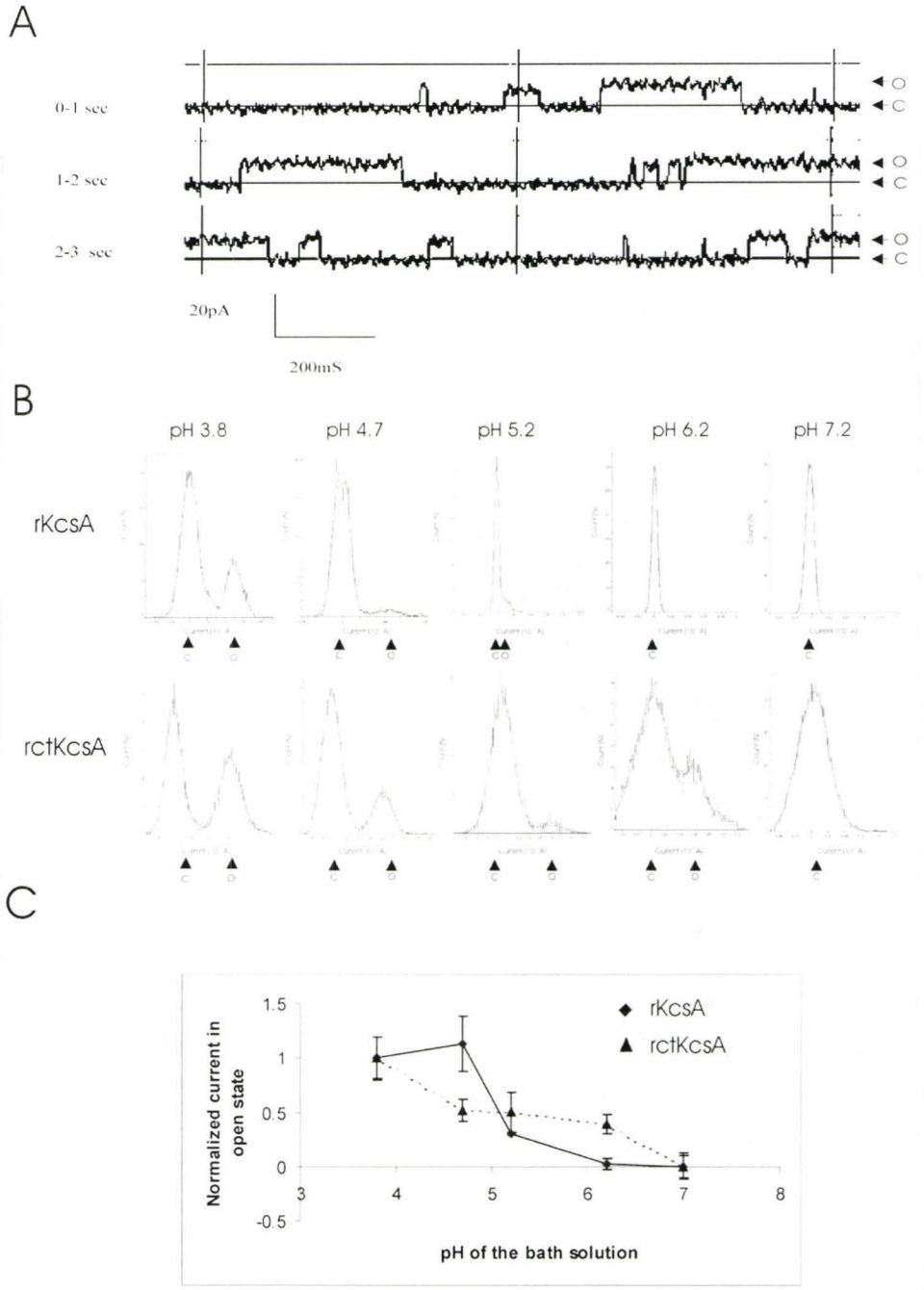

Figure 2.1 Measurement of current conducted by rKcsA and rctKcsA. Panel A: A typical record of current conducted by rKcsA at pH 3.8 for a period of 3 seconds with an applied voltage of 100 mV. The open and closed states are indicated by symbols C and O on the side of the figure. Panel B: Histograms of current conducted by rKcsA and rctKcsA at various pHs and recorded for periods of 20 seconds. The open and closed states are indicated by symbols C and O on the bottom of each histogram. No open state was observed at pHs (6.2 and 7.0) for rKcsA and at pH 7.0 for rctKcsA. Panel C: pH profile of current conducted by rKcsA and rctKcsA in its open states determined by fitting Gaussian curves to histograms in panel B. The current measured at different pHs for each construct was normalized to the current measured at pH 3.8. Currents of the closed state were used for pHs (6.2 and 7.2) of rKcsA and pH 7.0 of rctKcsA because no open state was observed. Standard derivations of the Gaussian peaks were calculated from the current values at the half-height positions and shown as error bars.

Thermal stability of tetrameric rKcsA and KcsA-CTD at various pHs.

Tetrameric KcsA is stable even in the presence of harsh detergent such as SDS and heating is required to dissociate it into monomer. Its thermal stability in SDS was used by Cortes et al. to determine the effect of various mutations (including CTD truncation) on the overall stability of the channel (81,87). It was reported that truncation of the CTD destabilized the channel. In addition, Rb^+ flux assay was also used to characterize the CTD deletion mutants and increased ion leakage at basic pH was observed. Cortes et al. concluded that the CTD stabilized the closed-form of the channel (81). In order to have a better understanding of the molecular basis of this observed phenomenon and to settle a recent claim by Molina et al. that truncation of the CTD did not destabilize KcsA tetramer (86), we extended the previous thermal stability studies carried out at a single pH to include a wide range of pHs.

The tetramer-monomer dissociation temperature (Tm) for rKcsA was pH-dependent. At pH 5.0 or higher it was about 80.0°C and shifted dramatically to about 37.4°C when pH was lowered to 4.0 (Figure 2.2 E). At pH 3.0, rKcsA existed mainly as monomer at all temperature tested (data not shown). The pH-dependent Tm profile of KcsA-CTD was quite different from its full-length counterpart. Tm of KcsA-CTD was about 20.0°C higher and 25.0°C lower than rKcsA at pH 4.0 and 8.0, respectively. When pH was lowered to 3.0, KcsA-CTD also existed as monomer.

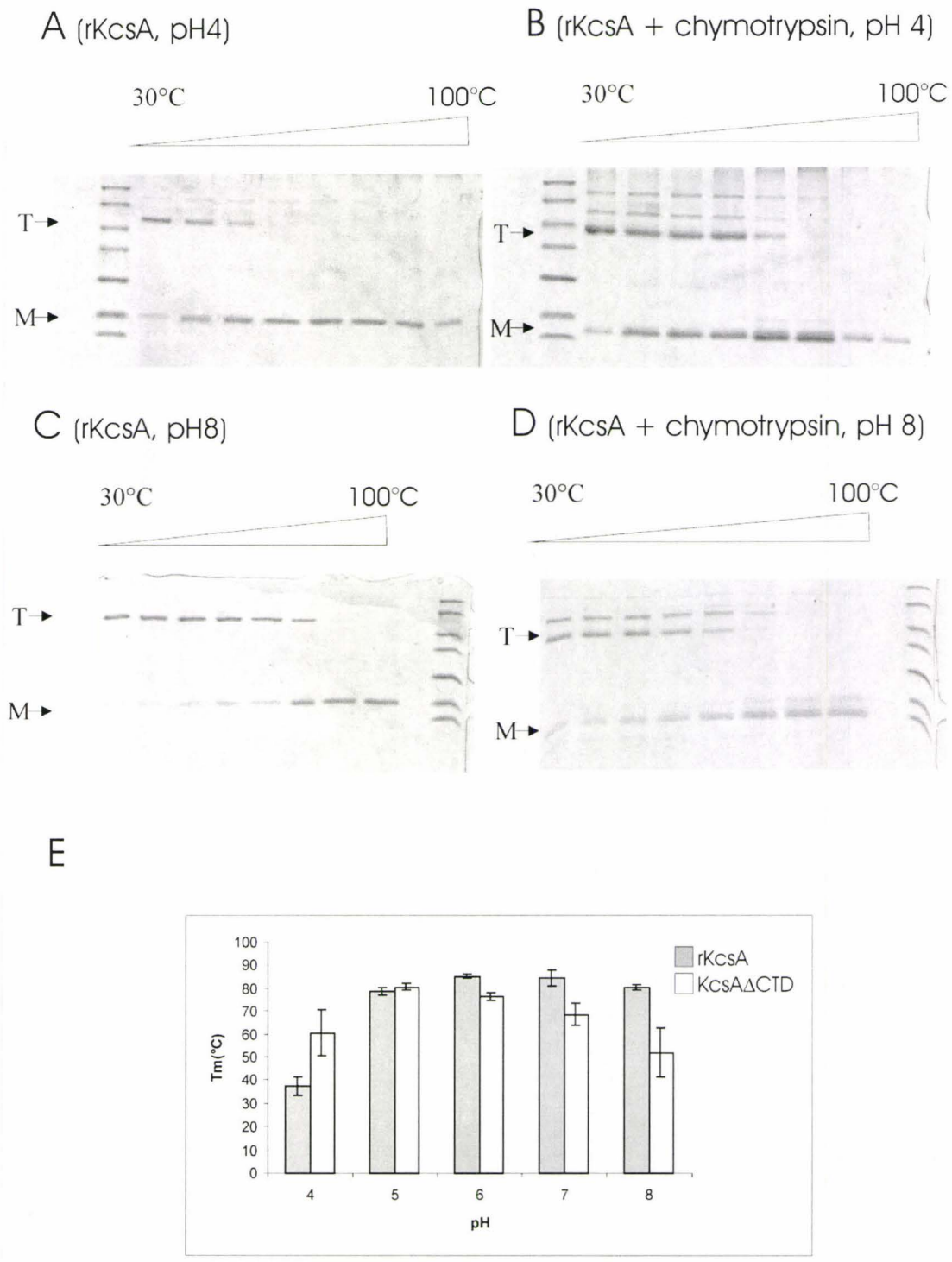

Figure 2.2 Panel A- D: Scanned images of representative SDS-PAGE gels used for thermal stability determination. T and M indicate rKcsA/KcsA CTD tetramer and monomer, respectively. The sizes of molecular weight markers from top to bottom are: 116 kDa, 66.2 kDa, 45.0 kDa, 35.0 kDa, 25.0 kDA, 18.4 kDa and 14.4 kDa. Panel E: pH profile of tetramer-monomer dissociation temperature (Tm) for rKcsA and KcsA CTD. For each pH, Tms from three independent experiments were determined. The results shown in this figure are given as mean +/- standard derivation (n = 3).

Oligomerization of rCTD at various pHs.

The observed contradicting contribution of the CTD to the stability of tetrameric rKcsA at pH 4.0 and 8.0 can be related to its modulating role in the open-closed switching of the channel. rKcsA is destabilized in the pH range where the gate is opened and stabilized by its CTD in the pH range where the gate is closed. This hypothetical role of the CTD requires it to oligomerize in a pH-dependent manner. We therefore constructed a His-tagged recombinant fragment of the CTD (residue 116 to 160, rHCTD) and expressed it in E coil. The expressed protein was purified to homogeneity as shown on 15% SDS-PAGE (Figure 2.3). After removal of the His-tag by thrombin digestion the mass of the recombinant CTD fragment (rCTD) was determined by mass-spectrometry to be 5729.0 Da, which is close to the predicted value of 5727.2 Da.

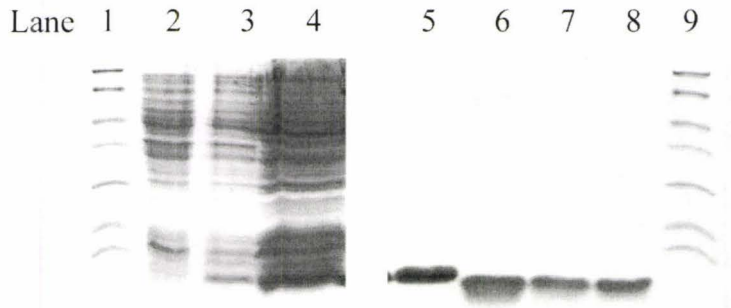

Figure 2.3 Overexpression and purification of rHCTD and rCTD analyzed on a 15% SDS-PAGE gel. Lanes 2 and 3: uninduced and induced cell cultures. Lane 4: supernatant of cell lysate after centrifugation. Lane 5: elution from Ni column. Lanes 6: after thrombin digestion. Lanes 7 and 8: elutions from Sep-pac C18 cartridge and Deltr-pac C18 column, respectively. Lanes 1 and 9 are molecular weight markers (from top to bottom: 116 kDa, 66.2 kDa, 45.0 kDa, 35.0 kDa, 25.0 kDA, 18.4 kDa and 14.4 kDa).

We used sedimentation equilibrium to monitor the apparent molecular weight of the rCTD at various pHs and the results are shown in Figure 2.4. When we fit the data to a single species model, the apparent molecular weights of the rCTD at acidic pHs of 4, 5 and 6 were 5049 ± 312, 5551 ± 373 and 5409 ± 298 Da (mean ± 95% confidence level generated by weighted function), respectively. These values were close to the expected

A

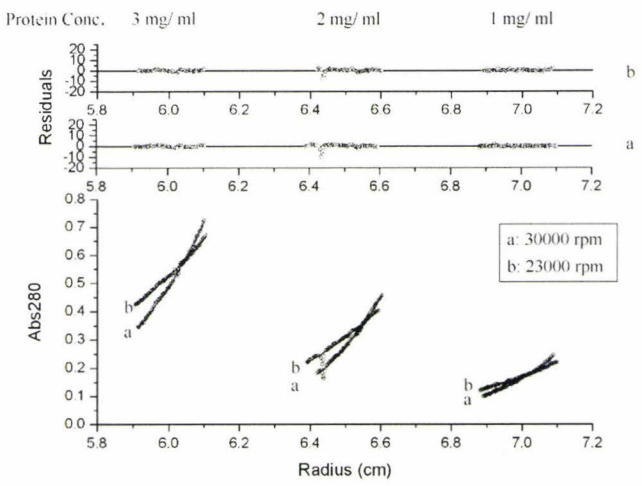

B

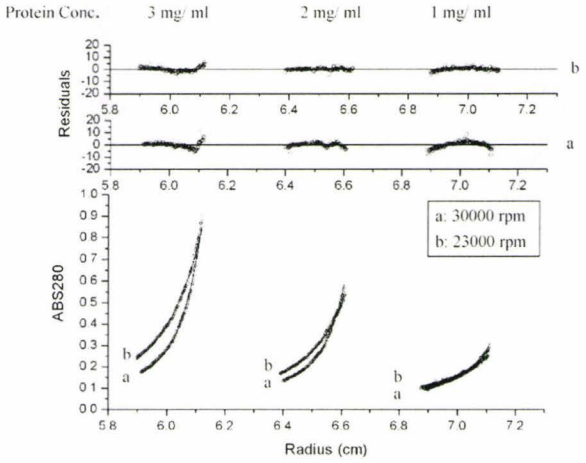

C

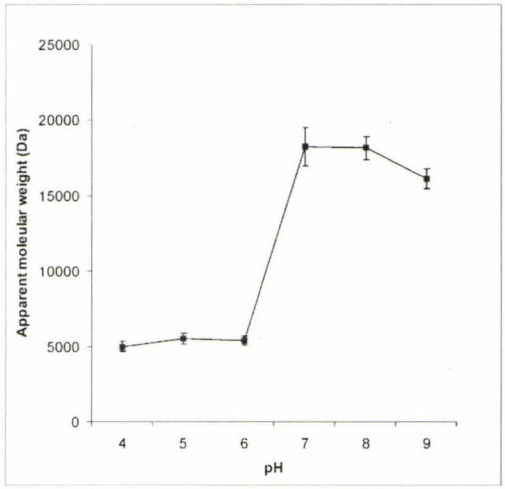

Figure 2.4 Molecular weight determination of rCTD by sedimentation equilibrium experiment at different pHs. Panel A and B: Composite absorbance scans of channels at equilibrium at pH 4 and pH 8, respectively. Data were fitted to a single species model. Residue plots are shown on the two top sub-panels. Circle and line represent experimental data and model predicted value, respectively. Panel C: Apparent molecular weight of rCTD at various pHs as determined by fitting all data sets to a single species model. Results shown in this figure are generated by the XL-A/ XL-I data analysis software (using weighted functions). The bars represent +/- 95% confidence levels.

mass of the rCTD in its monomeric form (5727.2 Da). The apparent molecular weight of the sample increased to about 17,000 Da at neutral and basic pHs (Figure 2.4 C). It was more than three times the molecular weight of a monomer at acidic pHs (e.g. 3 x 5409 Da). When the concentration of KCl was increased from 227 mM to 1.5 M, the apparent molecular weight increased and plateaued at 20,000 Da, which is close to that of a tetramer. Since rKcsA exists as homo-tetramer in nature, its CTD is likely to form tetramer. When we fit the data to monomer-tetramer, monomer-dimer-tetramer and monomer-trimer-tetramer models, all three models yielded similar Kd's for tetramer ($3.0*10^{-12}$ M^3). Since much higher Kd's for other oligomers (trimer: $1.2*10^4$ M^2, and dimer: $1.4*10^{12}$ M; data not shown) were obtained, the relative amount of these oligomers may be negligibly small.

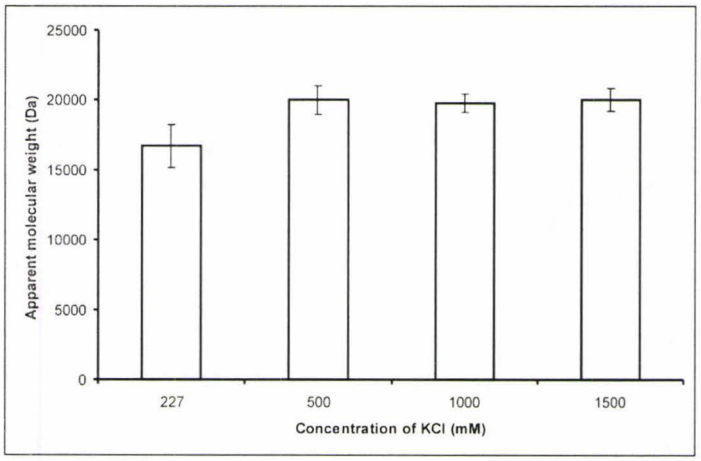

Figure 2.5 Apparent molecular weight of rCTD determined by sedimentation equilibrium experiment at different concentration of KCl at pH 8. The bars represent +/- 95% confidence levels.

2.4 DISCUSSION

Cortes et al. proposed that the CTD of KcsA may be involved in modulating the open-closed switching of the channel (81). Here, we examined this hypothesis by characterizing the biochemical and biophysical properties of the CTD. The primary structure of the CTD predicted that it is highly charged with a theoretical pI value around 10. About 44 percent of the CTD (22 out of 48 residues) are charged at neutral pH, with 12 positive and 10 negative residues, resulting in a theoretical net charge of about +2. Previous EPR studies showed close contacts amongst the CTDs at pH above neutral (81) despite its theoretical net charge of +2 indicating the existence of substantial attraction amongst the CTDs. One can imagine when the environment were acidified such that the net charge in this region is further increased, a stronger repulsion force will override the attraction force and prevent the CTDs to stay together. This pH/charge-based repulsion amongst the CTDs may contribute to channel opening while the attraction amongst the CTDs may contribute to the enhanced stability of the closed form as observed by Cortes et al. (81).

To test the hypothesis mentioned above, we measured the pH-dependent thermal stability of tetrameric KcsA and found that its denaturation profile was pH-dependent with close resemblance to the pH profile of its opening. The channel is more stable at neutral and basic pHs, where the gate of KcsA is mostly closed, than at acidic pHs where the gate opens (82,88). This close correlation between the denaturation and opening pH profiles suggest that factors that affect the stability of KcsA tetramer may also have an influence on channel opening. We therefore investigated the role of the CTD in gating by comparing the thermal stability of rKcsA and that of KcsA CTD at various pHs. We

found that the full-length channel is more stable than its CTD truncated counterpart at basic and neutral pHs presumably due to the extra contacts amongst the CTDs. Interestingly, the full-length channel is less stable than the CTD truncated form at acidic pH when the channel is supposed to be in its open state. This is in agreement with the hypothesis that the principal molecular interactions responsible for stabilizing the KcsA tetramer are contained within the transmembrance domain and the CTD is involved in modulating channel opening.

If gate opening and closing are modulated by the dissociation and association of the CTD as our data suggests, then the interactions between the CTDs have to be strong enough to stabilize its own oligomerization independent of other parts of the channel. We examined the oligomeric state of rCTD at various pHs by sedimentation equilibrium to determine whether rCTD alone was sufficient to form oligomer in a pH-dependent manner. As expected, we found that rCTD formed oligomer (probably tetramer) at basic pHs and no oligomer was detected at acidic pHs.

Taken together, our data supports the concept that interactions between the CTDs of rKcsA modulate gate opening and that the ionization state of residues within the CTD confers the pH-dependency of this process. The transition pH for the oligomerization of rCTD is about 2 pH units higher than the reported value for channel opening (82,88). This discrepancy may be due to the extra force required to pull the transmembrane domain apart and additional ionizable residues located at the CTD likely play a role in providing the required supplemental force.

We set out to determine the residues involved in the observed pH-dependent thermal stability of rKcsA. The transition pH for gating (pH 5.2 to 6.5; (81,82,88) and

oligomerization (pH 6.5) are close to the theoretical pKas of glutamic acid (4.25), aspartic acid (3.65) and histidine (6.00), which are abundant in the C-terminal domain (7 Glu, 3 Asp, 3 His). Amongst these three types of amino acid, the number of the histidines located in this region is the smallest and its theoretical pKa is close to the pH transition point for channel opening. Thus, the histidine residues (H124, H128 and H148) were chosen as targets for our mutation studies. Since removal of the last 20 residues from KcsA did not alter its pH-profile of opening whereas removal of the last 35 residues did (81), we only mutated H124 and H128. No observable changes to thermal stability of all mutants (H124A, H128A and H124A-H128A; data not shown) were detected. The pH-profiles of H124A in terms of gating as a full-length channel and oligomerization as a rCTD were also examined. Both profiles were the same as that of wild type (data not shown). These observations suggest that H124 and H128 are not the key residues in the pH-sensor and that other ionizible residues in the CTD may be responsible for the observed pH-dependent thermal stability. Nevertheless, our data provide compelling evidence to support that the pH-dependent oligomerization of the C-terminal domain plays a significant role in modulating the gating of KcsA in a pH-dependent manner.

2.5 MATERIALS AND METHODS

Material

Electrophoresis setups were purchased from BioRad Laboratories Ltd. (Ontario, Canada). All restriction enzymes, Taq polyermase, Pfu polymerase and T4 ligase were purchased from Fermentas Canada Inc. (Ontario Canada). HiTrap Chelating HP & HiTrap Heparin columns and pET28a were purchased from Amersham Biosciences Corp. (NJ, USA) and Novagen (CA, USA), respectively. Sep-pac Vac 12CC C18 Cartridge and

HPLC Delta-Pak C18 columns were purchased from Waters Corps (MA, USA). Thrombin was either purchased from Sigma-Aldrich Canada Ltd (Ontario, Canada) or purified from Thrombostat (Warner-Lambert Canada Inc., Ontario, Canada) with HiTrap Heparin column (89). 1-Palmitoyl-2-Oleoyl-*sn*-Glycero-3-Phosphoethanolamine (POPE) & 1-Palmitoyl-2-Oleoyl-*sn*-Glycero-3-[Phospho-*rac*-(1-glycerol)] (Sodium Salt) (POPG) and Specta/Por dialysis membrane with MWCO:3,500 & Viva spin concentrator with MWCO:50,000 were bought from Avanti Polar Lipid, Inc. (Al, USA) and VWR (Ontario, Canada), respectively. Other chemicals were purchased from Sigma-Aldrich Canada Ltd (Ontario, Canada).

Cloning of KcsA (rKcsA), C-terminal His tagged KcsA (chKcsA) & N-terminal His tagged rCTD of KcsA

The DNA coding for KcsA was amplified by PCR with Taq DNA polymerase (Fermentas) from pQE60/kcsa (A gift from Dr. MacKinnon) with an alanine inserted at the second position to form rKcsA and chKcsA (rKcsA & chKcsA forward primer, 5'GGTAACCATGGCTCCACCCATGCTGTCCGGTC3'; rKcsA reverse primer, 5'GCTAGAATTCCTATTACCGGCGGTTGTCGT3' and chKcsA reverse primer, 5'GATTACCTCGAGCCGGCGGTTGTCGTCGAG3'. NcoI, EcoRI and XhoI restriction enzyme recognition sites are underlined in the primer sequences). The amplified products were cloned into a pET28a expression vector (Novagen) at its respective restriction enzyme recognition sites.

The DNA coding for rCTD of KcsA (Residue 116 to 160) was also amplified by PCR from pQE60/kcsa (forward primer, 5'GGTAAGGATCCGGCCGGGAACAAGAGCGC3'

and reverse primer, 5'GCTAGAATTCCTATTACCGGCGGTTGTCGT3'. BamHI and EcoRI restriction enzyme recognition sites are underlined in the primer sequences). The amplified product was cloned into a modified pET28a expression vector (Novagen) using BamHI and EcoRI sites. The modified pET28a expression vector has a BamHI restriction enzyme recognition site incorporated into the thrombin recognition site's codons at the glycine and serine positions. Positive clones were selected by kanamycin. The plasmids for rKcsA, chKcsA and rCTD were sequenced (MOBIX, McMaster University) and named pET28a/rkcsa, pET28a/chkcsa and pET28a/hctd, respectively.

Overexpression of rKcsA and chKcsA

Overnight culture of BL21(DE3) transformed with either pET28a/rkcsa or pET28a/chkcsa was diluted 10 times with LB containing 100 μg/ml of kanamycin and incubated at 37°C. After one and a half hours, IPTG was added to the culture to a final concentration of 1 mM for induction. The culture was further incubated at 37°C for 3 hours. Cells were harvested by centrifuging the culture at 6,000 g for 15 minutes.

Purification of rKcsA - The cell pellet was resuspended in the lysis buffer (0.8% w/v NaCl, 0.04% w/v KCl, 0.12% w/v Na_2HPO_4, 0.04% w/v KH_2PO_4, 7.5 mM PMSF; pH7.4) and lysed by French press three times at 10,000 psi. The cell lysate was spun at 10,000 g for 60 minutes. rKcsA were purified from the pellet and the supernatant. rKcsA in the pellet was solubilized as follows: a) The pellet was resuspended in the binding buffer (see below) with ~0.8% w/v LDAO; b) the resuspension was incubated at room temperature with gentle mixing for one hour; c) the mixture was centrifuged at 100,000 g for 60 minutes at 22°C; d) the supernatant containing rKcsA was collected for further

purification. rKcsA in the supernatant of the low speed centrifugation (10,000 g) was further centrifuged at 100,000 g for 60 minutes at 22°C. rKcsA in this pellet was solubilized as previously stated. Solubilized rKcsA was purified using a HiTrap S column. The column was first equilibrated with binding buffer (25 mM Bicine, K^+; pH 8.0, 50mM KCl, 0.1% w/v LDAO) and the detergent solublized rKcsA was subsequently loaded onto the column. rKcsA was eluted with a linear gradient mixture of the binding buffer and elution buffer (25 mM Bicine, K^+; pH 8.0, 1.0 M KCl, 0.1% w/v LDAO). The protein came out at 0.2 M KCl.

Purification of chKcsA

The cell pellet was resuspended in the lysis buffer (20 mM Bicine, K^+; pH 8.0, 150mM KCl, 7.5 mM PMSF) and lysed by French press three times at 10,000 psi. The cell lysate was spun at 100,000 g for 60 minutes and chKcsA were solubilized by resuspending the pellet in lysis buffer with 1% w/v LDAO and incubating at room temperature with gentle mixing overnight. The mixture was centrifuged at 100,000 g for 60 minutes at 22°C and the supernatant was loaded onto a Ni^{2+} charged HiTrap Chelating HP column. The column was washed with the lysis buffer with 0.1% w/v LDAO and 0.05 M imidazole. The bound protein was eluted by increasing the concentration of imidazole to 0.15 M.

Chymotrypsin digestion of rKcsA and chKcsA

80 µl of chymotrypsin (0.1 mg/ml) was added to 4 ml of purified rKcsA or chKcsA (0.25 mg/ml) and incubated at 37°C for 2 hours. Subsequently, the reaction was

quenched by addition of 40 µl of 0.3M PMSF and further incubated for 30 minutes. Then, the sample was concentrated with Vivaspin concentrator (MWCO 50,000 Da) to a final volume of 1 ml. The rKcsA sample was used without further purification as KcsA CTD. The chKcsA sample was further purified by using a Ni^{2+} charged HiTrap Chelating HP column to remove the cleaved C-terminal domain as well as any uncleaved chKcsA to generate the C-terminal truncated KcsA (rctKcsA).

Reconstitution of rKcsA and rctKcsA in liposome and formation of giant liposome

Micellar solution of lipid-detergent (7.5 mg/ml POPE, 2.5 mg/ml POPG, 21 mg/ml CHAPS) in reconstitution buffer (450 mM KCl, 10 mM HEPES; pH 7.0) was prepared according to Heginbotham et al. (82,90). Purified rKcsA or rctKcsA was added to the micellar solution to a final concentration of 30-60 µg/ml. Mixture of lipid-detergent and rKcsA or chKcsA (1 ml) was dialyzed against reconstitution buffer (1 L) in a dialysis bag (MWCO of 3,500 Da) at room temperature for 12 hours with the buffer replaced once at the sixth hour. Liposomes containing rKcsA or rctKcsA were fused to form giant liposomes for electrophysiological studies according to the freeze-thaw method of Kasahara et al. (91). In brief, a glass culture tube with 0.5 mL of rKcsA or rctKcsA containing liposomes was put into liquid nitrogen for 2 minutes and thawed back to room temperature. This freeze-thaw cycle was repeated 5-6 times to produce giant liposomes.

Channel current measurement by cell-attached patch-clamp technique

All buffer solutions except the one at pH 7 contain 1 mM citric acid, 0.01 mM $CaCl_2$. The pHs (3.8, 4.7, 5.2 & 6.2) of each solution was adjusted by addition of KOH and KCl

to yield a final solution with exactly 100 mM [K^+]. The buffer solution at pH 7 contains 95 mM KCl, 5 mM KOH, 10 mM Hepes and 0.01 mM $CaCl_2$. The pH of this buffer was adjusted to 7 by addition of HCl.

5 µl of giant liposomes was deposited onto a petri dish (3.5 cm diameter) containing 200-300 µl of anchoring buffer (10 mM HEPES, 100mM KCl, 0.1 mM $CaCl_2$, pH 7.4). The petri dish was incubated at room temperature for 20 minutes to allow liposomes to anchor to the bottom of the dish. The petri dish was rinsed extensively using the pH 3.8 buffer to remove unanchored liposomes. Then, the pH 3.8 buffer was used as the bath solution.

The tip of a patch pipette containing a microelectrode and filled with the pH 3.8 buffer (10-20MΩ resistance for the open electrode) was apposed to an anchored liposome with the assistant of a micromanipulator to form a gigaseal (1-10GΩ) between the pipette and the liposome. 100 mV was applied across the gigaseal using a Model 2400 patch clamp amplifier (A-M System Inc, WA, USA) with the reference electrode sitting in the petri dish. Cell-attached current signal (filtered at 2 KHz) was sampled at a rate of 4096 Hz by a personal computer equipped with a USB-linked LabJack U12 DAQ device (LabJack Corporation, CO, USA). Different liposome would be patched if no channel activity were detected within thirty minutes. Cell-attached channel currents at different pHs were measured on the same liposome with the bath solution changed to corresponding buffers. The data set was analyzed using Molecular Devices pClamp 9.0 (Molecular Devices Corporation, CA, USA).

Thermal stability determination

200 µl samples of rKcsA and KcsA CTD were dialyzed in dialysis bags (MWCO 3,500 Da) at room temperature overnight against 200 ml solutions of 150 mM KCl, 0.1% v/v LDAO and 15 mM buffers (pH 3-6, K^+-citrate; pH 7, K^+-phosphate; pH8, K^+-Hepes). Two microlitre of thermal stability test solutions (10% w/v SDS, 9.3% w/v DTT and 38% w/v glycerol) were added to 8 µl of dialyzed samples and heated for 30 minutes at constant temperatures ranging from 30°C to 100°C at 10°C intervals. The heated samples were allowed to cool to room temperature and analyzed on 15% SDS PAGE. Scanned images of the gels were analyzed using ImageJ (program can be downloaded from *http://rsb.info.nih.gov/ij/*) in Integrated-Intensity-Mode to determine the amounts of tetramer and monomer in the samples. Fractional tetramer content was calculated by dividing the integrated density of tetramer by the combined integrated densities of tetramer and monomer. The thermal denaturation profiles (plots of fractional tetramer content vs temperature) for all pHs were analyzed to determine the temperatures at which half of the tetramers were dissociated (Tm) directly from the plot without curve fitting. Three independent experiments were performed for each pH and construct.

Overexpression and purification of His tagged rCTD, rHCTD

Procedures for overexpression of rHCTD and cell lysis were the same as those for rKcsA except that the *E. coli* BL21(DE3) was transformed with pET28a/hctd instead. Cell lysate was spun at 10,000 g and the supernatant was loaded onto a Ni^{2+} charged HiTrap Chelating HP column. The column was washed with the lysis buffer with the

addition of 0.1 M imidazole. The bound protein was eluted with 0.5 M imidazole in the lysis buffer.

Thrombin digestion of rHCTD and Purification of rCTD

Thrombin (144 units) was added to a 12 ml solution of purified rHCTD (1 mg/ml) and the reaction mixture was incubated at 37°C for 15 hours to remove the His-tag from the rHCTD. Then, the digested mixture was loaded onto a Sep-pac Vac 12CC C18 cartridge pre-equilibrated with 0.1% v/v trifluoroacetic acid. After sample loading, the cartridge was washed with 12 ml of 0.1% v/v trifluoroacetic acid and followed by 12 ml of 0.1% v/v trifluoroacetic acid in 20% v/v acetonitrile. rCTD was eluted from the cartridge by 12 ml of 0.1% v/v trifluoroacetic acid in 50% v/v acetonitrile. The eluted protein fraction was diluted three times with 0.1% v/v trifluoroacetic acid and rCTD was further purified using a Delta-Pak C18 column. The purified rCTD was lyophilized and analyzed on SDS PAGE. Its identity was confirmed by Mass spectrometry (McMaster Regional Center for Mass Spectrometry, McMaster University).

Oligomerization state determination of the rCTD

Sedimentation equilibrium experiments were performed on a Beckman Optima XL-I analytical ultracentrifuge (Beckman-Coulter, Palo Alto, CA) at 22°C. A cell with 6 channels of 12 mm optical path was used. The lyophilized rCTD was dissolved in water to a concentration of 10 mg/ml. The protein solutions of different concentrations (1, 2 and 3 mg per ml) at different pHs were prepared by adding KCl and corresponding buffers (pH 4-6, K^+-citrate; pH 7, K^+-phosphate/ Tris-HCl; pH 8-9, Tris-HCl. The citrate and

phosphate buffers were prepared by titrating citric acid and KH_2PO_4 against KOH to the desired pHs) to a final concentration of 227 mM KCl and 54 mM buffers. Sample channels were filled with 110 µl of protein solutions and the reference channels were loaded with 120 µl of corresponding solutions without protein. All runs were performed at two speeds: 23,000 and 30,000 rpm. Absorption profiles at 280nm of each centrifuged samples were collected after 17 and 19 hours of centrifugation. The absorption profiles at the two time points were compared to ensure equilibrium had been achieved. Absorption profiles were analyzed using the XL-A/ XL-I data analysis software (Beckman Coulter, CA). The partial specific volume of rCTD and the density of buffers were estimated with the program SEDNTERP (can be downloaded from www.jphilo.mailway.com/download.htm; (92).

2.6 REFERENCES

1. Clapham, D. E. (1998) *Nature structural biology* **5**(5), 342-344
2. Hille, B. (2001) *Ion Channels of Excitable Membrane*, 3rd Ed., Sinauer Associates, Inc, Sunderland, MA
3. Jiang, Y., Lee, A., Chen, J., Ruta, V., Cadene, M., Chait, B. T., and MacKinnon, R. (2003) *Nature* **423**(6935), 33-41
4. Long, S. B., Campbell, E. B., and Mackinnon, R. (2005) *Science* **309**(5736), 897-903
5. Jiang, Y., Lee, A., Chen, J., Cadene, M., Chait, B. T., and MacKinnon, R. (2002) *Nature* **417**(6888), 523-526
6. Ruta, V., and MacKinnon, R. (2004) *Biochemistry* **43**(31), 10071-10079
7. Liu, Y. S., Sompornpisut, P., and Perozo, E. (2001) *Nature structural biology* **8**(10), 883-887
8. Zagotta, W. N., Olivier, N. B., Black, K. D., Young, E. C., Olson, R., and Gouaux, E. (2003) *Nature* **425**(6954), 200-205
9. Cortes, D. M., and Perozo, E. (1997) *Biochemistry* **36**(33), 10343-10352
10. Schrempf, H., Schmidt, O., Kummerlen, R., Hinnah, S., Muller, D., Betzler, M., Steinkamp, T., and Wagner, R. (1995) *The EMBO journal* **14**(21), 5170-5178
11. Doyle, D. A., Morais Cabral, J., Pfuetzner, R. A., Kuo, A., Gulbis, J. M., Cohen, S. L., Chait, B. T., and MacKinnon, R. (1998) *Science* **280**(5360), 69-77
12. Zhou, Y., Morais-Cabral, J. H., Kaufman, A., and MacKinnon, R. (2001) *Nature* **414**(6859), 43-48
13. Noskov, S. Y., and Roux, B. (2006) *Biophysical chemistry* **124**(3), 279-291

14. Cortes, D. M., Cuello, L. G., and Perozo, E. (2001) *The Journal of general physiology* **117**(2), 165-180

15. Heginbotham, L., LeMasurier, M., Kolmakova-Partensky, L., and Miller, C. (1999) *The Journal of general physiology* **114**(4), 551-560

16. Li, J., Xu, Q., Cortes, D. M., Perozo, E., Laskey, A., and Karlin, A. (2002) *Proceedings of the National Academy of Sciences of the United States of America* **99**(18), 11605-11610

17. Iwamoto, M., Shimizu, H., Inoue, F., Konno, T., Sasaki, Y. C., and Oiki, S. (2006) *The Journal of biological chemistry* **281**(38), 28379-28386

18. Takeuchi, K., Takahashi, H., Kawano, S., and Shimada, I. (2007) *The Journal of biological chemistry*

19. Nordenman, B., and Bjork, I. (1977) *Thrombosis research* **11**(6), 799-808

20. Laue, T. M., Shah, B.D., Ridgeway, T.M., and Pelletier, S.L. (1992) *Analytical Ultracentrifugation*, The Royal Society of Chemistry, Cambridge, UK

21. Molina, M. L., Encinar, J. A., Barrera, F. N., Fernandez-Ballester, G., Riquelme, G., and Gonzalez-Ros, J. M. (2004) *Biochemistry* **43**(47), 14924-14931

22. Perozo, E., Cortes, D. M., and Cuello, L. G. (1999) *Science* **285**(5424), 73-78

23. Irizarry, S. N., Kutluay, E., Drews, G., Hart, S. J., and Heginbotham, L. (2002) *Biochemistry* **41**(46), 13653-13662

24. Heginbotham, L., Kolmakova-Partensky, L., and Miller, C. (1998) *The Journal of general physiology* **111**(6), 741-749

25. Kasahara, M., and Hinkle, P. C. (1977) *The Journal of biological chemistry* **252**(20), 7384-7390

Chapter 3

GCN4 Enhances the Stability of the Pore Domain of Potassium Channel KcsA

I wrote the manuscript and did the majority of all experiments except the following: Pau generated the clone of KcsA-GCN4; Yang supervised the project.

3.1 ABSTRACT

KcsA, a prokaryotic potassium channel, is the first channel that has a known crystal structure of the transmembrane domain. The crystal structure of its soluble C-terminal domain, however, still remains elusive. Biophysical and electrophysiological studies have previously implicated the essential roles of the C-terminal domain in pH sensing and *in vivo* channel assembly. We examined this functional assignment by replacing the C-terminal domain with an artificial tetramerization domain, GCN4-LI. The expression of KcsA is completely abolished when its C-terminal domain is deleted, but it can be rescued by fusion with GCN4-LI. The secondary and quaternary structures of the hybrid channel are very similar to those of the wild type channel according to circular dichroism and gel-filtration analyses. The thermostability of the hybrid channel at pH 8 is similar to that of the wild type but is insensitive to pH changes. This supports the notion that the pH sensor of KcsA is located in the C-terminal domain. Our result is in agreement with the proposed functions of the C-terminal domain and we show that the channel assembly role of the C-terminal domain can be substituted with a non-native tetrameric motif. Since tetramerization domains are found in different families of potassium channels and their

presence often enhances the expression of channels, replacement of the elusive C-terminal domains with a known tetrameric scaffold would potentially assist the expression of other potassium channels.

3.2 INTRODUCTION

Potassium channels selectively conduct potassium ions across the cell membrane and play a major role in membrane excitability (1). Most potassium channels are homo-tetramers, which compose a pore-forming domain that provides the passage for ions and regulatory domains that detect the presence of stimulants. Potassium channels can be classified based on the numbers of transmembrane helices (TM) and pore loops (P) within a monomeric unit. 2TM1P and 6TM1P are the two major classes, which can be represented by KcsA and Kv, respectively (1).

KcsA, a potassium channel from *Streptomyces lividans*, is the first ion channel which had its transmembrane domain structure determined by crystallography (2) (Figure 3.1 A). It can be structurally divided into an N-terminal helix, a transmembrane pore-domain and a C-terminal domain (Figure 3.1 B). The N-terminal helix has been proposed to be an amphiphilic helix lying on the membrane-cytoplasm interface (3,4); the transmembrane domain is the pore-forming part of the channel; the C-terminal domain is the regulatory domain that controls channel gating (3,5). The C-terminus is highly positively charged with a theoretical isoelectric point (pI) about 10, and its role in gating relies on its interaction with His-25 at the N-terminus (6,7). Previous *in vitro* studies showed that the C-terminal domain facilitates channel opening at pH<5 and closing at pH>7 (3,5,8-10). Nevertheless, since the native environment of KcsA in *Streptomyces lividans* can hardly

reach a pH as low as 4 (11), the physiological function of the C-terminal domain is still unclear.

Voltage-gated potassium (Kv) channels compose the largest family of potassium channels. All channels in this family contain a highly conserved sequence in the cytosolic N-terminal domain (12,13). This N-terminal domain by itself can spontaneously form a stable 4-fold tetramer and is referred to as the T1 domain (i.e. the first tetramerization domain). Its absence can significantly impair channel assembly (14-16). The tetramerizing function of the T1 domain was evidenced by a grafting study conducted by Zerangue and his colleagues (17), where they demonstrated that the assembly efficiency of a T1-deleted Kv can be fully restored by fusion with GCN4-LI, a 33-aa coiled-coil domain (Figure 3.1 A) which is capable of forming a parallel homo-tetramer (18). Since most potassium channels exist as tetramers, it is likely that they require tetramerization domain(s) to assist their assembly. Provided that KcsA shares a similar pore-forming domain with Kv and that the N-terminal helix of KcsA is very small and is spatially separated (thus not likely to play a role in tetramerization), there is a high chance that the C-terminal domain of KcsA would play a similar role as the T1 domain. Indeed, several studies on KcsA have implied the tetramerizing role of its C-terminal domain: our group has found that the C-terminal domain itself can form a tetramer *in vitro* at pH 7 or above (5), while Molina et al. have found that the C-terminal domain deleted KcsA cannot form tetramers *in vivo* like the wild type (19). Nevertheless, whether the lack of expression of the tetramer is caused by the absence of the tetramerization domain or by misfolding of the monomers before tetramer assembly can occur is still uncertain.

To examine the role of the C-terminal domain of KcsA, we generated wild type KcsA, C-terminus-deleted KcsA and KcsA-GCN4-LI hybrid constructs (for simplicity, GCN4-LI will be referred to as GCN4 for the remainder of this manuscript) (Figure 3.1 B). By comparing the protein expression level and stability of these constructs, we found that deletion of the C-terminus is detrimental to protein expression level and stability. We also found that the addition of GCN4 to the C-terminus-deleted KcsA could restore its expression level and its stability *in vitro*.

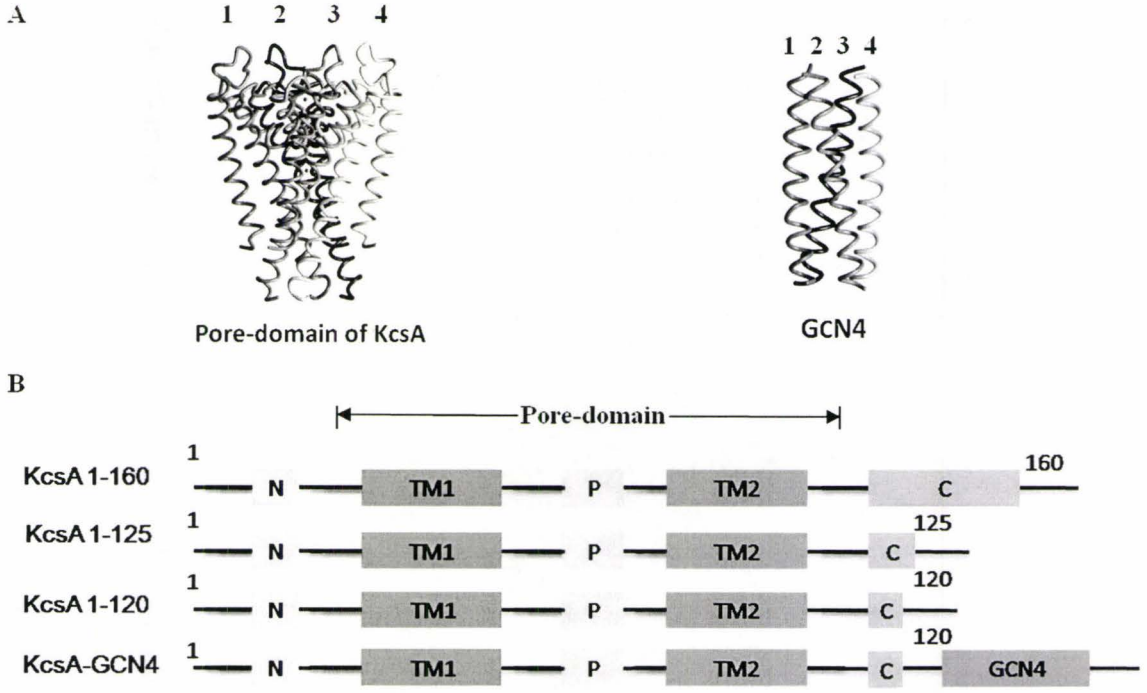

Figure 3.1 Design of KcsA constructs. (A) Crystal structure of pore-domain of KcsA (PDB ID: 1k4c) and GCN4 (PDB ID: 1gcl). Four subunits of KcsA and GCN4 are labeled 1, 2, 3, 4. (B) Schematic diagram of KcsA constructs. The numbers on this diagram represent the residue numbers of wild type KcsA counting from the N-terminus. Different domains of the channel are represented by different boxes: N, N-terminal helix; C, C-terminal domain; TM, transmembrane domain; P, P-loop.

Hence, our result is in agreement with the previous finding that deletion of the C-terminal domain of KcsA would impair the assembly of the channel *in vivo* (19). In addition, we also observed that the pH dependency disappeared in the KcsA-GCN4

hybrid construct, indicating that the pH-sensing domain of KcsA is located in its C-terminus. Based on our study, we conclude that the C-terminal domain of KcsA promotes channel assembly through its inherent tetramerization property and facilitates channel opening at low pH.

3.3 RESULT

Expression of different KcsA constructs

Recombinant KcsA 1-160 (wild type), KcsA 1-125, KcsA 1-120 and KcsA-GCN4 were expressed in *E.coli*. Protein expression levels of these constructs were examined by Western-blot analysis by using anti-His antibodies and they showed marked differences (Figure 3.2). While the yield of recombinant KcsA 1-125 was significantly less than that of the wild type, the expression of KcsA 1-120 was essentially negligible. However, the expression level of KcsA-GCN4 is about the same as the wild type.

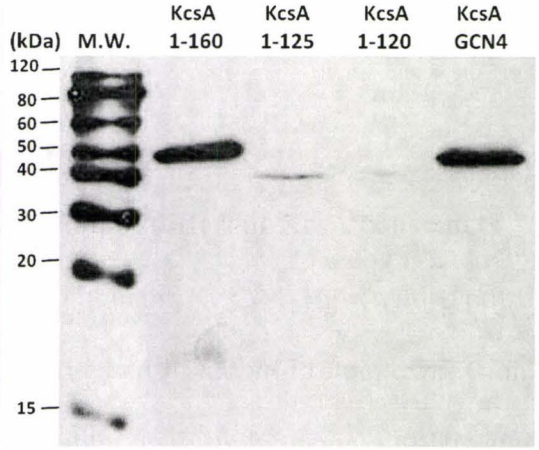

Figure 3.2 Western-blot analysis of KcsA constructs. Same amount of *E.coli* cells (quantified by OD_{600}) expressing different KcsA constructs were analyzed by 15% SDS-PAGE. KcsA was then identified by immunoblotting using an anti-His-tag antibody. The tetramer bands were quantified by densitometry by IMAGEJ (http://rsbweb.nih.gov/ij/). The ratio of intensities of KcsA 1-160, KcsA 1-125, KcsA-GCN4 is 9.7:1:10.

It was previously reported that residues 120-125 were crucial for the expression of tetrameric KcsA (19), and this protein segment was suggested to play a tetramerizing role. We wanted to investigate if an arbitrary sequence added on to the C-terminal end of the 1-120 construct would also enhance protein expression and therefore included a C-terminal His-tag to form the KcsA 1-120 construct. The addition of a C-terminal His-tag, however, did not rescue protein expression. Neither did the addition of an N-terminal His-tag rescue protein expression (data not shown). On the contrary, when an artificial tetramerization domain GCN4 was added to the C-terminal end of KcsA 1-120, the expression level was recovered. Similar effect was observed when GCN4 was added to the N-terminus of KcsA 1-120 (data not shown). It is worth mentioning that all constructs with observable expression level on Western-blot were found predominantly as SDS-resistant tetramers, which indicates that there is a strong correlation between protein expression level and tetramer stability.

Due to the low expression level of KcsA 1-125 and the lack of expression of KcsA 1-120, we decided to generate KcsA 1-125 for subsequent analysis via chymotrypsin digestion of the wild type channel according to a previously reported protocol (2,19). This construct is referred to as 'cdKcsA' (chymotrypsin digested KcsA).

Thermostabilities of KcsA constructs

To evaluate and compare the thermostabilities of KcsA 1-160, cdKcsA and KcsA-GCN4, a gel-shifting assay (3,5,19,20) that has been previously used to determine the effect of various mutations on the overall stability of KcsA was employed (Figure 3.3 A), and the dissociation temperatures (T_m's) at which a half of the tetrameric channels

dissociate into monomers in the presence of SDS at various pHs were determined for each construct. The thermostabilities of the wild type and mutant KcsA constructs were compared at basic and acidic pHs because the stability of KcsA depends on the pH of the solution: the tetrameric form of the wild type channel is more stable at basic than at acidic conditions (5).

At pH 8, the T_m of KcsA-GCN4 is higher than that of cdKcsA but lower than the T_m of KcsA 1-160 (Figure 3.3 B & D). This indicates that GCN4 stabilizes the tetrameric form of the channel although its stabilizing effect is not as strong as the wild type C-terminal domain. In contrast, the T_m's of KcsA-GCN4 and cdKcsA are very similar but are significantly higher than that of KcsA 1-160 at pH 4 (Figure 3.3 C & D). This result implies that the repulsive forces amongst the C-terminal domains of KcsA are stronger than those of GCN4 at pH 4. It is worth mentioning that the stability of KcsA-GCN4 at pH 4 was lower than that at pH 8, presumably due to an increase in the net positive charge attributable to protonation of multiple glutamates and histidines in GCN4 and the purification tag, respectively, at pH 4.

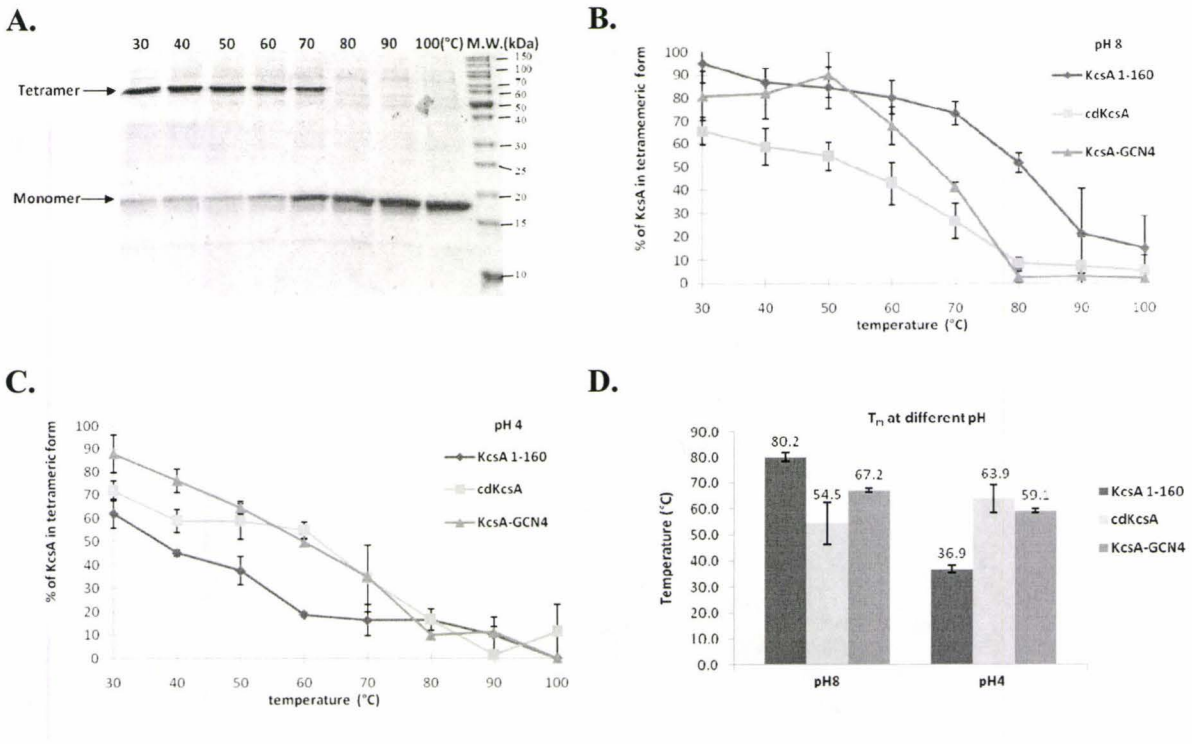

Figure 3.3 Thermostability determination of KcsA constructs. (A) Representative SDS-PAGE used in thermostability analyses (KcsA-GCN4 at pH 8). The tetramer and monomer bands of KcsA-GCN4 are indicated on the left side of the gel. The specific temperatures for heat treatment are indicated above the gel. (B and C) Comparison of stability of KcsA 1-160, cdKcsA and KcsA-GCN4 at different temperatures at pH 8 (B) and pH 4 (C). The fractional tetramer content in each sample was determined from the densitometry scans of SDS-PAGE. The results shown in panels B and C are given as mean±standard derivation (n = 3). (D) Comparison of T_m's of three KcsA constructs at pH 8 and pH 4. Each curve in panels B and C was fitted into the sigmoidal dose-responsive (variable-slope) model with $R^2 > 0.965$ by using GraphPad Prism software. The T_m values were calculated from the corresponding equations of the models.

Conformational states of KcsA constructs

To compare the folded states of KcsA-GCN4 and KcsA 1-160 in the absence of SDS, both samples were subjected to gel-filtration chromatography and circular dichroism analyses. Based on the result from chromatography analyses, we found that both constructs existed predominantly as tetramers in solution, albeit a small population of KcsA-GCN4 in a higher oligomeric state was also observed (Figure 3.4 A). As expected, KcsA-GCN4 displayed a circular dichroism spectrum that resembles that of an α-helical protein. The calculated helical content of KcsA-GCN4 based on this spectrum is slightly higher than that of the wild type channel (65% vs 62%, respectively; Figure 3.4 B). Very likely the increase of helical component is due to the high helical content of GCN4. The facts that KcsA-GCN4 can form a tetramer in solution and preserve a secondary structure profile similar to that of the wild type channel indicate that the folded state of KcsA-GCN4 is likely to be the same as the wild type KcsA 1-160.

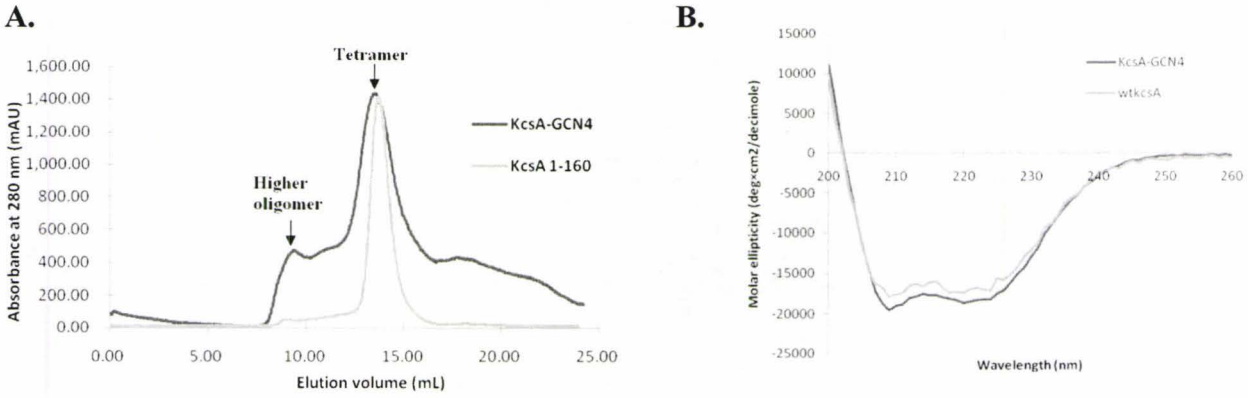

Figure 3.4 Biophysical characterization of KcsA constructs. (A) Chromatography profile of KcsA 1-160 and KcsA-GCN4 from size-exclusion column. The estimated molecular weights of the tetrameric LDAO-KcsA 1-160 and LDAO-KcsA-GCN4 micelles are 114 kDa and 127 kDa, respectively. (B) CD spectra of tetrameric KcsA 1-160 and KcsA-GCN4 in detergent LDAO. Estimated α-helical contents for KcsA 1-160 and KcsA-GCN4 are 62% and 65%, respectively.

Oligomerization state of KcsA-GCN4 after removal of GCN4 motif by chymotrypsin digestion

To determine if the tetramerization domain is only essential during initial channel assembly, we cleaved off GCN4 and the C-terminal domain from KcsA-GCN4 and KcsA 1-160, respectively after they were purified. The quaternary structures of the proteolytic products were then inspected. KcsA-GCN4 was designed to contain a TEV protease recognition site inserted between KcsA 1-120 and GCN4 such that GCN4 can be removed by the addition of TEV protease. However, the removal of GCN4 with TEV protease was not successful, presumably due to the inaccessibility of the protease to the cleavage site. Hence, chymotrypsin was used to generate the cleaved products from both constructs (2,19). Both digested products were identified to be SDS-resistant tetramers (Figure 3.5), indicating that the tetramerization domain is only required during initial assembly (i.e. immediately after channel expression *in vivo*).

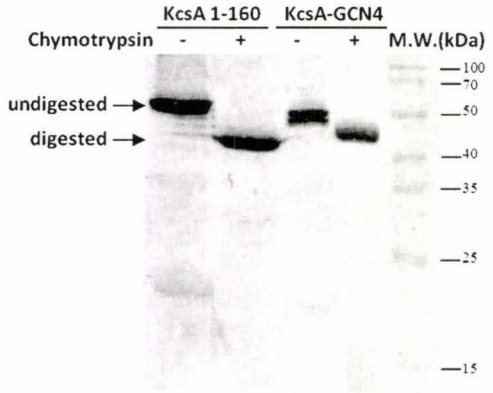

Figure 3.5 Chymotrypsin digestion of KcsA 1-160 and KcsA-GCN4. Labels on the top of the figure: -, protein samples before chymotrypsin digestion; +, protein samples after chymotrypsin digestion. The undigested and digested bands are indicated by arrows beside the gel.

3.4 DISCUSSION

Potassium channels are involved in many physiological processes, e.g. control of the excitability of membrane, release of neurotransmitter, regulation of osmotic pressure and regulation of the size of cell. Structural and functional understandings of these channels are therefore of paramount importance. However, studies of channels are often limited by their low expression level, and only very few channels have been expressed in sufficient quantities required for various studies. Overexpression of potassium channels has thus become the major hurdle to be overcome in this field. The C-terminal domain of KcsA was implicated to be important in its overexpression as well as in modulating channel opening (19). In this study, we clarified these dual functions of the C-terminal domain of KcsA.

The expression of KcsA was almost completely abolished when the last 40 residues of the channel were deleted. However, it could be rescued successfully by linking C-terminal domain deleted KcsA mutant to an artificial tetramerization domain, GCN4, which presumably reinforces the formation of KcsA tetramer by self-hybridizing into a tetrameric scaffold. The hybrid channel has similar properties as the wild type channel in terms of thermostability and secondary and quaternary structures. This result is consistent with our previous finding where the C-terminal domain itself was found to be capable of forming a tetramer (5) as well as a deletion study by Molina et al. (19), in which the sequence ERRGH (residues 120-124) was indicated to be a putative tetramerization domain. We showed that an artificial tetramerization domain can rescue the expression level of C-terminal domain deleted KcsA and the tendency of the channel to form tetramer during expression *in vivo* is highly correlated with its expression level.

The tetramer stability of potassium channel could be contributed by different parts of the channel, including N-terminal (12,21,22) and C-terminal (23-26) cytoplasmic domains as well as the transmembrane domain and the selectivity filter (8,14,27,28). Since the major subunit interactions mainly lie at the interface between the transmembrane domains, it is thus not surprising that the C-terminus-deleted KcsA generated by proteolytic digestion remains as a SDS-resistant tetramer. The poor expression of KcsA 1-120 is probably due to its poor efficiency of assembly *in vivo*. Based on the different expression levels of full length KcsA, KcsA 1-120 and KcsA-GCN4 (Figure 3.2), we speculate that channel assembly requires additional assistance from the cytoplasmic tetramerization domains (the C-terminal domain or GCN4). However, such assistance is not required for the molecule to stay as a tetramer once it is formed, as full length KcsA and KcsA-GCN4 hybrid could remain as a tetramer following chymotrypsin-mediated digestion. Hence, it is reasonable to suggest that the major *in vivo* function of the C-terminal domain in KcsA or GCN4 in KcsA-GCN4 hybrid is to facilitate channel assembly kinetically but not thermodynamically. We speculate the *in vivo* assembly pathway is like the following: First, monomeric channel subunits are inserted into the cell membrane; Then, tetramerization of the C-terminal domains brings the transmembrane domains in close proximity to each other to enhance their local concentration. In the end, the transmembrane domains form a stable tetramer (Figure 3.6).

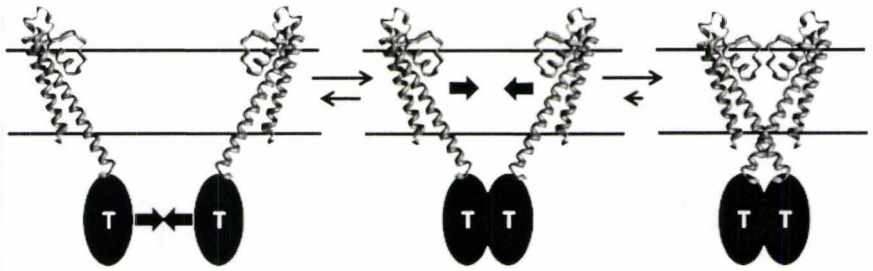

Figure 3.6 Mechanism of *in vivo* assembly of KcsA. Only two monomers are shown for clarity. Left panel: After translation and insertion of monomers into cell membrane, C-terminal tetramerization domain starts to interact with each other and bring subunits to the close vicinity. Middle panel: the association of C-terminal tetramerization domains increases the local concentration of KcsA monomers thus enhancing the rate of pore-domains assembly. Right panel: pore-domains finally associate and form tetrameric channel which is highly thermostable. T: tetramerization domain; thick arrows between different domains represent affinity forces; thin arrows among panels indicate the rate and direction of the assembly reaction.

The C-terminal domain of KcsA was also proposed to be a pH-sensing regulator. Cortes et al. (3) found that C-terminus-deleted KcsA displays less pH dependency in its opening probability than the wild type channel and they concluded that the C-terminal domain is involved in pH-dependent channel opening. Later studies by other groups then show that the pH-dependency of channel opening also involves His-25 in the N-terminal helix of KcsA (6,7). Here our data show that the stability of both constructs, cdKcsA and KcsA-GCN4, have much less response upon pH change compared to KcsA 1-160, indicating that part of the pH-sensing component of KcsA is located after residue 120.

On the other hand, GCN4 also displays some sensitivity upon pH change. From the thermostability analyses of our protein constructs, the T_m of KcsA-GCN4 at pH4 is 8°C less than that of KcsA-GCN4 at pH8. This observation agrees with the fact that GCN4 could be destabilized by lowering the pH level (29,30). Thus, GCN4 could act as a better tetramer stabilizer near neutral pH. Given that the intracellular environment is near neutral pH, GCN4 should be a very good candidate for assisting the expression of various tetrameric proteins, including other potassium channels.

Tetramerization domain is not unique to KcsA but is also present in various families of potassium channels – voltage-gated potassium channels, ERG (Ether-a-go-go) channels, Kir (potassium inwardly-rectifying) channels, calcium activated channels and CNG (cyclic nucleotide-gated) channels (12,13,16,31-36). Zerangue et al. previously showed that GCN4 can restore the functional expression of T1-deleted *Shaker* channel (17). Our current study indicates that although the 2TM1P channel KcsA is structurally different from the 6TM1P channel *Shaker*, they share similar property in terms of the dependency on tetramerization domain for channel assembly. Another common feature in these tetramerization domains is that most of them carry dual or even multiple functions instead of a single function. For examples, in addition to the self-tetramerizing property, the C-terminal domain of KcsA also serves as a pH-sensing modulator (3,5); the RCK (regulation of the conductance of K^+) domain of calcium-gated channel serves as a Ca^{2+}-sensing modulator (24,33,37); the C-terminal domain of CNG channel serves as a cyclic-nucleotide-sensing modulator (38,39); and the T1 domain of *Shaker* channel serves as a dock for auxiliary protein, i.e. an anchor for allocation to axonal locations as well as a modulator of gating activity (15,40-46). These tetramerization domains represent some of the best examples of how biological systems save energy by making good use of a small structure to accomplish multiple functions in the course of evolution.

To date, there are still many channels without a known tetramerization domain. We have conceived two possibilities: 1) they exist but are yet to be identified; 2) they do not exist. If the later is true, it could be one of the reasons to account for the low expression level of some particular channels. Through our findings in this report, we speculate that the expression yields of some of the hardly expressed ion channels can be significantly

improved by incorporating a non-native tetramerization domain at an appropriate site. Further examination of this hypothesis is thus warranted.

3.5 MSTERIALS AND METHODS

Constructs

The wild type KcsA construct (amino acid 1-160) was a gift from Dr. MacKinnon. The DNA sequence coding for KcsA 1-160, KcsA 1-125 and KcsA 1-120 were amplified from pQE60, which contains the wild type KcsA gene of *S. lividans*, by PCR using *Pfu* DNA polymerase (Fermentas), a forward primer for all three constructs (5′-GGTAACCATGGCTCCACCCATGCTGTCCGGTC-3′), and reverse primers specific for KcsA 1-160 (5′-GATTACCTCGAGCCGGCGGTTGTCG TCGAG-3′), KcsA 1-125 (5′-GATACTCTCGAGGAAGTGGCCCCGGCGCTC-3′) and KcsA 1-120 (5′-GATACTCTCGAGCTCTTG TTCCCGGCCGAC-3′). Note: NcoI and XhoI restriction enzyme recognition sites are underlined in the primer sequences. One extra alanine was introduced at the second position of KcsA in all three constructs in order to incorporate the recognition site for NcoI.

The KcsA-GCN4 construct containing KcsA 1-120, GCN4 and a TEV cleavage site as a linker between KcsA 1-120 and GCN4 was generated by fusion PCR technique (47). KcsA 1-120 was generated by PCR with the same forward primer as mentioned above and a reverse primer having the sequence of 5′-CCCTGAAAATACAGGTTTTC CTCTTGTTCCCGGCCGAC-3′ (overlapping sequence with the linker region is underlined). GCN4 and the TEV cleavage site were synthesized with a single synthetic oligonucleotide having the sequence of 5′-

GAAAACCTGTATTTTCAGGGCGGCACCCGCATGAAACAGATTGAGATAAACT GGAAGAAATTCTGAGCAAACTGTATCATATTGAAAACGAACTGGCGCGCATT AAAAAACTGCTGGGCGAACGC-3′ (DNA coding for linker region is underlined). The two halves of the gene were fused by PCR using the same forward primer for KcsA and a reverse primer having the sequence of 5′-GGACCGCTCGAG GCGTTCGCCCAGCAG-3′ (the recognition site of XhoI is underlined). All amplified products were digested with the corresponding restriction enzymes and cloned into the pET28 expression vector (Novagen) to generate the C-terminal 6-His constructs. The sequences of these plasmids were confirmed by dideoxynucleotide sequencing by MOBIX (a local university facility).

Protein Expression and Purification

E.coli BL21 (DE3) cells were transformed with the above constructs. Single colony was inoculated and grown in 100 mL LB (Luria Bertani) broth with 100 μg/mL kanamycin at 37°C overnight. The culture was then diluted 10 times with LB/kanamycin and further grown for 100 minutes. Expression of KcsA construct was induced by the addition of IPTG to a final concentration of 1 mM. Cells were pelleted after 3 hrs of incubation at 37°C, resuspended in lysis buffer (20 mM Tris, pH 8, 150 mM KCl, and 1 mM PMSF) and subsequently lysed by French Press at 10,000 psi. The cell lysate was centrifuged at 100,000 × g for 1 hr and the pellet was solubilized in 20 mL of 20 mM Tris, pH 8, 150 mM KCl, 1 mM PMSF and 1% v/v LDAO overnight at 4°C. The resuspended mixture was centrifuged at 100,000 × g for 1 hr and the supernatant was loaded onto a HiTrap Chelating HP column (Amersham Biosciences Corp.), which was

pre-equilibrated with the binding buffer containing 20 mM Tris, pH 8, 150 mM KCl, and 0.1% v/v LDAO. The column was washed with the binding buffer plus 0.05 M imidazole and the bound protein was eluted by increasing the final concentration of imidazole to 0.5 M. Purified proteins were analyzed by 15% SDS-PAGE with Coomassie blue staining and Western-blot by using an anti-His-tag antibody (Cell Signaling).

Chymotrypsin Digestion

Purified KcsA 1-160 was digested by chymotrypsin to generate cdKcsA (chymotrypsin digested KcsA). Specifically, the reaction was incubated at 37°C for 2 hrs with an enzyme:protein ratio of 1:100 (w/w). The reaction was quenched by the addition of PMSF to a final concentration of 3 mM. Digested product was purified by using a Ni^{2+} charged HiTrap Chelating HP column in order to remove the cleaved C-terminal domain as well as any uncleaved KcsA 1-160. Chymotrypsin digestion of the KcsA-GCN4 was conducted by the same method described here.

Thermostability Determination

Protein constructs KcsA 1-160, cdKcsA and KcsA-GCN4 were dialyzed overnight against the solution containing 150 mM KCl, 0.1% v/v LDAO, 20 mM Tris, pH 8 (or 15 mM potassium citrate, pH 4) in dialysis bags with a MWCO of 3,500 Da. Dialyzed samples were mixed with the loading solution containing 10% w/v SDS, 9.3% w/v DTT and 38% w/v glycerol (a modified loading solution that renders the pH of the samples unchanged), heated for 30 minutes at various temperatures ranging from 30°C to 100°C with the increment of 10°C interval, cooled to room temperature and analyzed by 15%

SDS PAGE. Three independent experiments were performed for each pH and construct. Scanned images of the gels were analyzed by using ImageJ (http://rsb.info.nih.gov/ij/) in Integrated-Intensity-Mode to determine the amounts of tetramer and monomer in the samples. Fractional tetramer content was calculated by dividing the integrated density of tetramer by the combined integrated densities of tetramer and monomer. Model fitting of the thermal denaturation curves was carried out by using Prism 4.00 (GraphPad software).

Gel-filtration Chromatography

Gel-filtration chromatography was run on a FPLC system (Amersham Biosciences Corp.) by using a Superdex 200 column (Amersham Biosciences Corp.) equilibrated in 50 mM Tris buffer, pH 8, 150 mM KCl and 0.1% v/v LDAO.

Circular Dichroism measurement

10 μM (monomeric protein concentration) protein samples were dissolved in 20 mM K_2HPO_4, pH 8, 150 mM KCl and 0.1% v/v LDAO. CD spectra of the samples were recorded in a 0.1 cm path length cell at 25°C by using a 410 circular dichroism spectrometer (AVIV Biomedical Inc.). The secondary structure content of each sample was quantified by using the CD spectrum analysis program CDSSTR of the CDPro suite (http://lamar.colostate.edu/~sreeram/CDPro/main.html).

3.6 REFERENCES

1. Hille, B. (2001) *Ion Channels of Excitable Membrane*, Sinauer Associates, Inc, Sunderland, MA
2. Doyle, D. A., Morais Cabral, J., Pfuetzner, R. A., Kuo, A., Gulbis, J. M., Cohen, S. L., Chait, B. T., and MacKinnon, R. (1998) *Science* **280**, 69-77
3. Cortes, D. M., Cuello, L. G., and Perozo, E. (2001) *J Gen Physiol* **117**, 165-180
4. Li, J., Xu, Q., Cortes, D. M., Perozo, E., Laskey, A., and Karlin, A. (2002) *Proc Natl Acad Sci U S A* **99**, 11605-11610
5. Pau, V. P., Zhu, Y., Yuchi, Z., Hoang, Q. Q., and Yang, D. S. (2007) *J Biol Chem* **282**, 29163-29169
6. Takeuchi, K., Takahashi, H., Kawano, S., and Shimada, I. (2007) *J Biol Chem*
7. Thompson, A. N., Posson, D. J., Parsa, P. V., and Nimigean, C. M. (2008) *Proc Natl Acad Sci U S A* **105**, 6900-6905
8. Irizarry, S. N., Kutluay, E., Drews, G., Hart, S. J., and Heginbotham, L. (2002) *Biochemistry* **41**, 13653-13662
9. Heginbotham, L., LeMasurier, M., Kolmakova-Partensky, L., and Miller, C. (1999) *J Gen Physiol* **114**, 551-560
10. Cuello, L. G., Romero, J. G., Cortes, D. M., and Perozo, E. (1998) *Biochemistry* **37**, 3229-3236
11. Corvini, P. F., Gautier, H., Rondags, E., Vivier, H., Goergen, J. L., and Germain, P. (2000) *Microbiology* **146 (Pt 10)**, 2671-2678
12. Li, M., Jan, Y. N., and Jan, L. Y. (1992) *Science* **257**, 1225-1230

13. Shen, N. V., Chen, X., Boyer, M. M., and Pfaffinger, P. J. (1993) *Neuron* **11**, 67-76

14. Tu, L., Santarelli, V., Sheng, Z., Skach, W., Pain, D., and Deutsch, C. (1996) *J Biol Chem* **271**, 18904-18911

15. Deutsch, C. (2002) *Annu Rev Physiol* **64**, 19-46

16. Kreusch, A., Pfaffinger, P. J., Stevens, C. F., and Choe, S. (1998) *Nature* **392**, 945-948

17. Zerangue, N., Jan, Y. N., and Jan, L. Y. (2000) *Proc Natl Acad Sci U S A* **97**, 3591-3595

18. Harbury, P. B., Zhang, T., Kim, P. S., and Alber, T. (1993) *Science* **262**, 1401-1407

19. Molina, M. L., Encinar, J. A., Barrera, F. N., Fernandez-Ballester, G., Riquelme, G., and Gonzalez-Ros, J. M. (2004) *Biochemistry* **43**, 14924-14931

20. Perozo, E., Cortes, D. M., and Cuello, L. G. (1999) *Science* **285**, 73-78

21. Shen, N. V., and Pfaffinger, P. J. (1995) *Neuron* **14**, 625-633

22. Strang, C., Cushman, S. J., DeRubeis, D., Peterson, D., and Pfaffinger, P. J. (2001) *J Biol Chem* **276**, 28493-28502

23. Fujiwara, Y., and Minor, D. L., Jr. (2008) *J Mol Biol*

24. Jiang, Y., Lee, A., Chen, J., Cadene, M., Chait, B. T., and MacKinnon, R. (2002) *Nature* **417**, 515-522

25. Dong, J., Shi, N., Berke, I., Chen, L., and Jiang, Y. (2005) *J Biol Chem* **280**, 41716-41724

26. Howard, R. J., Clark, K. A., Holton, J. M., and Minor, D. L., Jr. (2007) *Neuron* **53**, 663-675

27. Heginbotham, L., Odessey, E., and Miller, C. (1997) *Biochemistry* **36**, 10335-10342

28. Krishnan, M. N., Trombley, P., and Moczydlowski, E. G. (2008) *Biochemistry* **47**, 5354-5367

29. Moran, L. B., Schneider, J. P., Kentsis, A., Reddy, G. A., and Sosnick, T. R. (1999) *Proc Natl Acad Sci U S A* **96**, 10699-10704

30. Steinmetz, M. O., Jelesarov, I., Matousek, W. M., Honnappa, S., Jahnke, W., Missimer, J. H., Frank, S., Alexandrescu, A. T., and Kammerer, R. A. (2007) *Proc Natl Acad Sci U S A* **104**, 7062-7067

31. Jenke, M., Sanchez, A., Monje, F., Stuhmer, W., Weseloh, R. M., and Pardo, L. A. (2003) *The EMBO journal* **22**, 395-403

32. Tinker, A., Jan, Y. N., and Jan, L. Y. (1996) *Cell* **87**, 857-868

33. Jiang, Y., Pico, A., Cadene, M., Chait, B. T., and MacKinnon, R. (2001) *Neuron* **29**, 593-601

34. Quirk, J. C., and Reinhart, P. H. (2001) *Neuron* **32**, 13-23

35. Schmalhofer, W. A., Sanchez, M., Dai, G., Dewan, A., Secades, L., Hanner, M., Knaus, H. G., McManus, O. B., Kohler, M., Kaczorowski, G. J., and Garcia, M. L. (2005) *Biochemistry* **44**, 10135-10144

36. Zhou, L., Olivier, N. B., Yao, H., Young, E. C., and Siegelbaum, S. A. (2004) *Neuron* **44**, 823-834

37. Ptak, C. P., Cuello, L. G., and Perozo, E. (2005) *Biochemistry* **44**, 62-71

38. Young, E. C., and Krougliak, N. (2004) *J Biol Chem* **279**, 3553-3562

39. Trudeau, M. C., and Zagotta, W. N. (2002) *Proc Natl Acad Sci U S A* **99**, 8424-8429

40. Shi, G., Nakahira, K., Hammond, S., Rhodes, K. J., Schechter, L. E., and Trimmer, J. S. (1996) *Neuron* **16**, 843-852

41. Yu, W., Xu, J., and Li, M. (1996) *Neuron* **16**, 441-453

42. Gulbis, J. M., Zhou, M., Mann, S., and MacKinnon, R. (2000) *Science* **289**, 123-127

43. Gu, C., Jan, Y. N., and Jan, L. Y. (2003) *Science* **301**, 646-649

44. Cushman, S. J., Nanao, M. H., Jahng, A. W., DeRubeis, D., Choe, S., and Pfaffinger, P. J. (2000) *Nature structural biology* **7**, 403-407

45. Minor, D. L., Lin, Y. F., Mobley, B. C., Avelar, A., Jan, Y. N., Jan, L. Y., and Berger, J. M. (2000) *Cell* **102**, 657-670

46. Kurata, H. T., Soon, G. S., Eldstrom, J. R., Lu, G. W., Steele, D. F., and Fedida, D. (2002) *J Biol Chem* **277**, 29045-29053

47. Shevchuk, N. A., Bryksin, A. V., Nusinovich, Y. A., Cabello, F. C., Sutherland, M., and Ladisch, S. (2004) *Nucleic Acids Res* **32**, e19

Chapter 4

An Engineered Right-handed Coiled-coil Domain Imparts Extreme Thermostability to the KcsA Channel

Reproduced in part with permission from [Zhiguang Yuchi, Victor P. T. Pau Bridget X. Lu, Murray Junop and Daniel S. C. Yang (2009). An Engineered Right-handed Coiled-coil Domain Imparts Extreme Thermostability to the KcsA Channel *FEBS J,* **accepted**]

I wrote the manuscript and did the majority of all experiments except the following: Pau generated the clone of KcsA-RHCC; Lu did part of the electrophysiological experiments; Junop assisted and supervised the gel-filtration experiments; Yang supervised the project.

4.1 ABSTRACT

KcsA, a potassium channel from Streptomyces lividans, is the first ion channel which had its transmembrane domain structure determined by crystallography. Previously, we demonstrated that its C-terminal cytoplasmic domain is crucial for the thermostability and expression of the channel. Expression was almost abolished in its absence but could be rescued by the presence of an artificial left-handed coiled coil tetramerization domain GCN4. In this study, we noticed that the handedness of GCN4 is not the same as the bundle crossing of KcsA. We identified a compatible right-handed coiled coil structure, RHCC, from the Protein Data Bank and used it to replace the C-terminal domain of KcsA. The hybrid channel exhibited higher expression level than the wild type and it is extremely thermostable. Surprisingly, this stable hybrid channel is equally active as the wild type channel in conducting potassium ions through lipid bilayer at acidic pH. We suggest similar engineering strategy could be applied to other ion channels for both functional and structural studies.

4.2 INTRODUCTION

Tetrameric architecture is a common character shared by cation channels, including K^+, Na^+, Ca^{2+}, non-selective, glutamate-gated, cyclic nucleotide-gated, transient receptor potential (Trp) channels, and other ion channels (1,2). Although they differ from each other in terms of

selectivity and physiological activator, they all have to organize to a tetrameric arrangement in order to be functional. The ion conducting function is fulfilled by a central ion-conducting pore composed of selectivity filters and α-helices arranged in 4-fold or pseudo 4-fold symmetry.

Most potassium channels form homo-tetramers. Several different cytoplasmic tetramerization domains have been found to be important for proper channel assembly. For example, T1, a N-terminal tetramerization domain is used by the Kv channel while C-terminal tetramerization domains are used by EAG (Ether-a-go-go) channels, Kir (potassium inwardly-rectifying) channels, calcium activated channels and CNG (cyclic nucleotide-gated) channels (3-11).

Despite different families of K^+ channels are structurally similar and often co-expressed in the same cell type, they seldom mix with each other to form hetero-tetramers (12,13). This important intra-family recognition is also carried out by the tetramerization domains. For example, the specificity of T1 determines the compatibility of channels from different families during Kv channel assembly (3,5,13-19). It was also shown that the replacement of the T1 domain of DRK1 channel with the corresponding domain from a distantly related Drosophila Shaker B (ShB) channel allowed the hybrid DRK1 channel to coassemble with the ShB channel (5).

KcsA, a potassium channel from *Streptomyces lividans*, is a good model for investigating the working mechanism of potassium channels since it has a relatively simple structure but contains most typical components of potassium channels. It has been proposed that the C-terminal domain of KcsA acts as a tetramerization domain (20-22). This domain can self-associate to form stable tetramer (20) and its presence is required for proper expression of tetrameric KcsA (21). This domain could be replaced by an artificial tetramerization domain GCN4-LI (23) without affecting the expression of functional channel, however the thermostability of the hybrid channel is slightly diminished (22). In order to determine the cause of the reduced thermostability we

inspected the crystal structure of GCN4-LI and KcsA. We found the GCN4-LI forms a left-handed coiled coil but the bundle crossing on KcsA is a right-handed coiled coil. We hypothesized that the splicing of two different handed coiled coil structures may be the culprit of the reduction in thermostability.

In this study we set out to pursue a more stable hybrid channel of KcsA for structural studies. We chose to use RHCC, a right-handed coiled coil (24), to replace the C-terminal domain of wild type KcsA. The hybrid channel, KcsA-RHCC, was computationally designed to form a continuous right-handed coiled coil at the bundle crossing. As expected, this hybrid channel was expressed at higher level than the wild type channel in *E. coli* and exhibited extreme *in vitro* thermostability. It remained mainly as tetramer even after prolonged treatment at 100°C in the presence of SDS. Surprisingly, this stable hybrid channel without the native pH sensor domain could still sense pH change and conduct potassium ions.

One of the reasons for the scarcity of structural data on channels is their relatively low protein expression level. Since tetramer stabilities of Kv and KcsA had been found to correlate with their expression level (22,25), a better tetramerization construct by protein engineering may assist channel expression. Besides protein expression level, inter-domain flexibility is another reason for the scarcity of structural data because of their negative effects on the diffraction quality of protein crystals. Therefore the replacement of original flexible inter-domain linker by a rigid continuous coiled coil should facilitate the structure determination of ion channels. We propose that similar engineering effort may be applicable to other ion channels to assist their expression as well as structural and functional studies.

4.3 RESULTS

Computational design of KcsA-RHCC

The hybrid channel KcsA-GCN4 previously reported by our lab is composed of a transmembrane domain of KcsA (residues 1-120) linked to a left-handed coiled coil GCN4-LI (pdb code: 1GCL) (23) with a linker containing a TEV recognition sequence (22) (Figure 4.1 A & B). In this study, we examined the effect of coiled coil handedness of the tetramerization domain on the stability of KcsA. Four tetrameric coiled coils were selected for this testing: $NSP4_{95-137}$ (pdb code: 1G1I) (26), RH4B (pdb code: 2O6N) (27), VASP TD (pdb code: 1USE) (28) and RHCC (pdb code: 1FE6) (24). $NSP4_{95-137}$ is the coiled coil domain of a virally-encoded receptor (26). RH4B is a *de novo* designed 33-residue peptide comprising three 11-residue repeats, which can form a stable, right-handed parallel tetrameric coiled coil (27). VASP TD is a 45-residue tetramerization domain from human vasodilator-stimulated phosphoprotein, a key regulator of actin dynamics (28). RHCC is a naturally occurring parallel right-handed coiled coil tetramer found in the surface layer protein tetrabrachion from *Staphylothermus marinus* (24). All of them display as winding of the supercoil in a right-handed fashion except $NSP4_{95-137}$, which forms left-handed coiled coil.

In our initial trials, we simply replaced the GCN4 fragment in KcsA-GCN4 with RH4 or RHCC and kept the linker between KcsA pore domain and the tetramerization domain. Both constructs showed similar expression level and thermostability as KcsA-GCN4 (data not shown). Since no obvious improvement was observed, we suspected that the linker between the transmembrane domain and the tetramerization domain may impair the cooperative effect on the assembly of these two domains. Thus, new attempts were made to build a continuous coiled coil structure without intervening flexible linker. Since crystal structures of KcsA and all selected

tetramerization domains are available, we decided to structurally align the inner helices of KcsA with the foreign coiled coils. Among the four tetramerization domains, RHCC displays the smallest RMS deviation when compared to the other three coiled coils (Table 4.1). The top ranking hybrid structures of KcsA-RHCC (Figure 4.2) were modeled and Monte Carlo minimized by program ZMM-MVM. The result shows that RHCC (residues 16-55) could be best spliced onto KcsA (residues 23-115) (Figure 4.1 A & B). This chimeric channel was cloned with N-terminal his-tag and named KcsA-RHCC.

Coiled coils / RMS Ranking	NSP4 95-137	RH4B	VASP TD	RHCC
1	1.859	1.143	0.862	0.619
2	1.929	1.202	0.891	0.709
3	2.032	1.221	0.894	0.774
4	2.095	1.259	0.898	0.838
5	2.12	1.274	0.911	0.871

Table 4.1 RMS deviations of overlapping atoms at splice junctions from structural alignments between KcsA inner helices and four coiled coil structures output by Program FitHelices. Five constructs with the smallest RMS are listed for each coiled coil structures. The unit is in angstrom.

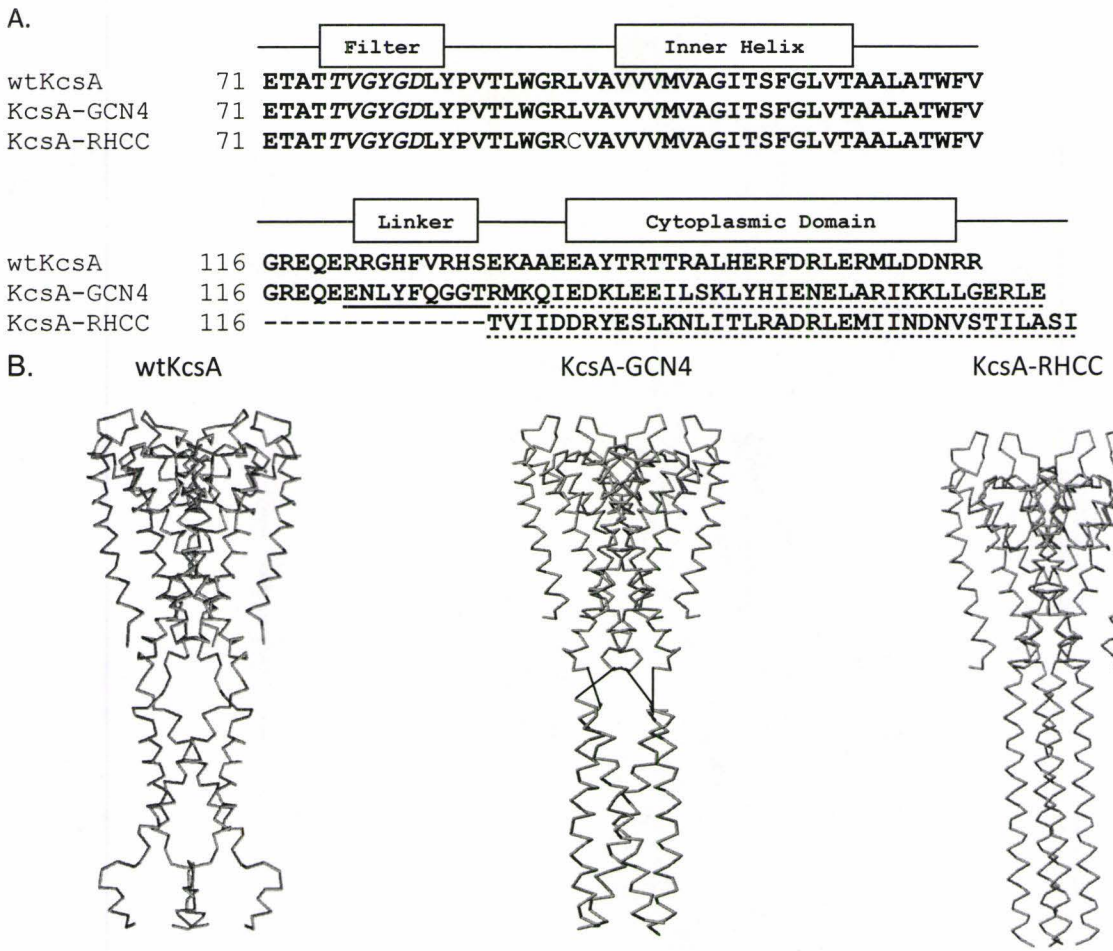

Figure 4.1 (A) Partial sequence alignment of wtKcsA, KcsA-GCN4 and KcsA-RHCC. The alignment starts at conserved selective filter sequence (in Italic) and ends at the ends of C-terminal tetramerization domains. The different structural domains are indicated by the bars above the protein sequence. The linker between KcsA pore-domain and GCN4 is underlined. The tetramerization peptides GCN4 and RHCC are dotted underlined. (B) Models of wtKcsA, KcsA-GCN4 and KcsA-RHCC. The PDB files used in these models are: 3EFF (29) for full length wtKcsA; 1K4C (30) for the pore domain of KcsA in KcsA-GCN4 and KcsA-RHCC; 1GCL (23) for GCN4; 1FE6 (24) for RHCC. The model of KcsA-RHCC was calculated by structural alignment and followed by iterative energy minimization (see results for details). The pictures of three models are generated by program ZMM-MVM.

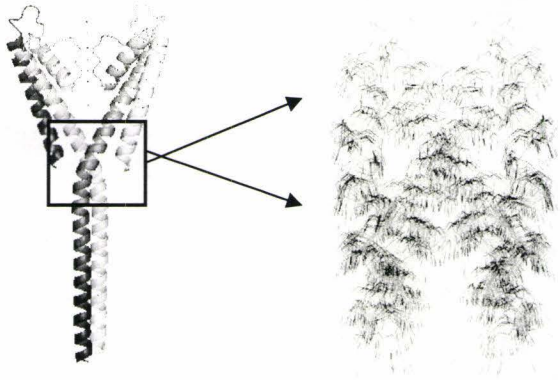

Figure 4.2 Splicing of KcsA and RHCC. The left picture shows the model of KcsA-RHCC. Only two subunits are shown for clarity. The area enclosed by the square is where different splicing motifs are tested *in silico*. It is displayed on the right in enlarged format showing overlaps of different spliced structures.

Expression and purification of KcsA-RHCC

Recombinant KcsA-RHCC was expressed in *E.coli*. The yield is about 1.5 mg/L. Previously we found that deletion of the C-terminal domain (residue 121-160) almost completely abolished the expression of wtKcsA but the addition of an artificial tetramerization domain GCN4 rescued the expression to wild type level. KcsA-RHCC can reach higher expression level than wtKcsA. The protein was purified to homogeneity by using a HisTrap^{TM} HP column (Figure 4.3).

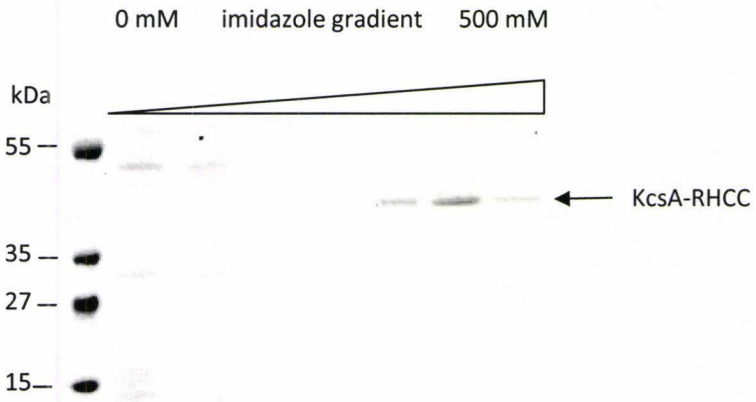

Figure 4.3 Purification of KcsA-RHCC by HisTrap^{TM} HP column. Proteins samples were run on 4-12% SDS-PAGE and stained with Commassie Blue. There was increasing amount of imidazole for the elution of protein samples from the column present in the lanes from left to right. Arrows indicates the position of purified KcsA-RHCC protein.

Biophysical characterization

The secondary and quaternary structures of KcsA-RHCC were characterized by circular dichroism (CD) and gel-filtration chromatography (GFC) respectively. The CD data shows that KcsA-RHCC is slightly more α-helical than the wtKcsA (64% vs 62%, respectively; Figure 4.4 A). This is not surprising because RHCC existed predominantly as an α-helix in its crystallized form. The GFC data shows that the majority of KcsA-RHCC is in tetrameric form while a very small portion of it is in higher oligomeric form. This is very similar to that of wtKcsA (Figure 4.4 B). Taken together, these two results indicated that the gross biophysical nature of KcsA is not altered by the addition of RHCC.

A.

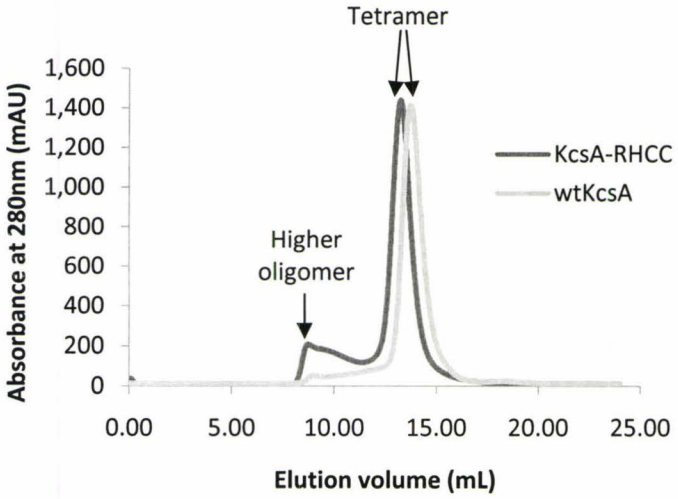

B.

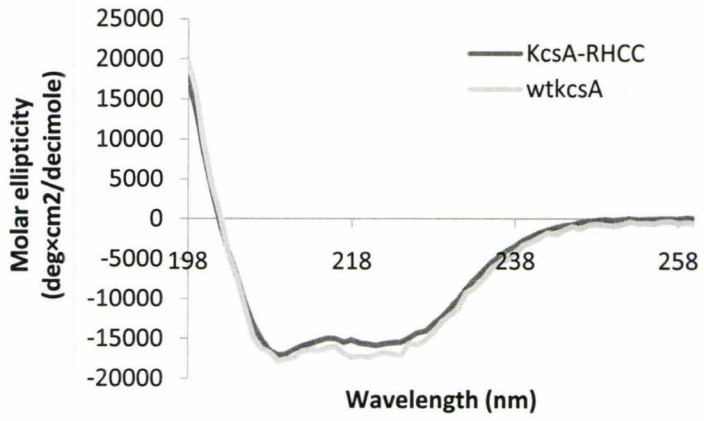

Figure 4.4 Biophysical characterization of KcsA-RHCC. (A) Elution profile of wtKcsA and KcsA-RHCC from gel-filtration chromatography column. The estimated molecular weights of the tetrameric LDAO-wtKcsA and LDAO-KcsA-RHCC micelles are 114 kDa and 149 kDa, respectively. (B) CD spectra of tetrameric wtKcsA and KcsA-RHCC in LDAO. Estimated α-helical contents for wtKcsA and KcsA-RHCC are 62% and 64%, respectively.

Thermostability test

The thermostability of wtKcsA, cdKcsA, KcsA-GCN4, KcsA-RHCC and RHCC were compared by gel-shift assay. Tetrameric KcsA is very stable and displays properties of SDS-resistant and heat-resistant. Thermostability in the presence of SDS is generally used to indicate the stability of ion channels (20-22,31,32). It is usually reported as the temperature at which half of the tetrameric channels dissociate into monomers (Tm). At pH 8, the order of thermostability of the various constructs is KcsA-RHCC > wtKcsA > KcsA-GCN4 > cdKcsA ≈ RHCC (Figure 4.5 A & C). Clearly, the continuous coiled coil in KcsA-RHCC provided a strong tetramerization force, as indicated by its ultra high Tm value which is much higher than 100°C. However, when two parts of KcsA-RHCC, namely, cdKcsA and RHCC, were tested individually, both of them display relatively low Tm, suggesting the high stability of KcsA-RHCC is the result of cooperative effect. At pH4, the order of thermostability is KcsA-RHCC > cdKcsA > KcsA-GCN4 > wtKcsA > RHCC (Figure 4.5 B & C). All constructs except cdKcsA show a decrease in Tm upon pH change from 8 to 4, showing all three tetramerization domains are somewhat sensitive to pH change. The pH effect on wtKcsA is well documented; however the acid labile nature of wild type RHCC is not known until this investigation. The acid labilities of GCN4 and RHCC may be due to the weakening of intra- and/or inter-helical salt bridges that stabilize their respective coiled coil structures (23,24).

A.

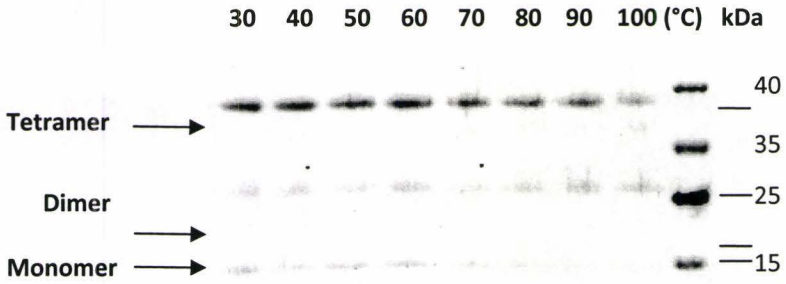
30 40 50 60 70 80 90 100 (°C) kDa
Tetramer
Dimer
Monomer
40
35
25
15

B.

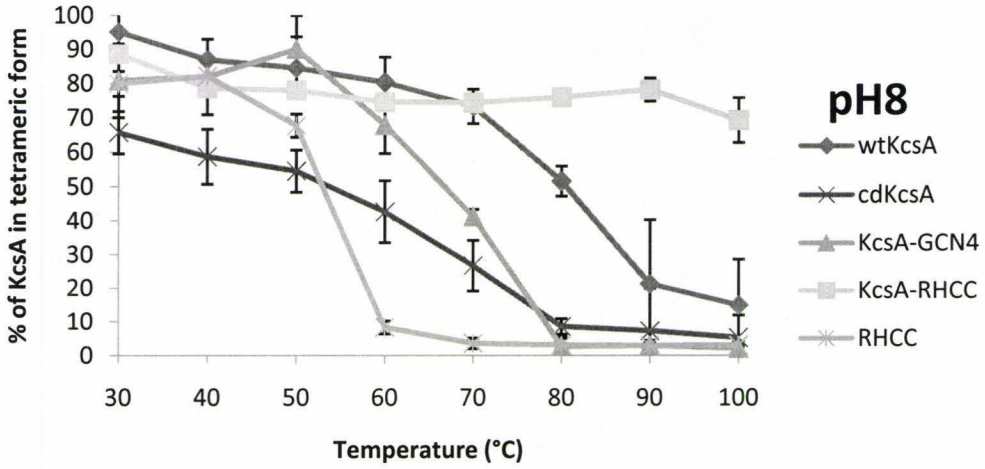
% of KcsA in tetrameric form
Temperature (°C)
pH8
wtKcsA
cdKcsA
KcsA-GCN4
KcsA-RHCC
RHCC

C.

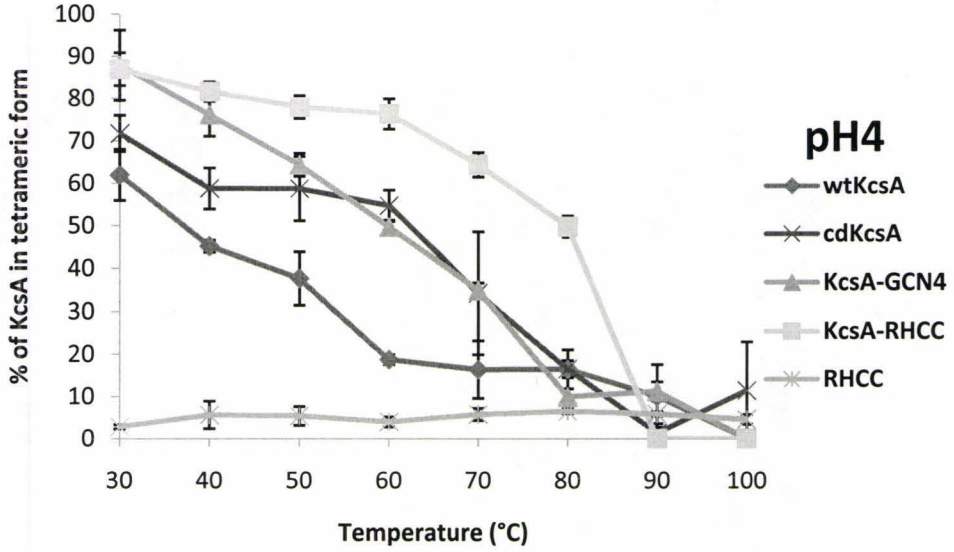
% of KcsA in tetrameric form
Temperature (°C)
pH4
wtKcsA
cdKcsA
KcsA-GCN4
KcsA-RHCC
RHCC

D.

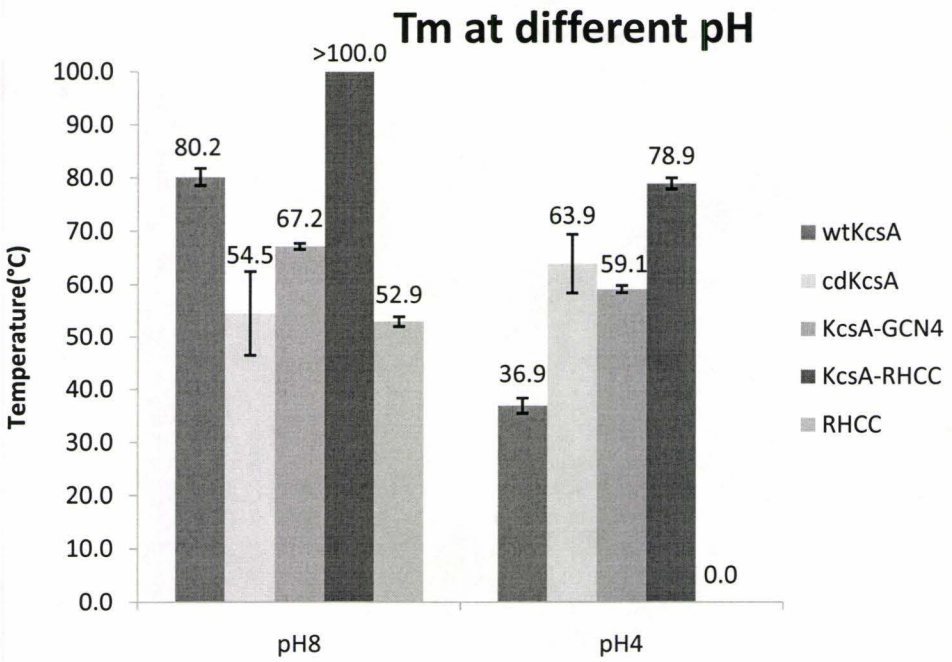

Figure 4.5 Thermostability determination of KcsA constructs. (A) Representative SDS-PAGE used in thermostability analyses (KcsA-RHCC at pH 8). The tetramer, dimer and monomer bands of KcsA-RHCC are indicated on the left side of the gel. The specific temperatures for heat treatment are indicated above the gel. (B and C) Comparison of stability of wtKcsA, cdKcsA, KcsA-GCN4, KcsA-RHCC and RHCC at different temperatures at pH 8 (B) and pH 4 (C). The fractional tetramer content in each sample was determined from the densitometry scans of SDS-PAGE. The results shown in panels B and C are given as mean standard derivation (n = 3). (D) Comparison of Tm's of three KcsA constructs at pH 8 and pH 4. Each curve in panels B and C was fitted into the sigmoidal dose-responsive (variable-slope) model with R2 > 0.97 by using GraphPad Prism software. The Tm values were calculated from the corresponding equations of the models.

Electrophysiological test of KcsA-RHCC

When we design the KcsA-RHCC hybrid channel, we expected the continuous coiled coil structure to keep the inner helices and the channel permanently in the close form. However, the observed pH sensitive nature of the hybrid channel led us to speculate that KcsA-RHCC may be conducting at acidic pH. We therefore measured its potassium conducting activity with a planar bilayer system. KcsA-RHCC can be opened at pH 4 and its apparent opening probability, NPo, is 0.13 (Figure 4.6 A & B). It is a weak outward rectifier as indicated by an I-V curve at pH 4

(Figure 4.6 C). The above two properties are very similar to that of the wtKcsA (33). However, when the buffer was exchanged to pH 8, the channel activity could barely be observed (Figure 4.6 A & B).

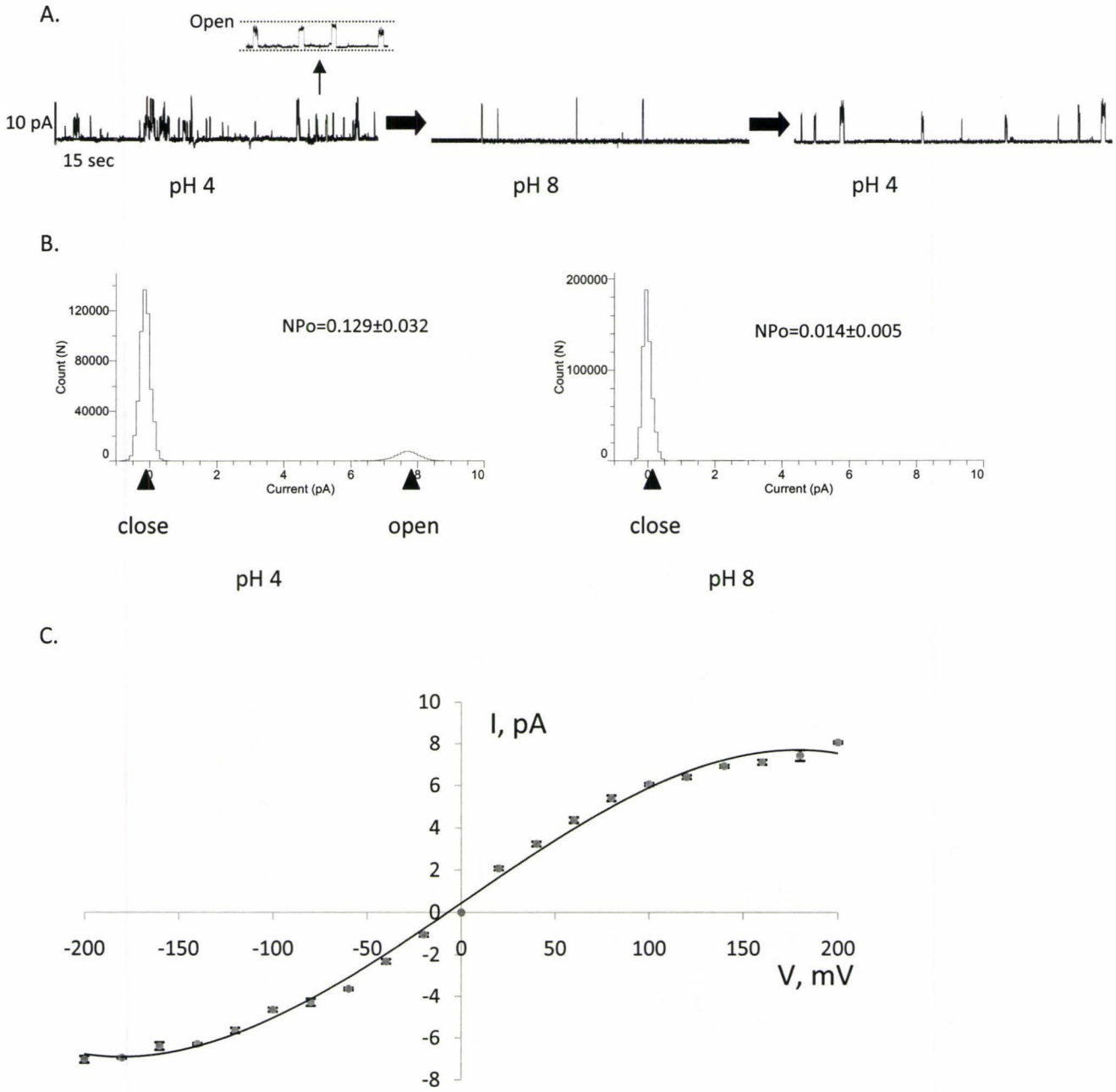

Figure 4.6 Measurement of currents conducted by KcsA-RHCC. (A) Representative current traces from lipid bilayer containing KcsA-RHCC at pH 4 (left panel) for a period of 1 minute with an applied voltage of 200 mV followed by buffer exchange to pH 8 (middle panel) and back to pH 4 again (right panel). A high-resolution detail of measured current was shown on the top of left panel with the open and closed states indicated on the side. (B) All-

points amplitude histogram of single-channel recordings, for KcsA-RHCC at pH 4 and 8 respectively. The open and close states are indicated on the bottom of the chart. The nominal open probabilities (NPo) at pH 4 and pH 8 respectively are indicated above the graphs. They are indicative of the mean levels of activity from three recordings. (C) I-V curve constructed from data of KcsA-RHCC at pH 4 reflects weak outward rectification property. Each data point represents mean current (± S.E., n=3).

4.4 DISCUSSION

Chimeric channel KcsA-RHCC was designed with the aim of generating a more stable and robust channel for structural and functional studies. Tetramerization domains are present in many different families of ion channels. Our previous study established the importance of the native tetramerization domain in KcsA and found that it can be replaced by an artificial tetramerization domain GCN4 (22).

In this paper, we investigated the effects of different non-native tetramerization domains and modes of linkage on the stability of KcsA hybrid channel. We found little differences between tetramerization domains whenever a flexible linker is used. However, more stable construct was obtained when two structurally compatible domains were linked directly without a flexible linker. Although GCN4 itself can form stable tetramer, its left-handed supercoil structure is not compatible with the right-handed inner helix of KcsA. The linking of these two structures could not be done without distorting one or both of the contributing structures thus we can expect the resultant structure to be not very stable (Figure 4.1 B middle). On the other hand, the C-terminal domain of wild type KcsA was shown to adopt a right-handed four-helix bundle structure linked to the inner helix via a less helical structure (31,34) (Figure 4.1 B left). The discontinuity in the coiled coil structure may allow for flexibility and suit its gating function; however it will inevitably compromise stability. In contrast, the continuous right-handed coiled coil design in KcsA-RHCC overcomes this problem and dramatically improves the stability of the hybrid channel (Figure 4.1 B right).

Previously we proposed a model of *in vivo* channel assembly describing the correlation between channel stability and protein expression level (22). Our result reported in this study is consistent with this model. The stability order deduced from gel-shift assay is: KcsA-RHCC > wtKcsA > KcsA-GCN4 > KcsA 1-125, which directly correspond to the order of their respective protein expression levels (data not shown).

Coiled coil motif is a commonly found structure in proteins. A statistical study from genomic analysis suggested that approximately 5-10% of all protein sequences are in coiled coils of various oligomeric states (35). Typically two to six α-helices wind around each other to form supercoil (36,37). They are widely found in diverse array of proteins, such as transcription factors and extracellular matrix proteins (38,39). Due to its simple and predictable folding properties, coiled coils have been used as temperature regulators, antibody stabilizers, anticancer drugs, purification tags, hydrogels, and linker systems, etc (37).

In this study, we intended to fuse a right-handed tetrameric coiled coil to KcsA to form a continuous coiled coil. The multiplicity of coiled coil candidates and the multiple possible splice junctions render exhaustive experimental testing intractable. We therefore resorted to *in silico* selection to identify the optimal splice variants. We included both right-handed and left-handed coiled coils as our target candidates and our algorithm easily identified the right-handed coiled coils as better candidates. The robustness of our computational algorithm was later confirmed by the extreme thermostability of the selected hybrid channel. This selection algorithm is applicable to the design of other chimeric channels.

The fact that KcsA-RHCC can conduct current opens up the possibility of using RHCC as an alternative sensor domain to the pore domain of other ion channels for functional assays and drug screening. The pH dependency of RHCC gating stems from its tetramerization property. Its

tetramer completely dissociates at acidic pH (Figure 4.5 C & D), which is similar to the wild type C-terminal domain (20).

Structural flexibility is a major obstacle in the production of well diffracting protein crystals due to its effect on ordered crystal packing. The presence of a flexible inter-domain linker on wtKcsA reduced the diffraction quality of its crystals (Pau, unpublished) (34). Stiffening of KcsA by the addition of RHCC should make it more prone to the yielding of well diffracting crystals. Currently we are in the process of screening for crystallization conditions.

We propose that similar engineering design may also be applied to other ion channels since they are all likely to possess a right-handed coiled coil structure at their respective bundle crossing (1,40-44). Functional minimal ion conducting modules composed of S5-S6 helices from various channels have been produced (45-48). We envisage that the expression of minimal channels may be facilitated by appropriate tetramerization domains and the success of this effort will certainly open up the possibilities in structural and functional characterization of ion channels.

4.5 MSTERIALS AND METHODS

Computational design of KcsA-RHCC

A comprehensive search of the Protein Data Bank (49) for right-handed or parallel coiled coil structures that have four-fold rotational symmetry retrieved four candidates. Program FitHelices (Yang unpublished 2007, available upon request) was used to determine the optimal splicing positions for joining the coiled coil fusion candidate to KcsA. The indicator used by the program is the root mean square deviation of the overlapping atoms at the spliced site. Coordinates of the

best spliced structure for each fusion candidates were then Monte Carlo minimized by program ZMM-MVM (http://www.zmmsoft.com/).

Molecular cloning

The DNA sequence encoding residues Ala 23-Val 115 of KcsA was amplified from pET28-KcsA (22), which contains the wild type KcsA (wtKcsA) gene of *S. lividans*, by PCR using *Pfu* DNA polymerase (Fermentas) with a forward primer 5'-GATTCGGATCCGCGCTGCACTGG AGGGC-3' and a reverse primer 5'-TGATAACG GTGACGAACCAGGTGGCCAGCG-3'. A gene encoding residues Thr 16-Ile 52 of RHCC (Table 4.2) was synthesized with optimal codon usage for *E. coli* (50) and PCR amplified with the following primers, forward: 5'-CTGGTTCGTCACCGTTATCATCGACGAC-3' and reverse: 5'-GACTGA GAATTCTCATTAAATTGACGCCAGGATGGT-3' (the recognition sites of BamHI and EcoRI are underlined). The two amplified fragments were joined by fusion PCR (51), digested with the corresponding restriction enzymes and cloned into pET28M, a modified pET28a expression vector (20). The sequence of this N-terminal His-tagged construct, pET28M/kcsa-rhcc, was confirmed by dideoxynucleotide sequencing. The cloning of wtKcsA and KcsA-GCN4 is as described before (22). RHCC cloned in pET15b is a gift from Dr. Richard Kammerer.

ACCGTTATCATCGACGACCGTTACGAATCTCTGAAAAACCTGATCACCCTGCGTGCG
GACCGTCTGGAAATGATTATCAACGACAACGTTTCTACCATCCTGGCGTCAATT

Table 4.2 DNA sequence of the synthesized rhcc gene.

Protein Expression and Purification

E.coli BL21(DE3) cells were transformed with pET28M/kcsa-rhcc. Single colony was inoculated and grown in 100 mL LB (Luria Bertani) broth with 100 μg/mL kanamycin (as the final concentration) at 37°C overnight. The culture was then diluted into 1 L LB broth with 100 μg/mL kanamycin and further grown for 100 minutes. Protein expression was induced by the addition of IPTG to a final concentration of 1 mM. Cells were pelleted after 3 hrs of incubation at 37°C, resuspended in lysis buffer (20 mM Tris, pH 8, 150 mM KCl, and 1 mM PMSF) and subsequently lysed by French Press at 10,000 psi. The cell lysate was centrifuged at 100,000 × g for 1 hr and the pellet was solubilized in 20 mL of 20 mM Tris, pH 8, 150 mM KCl, 1 mM PMSF and 1% v/v LDAO overnight at 4°C. The resuspended mixture was centrifuged at 100,000 × g for 1 hr and the supernatant was loaded onto a HisTrap™ HP column (GE Healthcare). Protein was purified using a FPLC system (Pharmacia) with a linear gradient of 0 - 500 mM imidazole. Purified proteins were analyzed by NuPAGE Novex 4-12% Bis-Tris Midi Gel (Invitrogen) with Coomassie blue staining. wtKcsA, KcsA-GCN4 and RHCC were expressed and purified in similar manner except the absence of detergent during RHCC purification. cdKcsA (C-terminal deleted KcsA) was generated by chymotrypsin digestion of wtKcsA (22).

Thermal Stability Determination

Protein of KcsA-RHCC was dialyzed overnight against a solution containing 150 mM KCl, 0.1% v/v LDAO, 20 mM Tris, pH 8 (or 15 mM potassium citrate, pH 4) in dialysis bags with a MWCO of 3,500 Da. Dialyzed sample was mixed with the loading solution containing 10% w/v SDS, 9.3% w/v DTT and 38% w/v glycerol, heated for 30 minutes at various temperatures ranging from 30°C to 100°C with the increment of 10°C interval, cooled to room temperature

and analyzed by SDS-PAGE. Three independent experiments were performed. Scanned images of the gels were analyzed by using ImageJ (http://rsb.info.nih.gov/ij/) in Integrated-Intensity-Mode to determine the amounts of tetramer and monomer in the samples. Fractional tetramer content was calculated by dividing the integrated density of tetramer by the combined integrated densities of tetramer and monomer. Model fitting of the thermal denaturation curves was carried out using prism 4.00 (GraphPad Software Inc., San Diego, CA, USA).

Gel-filtration Chromatography

Gel-filtration chromatography was run on a FPLC system (Amersham Biosciences Corp.) using a Superdex 200 column (Amersham Biosciences Corp.) equilibrated in 50 mM Tris buffer (pH 8), 150 mM KCl and 0.1% v/v LDAO.

Circular Dichroism measurement

Protein samples at a 10 μM monomeric protein concentration were dissolved in 20 mM K_2HPO_4 (pH 8), 150 mm KCl and 0.1% v/v LDAO. CD spectra of the samples were recorded in a 0.1 cm path length cell at 25°C using a 410 CD spectrometer (AVIV Biomedical Inc., Lakewood, NJ, USA). The secondary structure content of each sample was quantified using the CD spectrum analysis program cdsstr of the cdpro suite (http://lamar.colostate.edu/~sreeram/CDPro /main.html).

Electrophysiology

Channel recordings were performed in a horizontal planar lipid bilayer of POPE and POPG (15 mg/ml and 5 mg/ml respectively) at room temperature. Both cis and trans chambers were

filled with solution at pH 4 (150 mM KCl, 20 mM potassium acetate) in the beginning which was changed to pH 8 (150 mM KCl, 20 mM Tris) when needed. Current records were acquired at a sampling frequency of > 10 kHz and filtered to 1 kHz.

4.6 REFERENCES

1. Doyle, D. A., Morais Cabral, J., Pfuetzner, R. A., Kuo, A., Gulbis, J. M., Cohen, S. L., Chait, B. T., and MacKinnon, R. (1998) *Science* **280**, 69-77
2. Hille, B. (2001) *Ion Channels of Excitable Membrane*, Sinauer Associates, Inc, Sunderland, MA
3. Shen, N. V., Chen, X., Boyer, M. M., and Pfaffinger, P. J. (1993) *Neuron* **11**, 67-76
4. Kreusch, A., Pfaffinger, P. J., Stevens, C. F., and Choe, S. (1998) *Nature* **392**, 945-948
5. Li, M., Jan, Y. N., and Jan, L. Y. (1992) *Science* **257**, 1225-1230
6. Jenke, M., Sanchez, A., Monje, F., Stuhmer, W., Weseloh, R. M., and Pardo, L. A. (2003) *The EMBO journal* **22**, 395-403
7. Tinker, A., Jan, Y. N., and Jan, L. Y. (1996) *Cell* **87**, 857-868
8. Jiang, Y., Pico, A., Cadene, M., Chait, B. T., and MacKinnon, R. (2001) *Neuron* **29**, 593-601
9. Quirk, J. C., and Reinhart, P. H. (2001) *Neuron* **32**, 13-23
10. Schmalhofer, W. A., Sanchez, M., Dai, G., Dewan, A., Secades, L., Hanner, M., Knaus, H. G., McManus, O. B., Kohler, M., Kaczorowski, G. J., and Garcia, M. L. (2005) *Biochemistry* **44**, 10135-10144
11. Zhou, L., Olivier, N. B., Yao, H., Young, E. C., and Siegelbaum, S. A. (2004) *Neuron* **44**, 823-834
12. Wei, A., Jegla, T., and Salkoff, L. (1996) *Neuropharmacology* **35**, 805-829
13. Covarrubias, M., Wei, A. A., and Salkoff, L. (1991) *Neuron* **7**, 763-773
14. VanDongen, A. M., Frech, G. C., Drewe, J. A., Joho, R. H., and Brown, A. M. (1990) *Neuron* **5**, 433-443
15. Schulteis, C. T., Nagaya, N., and Papazian, D. M. (1998) *J Biol Chem* **273**, 26210-26217
16. Hopkins, W. F., Demas, V., and Tempel, B. L. (1994) *J Neurosci* **14**, 1385-1393

17. Deal, K. K., Lovinger, D. M., and Tamkun, M. M. (1994) *J Neurosci* **14**, 1666-1676

18. Xu, J., Yu, W., Jan, Y. N., Jan, L. Y., and Li, M. (1995) *J Biol Chem* **270**, 24761-24768

19. Shen, N. V., and Pfaffinger, P. J. (1995) *Neuron* **14**, 625-633

20. Pau, V. P., Zhu, Y., Yuchi, Z., Hoang, Q. Q., and Yang, D. S. (2007) *J Biol Chem* **282**, 29163-29169

21. Molina, M. L., Encinar, J. A., Barrera, F. N., Fernandez-Ballester, G., Riquelme, G., and Gonzalez-Ros, J. M. (2004) *Biochemistry* **43**, 14924-14931

22. Yuchi, Z., Pau, V. P., and Yang, D. S. (2008) *FEBS J* **275**, 6228-6236

23. Harbury, P. B., Zhang, T., Kim, P. S., and Alber, T. (1993) *Science* **262**, 1401-1407

24. Stetefeld, J., Jenny, M., Schulthess, T., Landwehr, R., Engel, J., and Kammerer, R. A. (2000) *Nat Struct Biol* **7**, 772-776

25. Zerangue, N., Jan, Y. N., and Jan, L. Y. (2000) *Proc Natl Acad Sci U S A* **97**, 3591-3595

26. Bowman, G. D., Nodelman, I. M., Levy, O., Lin, S. L., Tian, P., Zamb, T. J., Udem, S. A., Venkataraghavan, B., and Schutt, C. E. (2000) *J Mol Biol* **304**, 861-871

27. Sales, M., Plecs, J. J., Holton, J. M., and Alber, T. (2007) *Protein Sci* **16**, 2224-2232

28. Kuhnel, K., Jarchau, T., Wolf, E., Schlichting, I., Walter, U., Wittinghofer, A., and Strelkov, S. V. (2004) *Proc Natl Acad Sci U S A* **101**, 17027-17032

29. Alam, A., and Jiang, Y. (2009) *Nat Struct Mol Biol* **16**, 30-34

30. Zhou, Y., Morais-Cabral, J. H., Kaufman, A., and MacKinnon, R. (2001) *Nature* **414**, 43-48

31. Cortes, D. M., Cuello, L. G., and Perozo, E. (2001) *J Gen Physiol* **117**, 165-180

32. Perozo, E., Cortes, D. M., and Cuello, L. G. (1999) *Science* **285**, 73-78

33. LeMasurier, M., Heginbotham, L., and Miller, C. (2001) *J Gen Physiol* **118**, 303-314

34. Uysal, S., Vasquez, V., Tereshko, V., Esaki, K., Fellouse, F. A., Sidhu, S. S., Koide, S., Perozo, E., and Kossiakoff, A. (2009) *Proc Natl Acad Sci U S A* **106**, 6644-6649

35. Mewes, H. W., Frishman, D., Gruber, C., Geier, B., Haase, D., Kaps, A., Lemcke, K., Mannhaupt, G., Pfeiffer, F., Schuller, C., Stocker, S., and Weil, B. (2000) *Nucleic Acids Res* **28**, 37-40

36. Wolf, E., Kim, P. S., and Berger, B. (1997) *Protein Sci* **6**, 1179-1189

37. Mason, J. M., and Arndt, K. M. (2004) *Chembiochem* **5**, 170-176

38. Glover, J. N., and Harrison, S. C. (1995) *Nature* **373**, 257-261

39. Frank, S., Schulthess, T., Landwehr, R., Lustig, A., Mini, T., Jeno, P., Engel, J., and Kammerer, R. A. (2002) *J Biol Chem* **277**, 19071-19079

40. Jiang, Y., Lee, A., Chen, J., Ruta, V., Cadene, M., Chait, B. T., and MacKinnon, R. (2003) *Nature* **423**, 33-41

41. Long, S. B., Campbell, E. B., and Mackinnon, R. (2005) *Science* **309**, 897-903

42. Jiang, Y., Lee, A., Chen, J., Cadene, M., Chait, B. T., and MacKinnon, R. (2002) *Nature* **417**, 515-522

43. Shi, N., Ye, S., Alam, A., Chen, L., and Jiang, Y. (2006) *Nature* **440**, 570-574

44. Kuo, A., Gulbis, J. M., Antcliff, J. F., Rahman, T., Lowe, E. D., Zimmer, J., Cuthbertson, J., Ashcroft, F. M., Ezaki, T., and Doyle, D. A. (2003) *Science* **300**, 1922-1926

45. Pincin, C., Ferrera, L., and Moran, O. (2005) *Biochem Biophys Res Commun* **334**, 140-144

46. Kang, G. B., Song, H. E., Song, D. W., Kim, M. K., Rho, S. H., Kim do, H., and Eom, S. H. (2007) *Protein Pept Lett* **14**, 742-746

47. Chen, Z., Alcayaga, C., Suarez-Isla, B. A., O'Rourke, B., Tomaselli, G., and Marban, E. (2002) *J Biol Chem* **277**, 24653-24658

48. Santos, J. S., Grigoriev, S. M., and Montal, M. (2008) *J Gen Physiol* **132**, 651-666

49. Berman, H. M., Westbrook, J., Feng, Z., Gilliland, G., Bhat, T. N., Weissig, H., Shindyalov, I. N., and Bourne, P. E. (2000) *Nucleic Acids Res* **28**, 235-242

50. Dong, H., Nilsson, L., and Kurland, C. G. (1996) *Journal of molecular biology* **260**, 649-663

51. Shevchuk, N. A., Bryksin, A. V., Nusinovich, Y. A., Cabello, F. C., Sutherland, M., and Ladisch, S. (2004) *Nucleic Acids Res* **32**, e19

Chapter 5.

Design of Minimal Ion Channels

5.1 ABSTRACT

Ion channels are pore-forming proteins that are widely distributed in all living cells. They are involved in many physiological functions, such as neuronal signal transduction, contraction of muscle and secretion of hormone. The structural information of a few potassium channels shed light on the mechanism of K+ selectivity, conductivity and ligand-binding property. However, the efficiency of determining the structures of ion channels is far below what is actually required, especially for understanding the selectivity of Ca^{2+} and Na^{+} channels, the relationship between diverse stimulus and gating of channels as well as important application in rational drug designs. Here, we designed some universal platforms for easy overexpression and crystallization of a wide range of ion channels. We found that the pore-forming domains of voltage-gated or ligand-gated ion channels can be expressed with the assistance of non-native cytoplasmic tetramerization domains. These minimized eukaryotic ion channels kept the properties as selectivity, conductivity and drug-binding as wild type channels when expressed in *E.coli* system. A number of constructs with high expression level and good homogeneity are under crystallization trials.

5.2 INTRODUCTION

Ion channels are special protein catalysts existing in the cell membrane that passively allow ions to move down their electrochemical gradient across the membrane barrier (1). This movement will cause a membrane potential change, which in turn is used as an important signal inside the body. This electric signal is involved in many cellular functions including nerve pulse, T-cell activation, hormone release, and etc.

There are three major topologies of ion channels (Figure 5.1 A & B). Functional channels all have homotetrameric or pseudo-homotetrameric arrangement. For each monomer subunit, the type I channel is composed of two transmembrane (TM) helices forming an ion-conducting pore with a P-loop forming the selectivity filter in the middle. And it also has relatively small N-terminal and C-terminal cytoplasmic domains. The type II differs from type I by a big C-terminal cytoplasmic domain which has the role of ligand-sensing. Type III differs from type I and II by four extra transmembrane helices which compose voltage-sensor domain (VS). In addition, it has a big N-terminal cytoplasmic domain which interacts with β–subunit inside the cell and regulates the channel function. From the representative crystal structures of three types of channels, one can see although they differ in size and accessory domains, they all have a pore-forming domain (PF) which is composed of the most inner two helices and a selectivity filter (Figure 5.1 C). In human, ion channels can be divided into more sub-families in terms of function and property, but about two thirds of them belong to type III in our classification according to their signature 6-TM topology.

The modular property of ion channels has been demonstrated from three different aspects. First, in the crystal structures of KvAP and rKv1.2, the four VS modules sit

peripherally to the PF with very little buried surface area (2,3). The only interaction between these two independent modules is a hydrophobic patch on S4 helix facing the neighbouring S5 helix. Second, when the PF domains of IRK1 (type II), *Shaker* (type III) or cyclic nucleotide-gated channels (type III) were replaced by the counterpart of KcsA (type I), all of the chimeric channels were proven to be functional (4,5). And last, the finding of Ci-VSP, a phosphatase controlled by a VS domain conserved with VS from voltage-gated ion channels, gave another piece of solid evidence about this modular property (6-9). These findings clearly validate evolutionary modularity of both VS and PF domains.

Ion channels are a family of favourite drug targets because they are related to a number of diseases such as vascular diseases, neurological diseases, multiple sclerosis and etc (10-12). There are two major drug-binding sites in ion channels, one is at the entrance of selectivity filter; the other is in the central cavity of the ion-conducting pore (13-15). Both of them are located in the PF. There are a few drugs targeting the VS or other intracellular regulatory domain (16-18), but most drugs directly interact with the PF and affect channel function by blocking. Therefore, the structural information about this part of the channel is very valuable in terms of rational drug designs.

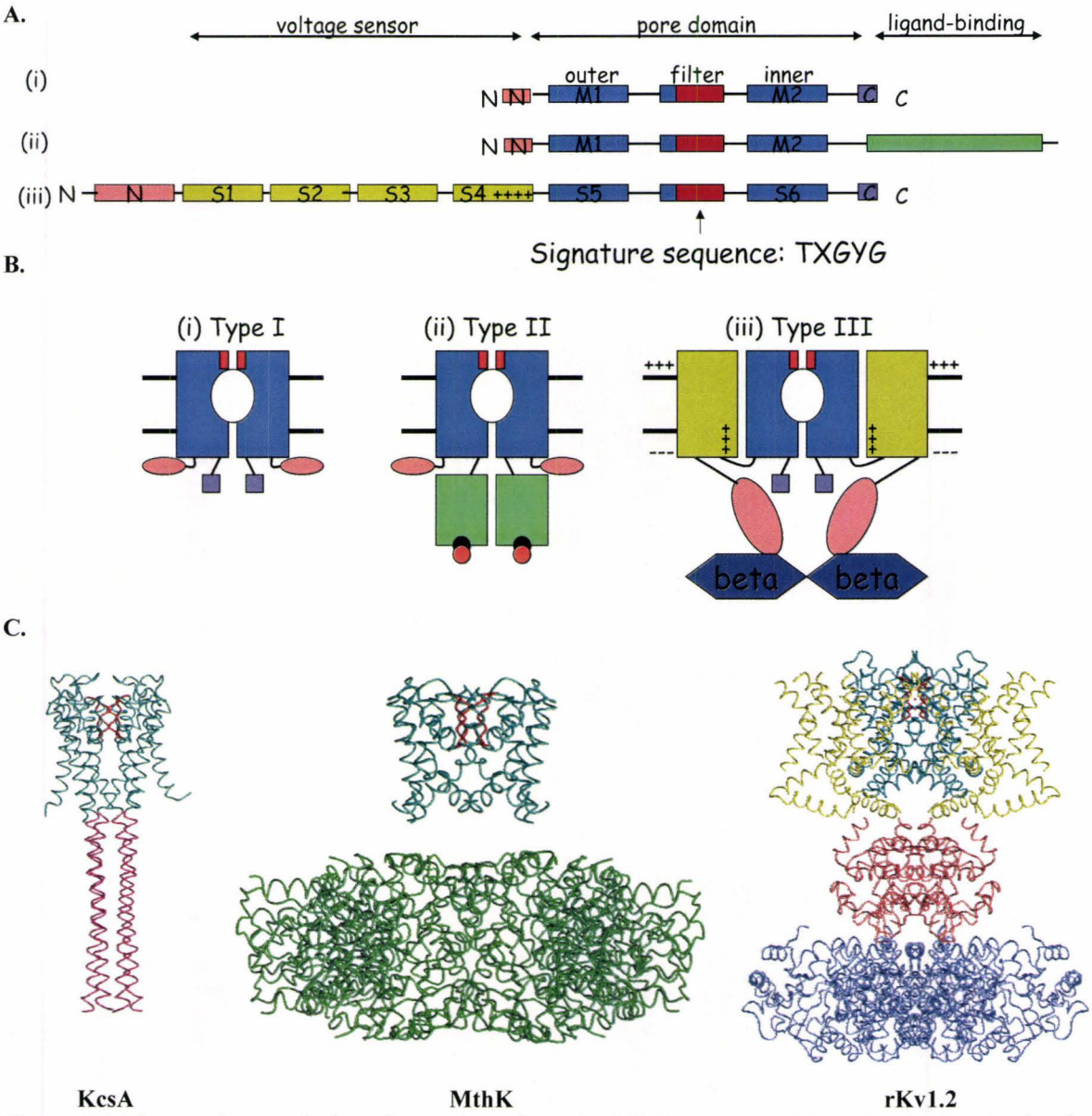

Figure 5.1 Three major topologies of potassium channels. (A) Gene composition of a single subunit of potassium channels. Domains are described in different colours. Sequence of selectivity filter is indicated by the arrow. (B) Symbolic description of different types of potassium channels in the cell membrane. Only two subunits instead of four are shown to represent their structures for clarity. (C) Representative crystal structures for three types of potassium channels. The colour scheme is same as in (A) and (B). The PDB codes are 3EFF (KcsA), 1LNQ (MthK) and 2A79 (rKv1.2). The picture was generated by program ZMM-MVM.

Since PF is in charge of selectivity, conductivity and drug binding properties, we should be able to simplify the system and improve the rate of structural and functional characterization of potassium channels by making use of its modular property and

expressing the PF of type II and type III channels in the absence of VS or ligand-binding domain. The function of this wild type C-terminal domain can be replaced by other artificial tetramerization domain if proper considerations of other factors like handedness of non-native coiled coil and splicing positions were given (20). The tetramerization domains have been found not only in KcsA but also a variety of other ion channels, such as voltage-gated potassium channels, ether-a-go-go channels, potassium inwardly-rectifying channels, calcium activated channels and cyclic nucleotide-gated channels (21-29). There are also many ion channels containing a C-terminal cytoplasmic domain with un-characterized functions, which may also involve in the tetramerization effect. In this study, we built chimeric channels by connecting the PF from type II and type III channels with KcsA C-terminal domain or tetramerization domains from other protein sources. We discovered that several of these PF modules can be functionally expressed independently with the assistance of cytoplasmic tetramerization domains and maintain the native functions as a normal ion channel.

5.3 RESULT

Structural comparison of PF domains of potassium channels

Among the six ion channels with known crystal structures, KcsA and NaK belong to type I (30,31); KirBac and MthK belong to type II (32,33); KvAP and Kv1.2 belong to type III (2,3). KcsA, KirBac and NaK were crystallized in closed form and the other three were crystallized in open form. We compare their isolated PF domains from different angels (Figure 5.2). By visual comparison, all PFs are structurally similar, especially the upper half of these domains because of their independence of the gating status in the

crystal structures. The structural alignments from modeling program shows that the RMSD of the whole pore-forming domain is about 3.442 Å and the RMSD of the top half is about 1.611 Å (Table 5.1). Since type I channel like KcsA and NaK can exist as an independent functional entity on their own, the PF of other type II and type III channels should also have chance to exist independently.

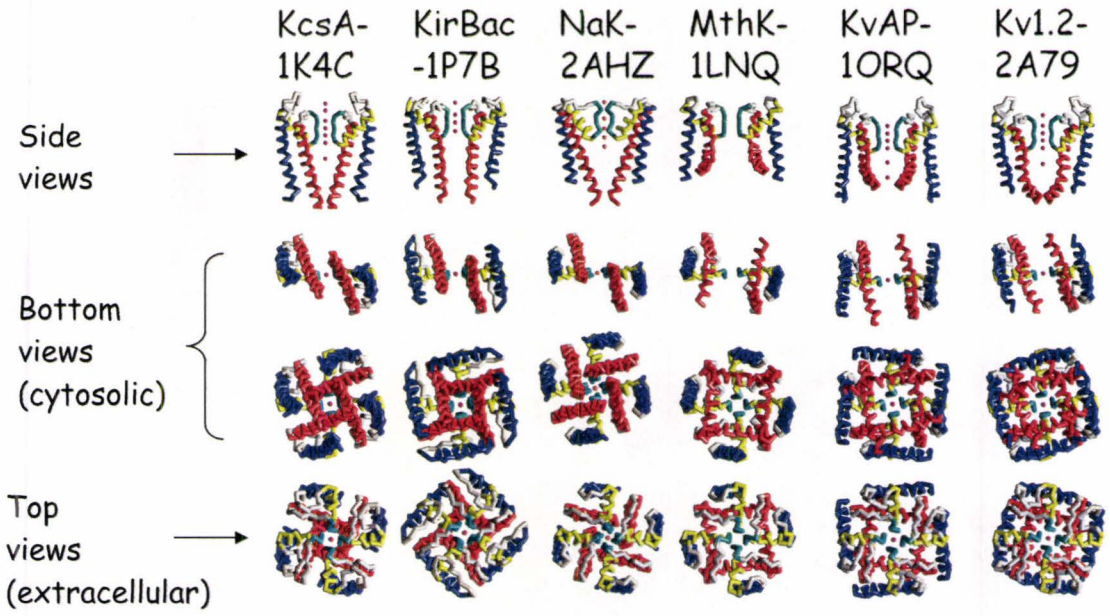

Figure 5.2 Structural comparison of pore-forming domains of different channels. PDBs of six channels (codes labeled above the picture), KcsA, KirBac, NaK, MthK, KvAP and Kv1.2, are used to generate this picture by program ZMM-MVM.

RMSD (Whole/Top)	KcsA	KirBac	NaK	MthK	KvAP
KcsA	-	-	-	-	-
KirBac	2.720/1.810	-	-	-	-
NaK	2.394/1.808	2.988/1.940	-	-	-
MthK	4.243/1.601	4.702/2.062	4.575/1.557	-	-
KvAP	3.987/1.454	3.686/1.636	4.675/1.611	2.683/1.500	-
Kv1.2	2.544/0.979	2.274/1.333	3.795/1.900	3.794/1.718	2.574/1.250

Table 5.1 Structural alignments of pore-forming domains of different channels by program FITCHANNEL (Yang unpublished 2008, available upon request). Only the main chain atoms were used for alignment. The first number is the root mean square deviation (RMSD) from the alignment by whole pore-forming domains (specifically for two fragments: residue 28-49 and 61-114 in KcsA and corresponding parts in other channels), and the second is from the alignment by top half of pore-forming domains, (specifically for two fragments: residue 36-49 and 61-98 in KcsA and corresponding parts in other channels). The unit is in angstrom.

Targets selection

Our goal in this study is to develop a minimal channel platform that can be applied to ion channels of many different families. At the first step, we decided to focus on potassium channels and prokaryotic sodium channels because their homotetrameric structures are much simpler than the heterotetrameric channels. We selected eleven channels from five different families as our targets. In voltage-gated potassium channel family, we chose Kch, an *E.coli* Kv channel; three Kv channels from other bacteria strains (*Salinispora arenicola, Mycobacterium ulcerans, Bifidobacterium adolescentis*); rat Kv1.2 and human Kv1.5 channel. In Ca^{2+}-gated potassium channel family, we chose Mthk and human BK1 channels. In inward-rectifying potassium channel family, we chose human Kir2.1 channel. In cyclic nucleotide-gated potassium channel family, we chose Mlok1 channel. We also chose one of the sodium channels, NaChBac, which is a bacteria sodium channel that has similar topology as our type III potassium channels. We synthesized the genes of PF domains for all these ten channels in the optimal codon for *E.coli* expression.

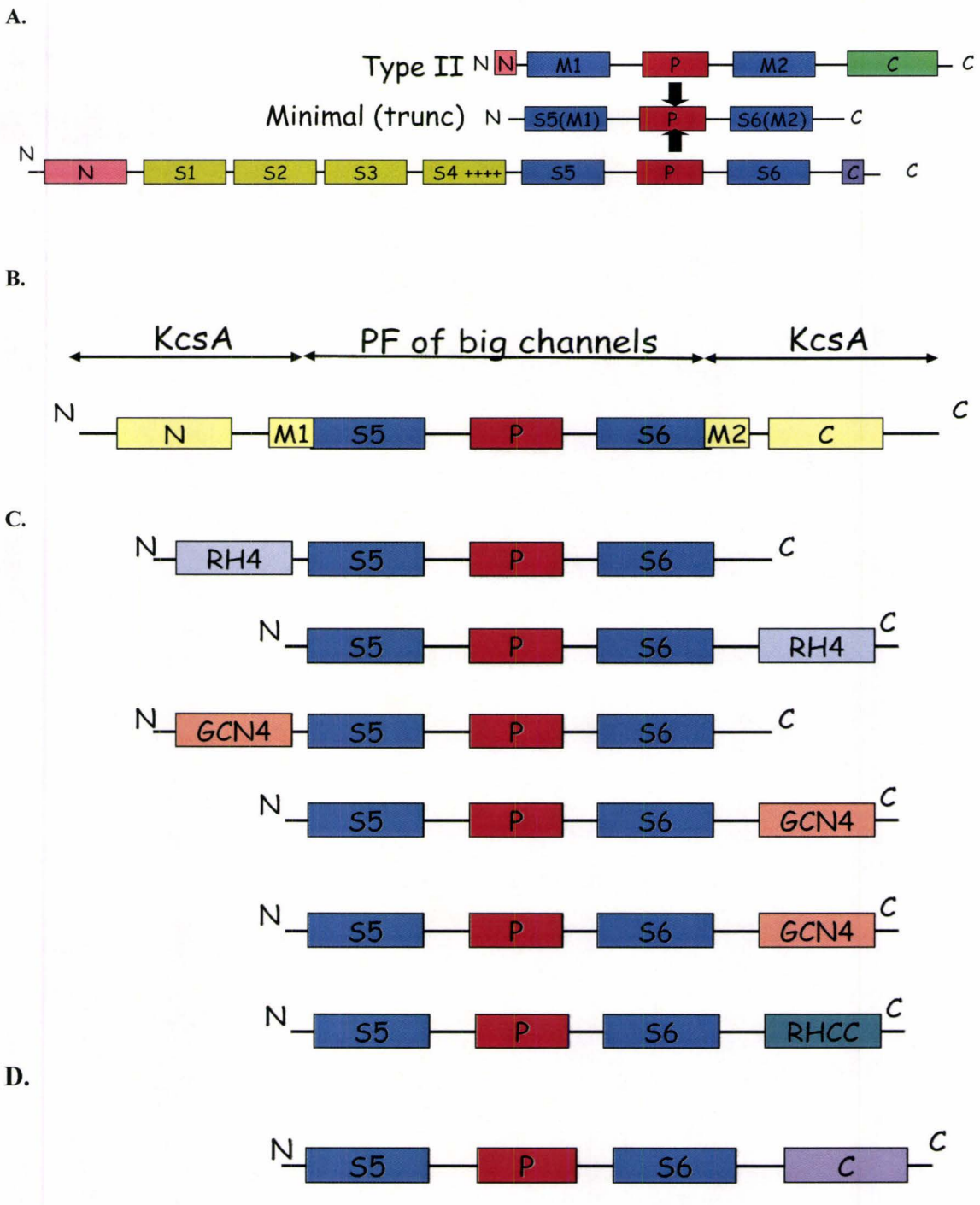

Figure 5.3 Strategies to build minimal potassium channels. (A) Minimal channels generated by direct truncation. (B) Minimal channels generated by connecting PF of big channels with N- and C-terminal domain of KcsA. (C) Minimal channels generated by connecting PF of big channels with artificial tetrameric coiled coils. (D) Minimal channels generated by connecting PF of big channels with their native C-terminal domains.

Minimal channels generated by direct truncation

From KcsA study, we knew the PF domain alone can hardly be expressed. To verify this observation, in our first trials, we repeated the similar experiments by directly truncating all the accessory domains from four of our target channels (Figure 5.3 A) and cloned their PF domains into *E.coli* expression vector pET28 KcsA (see supplementary data for detailed sequences). When we induced the expression of these constructs, two Kv channels cannot be expressed at all, and the other two channels hKir2.1 and NaChBac were induced with very low expression level and only showed protein band at monomer size on SDS-PAGE (Figure 5.4).

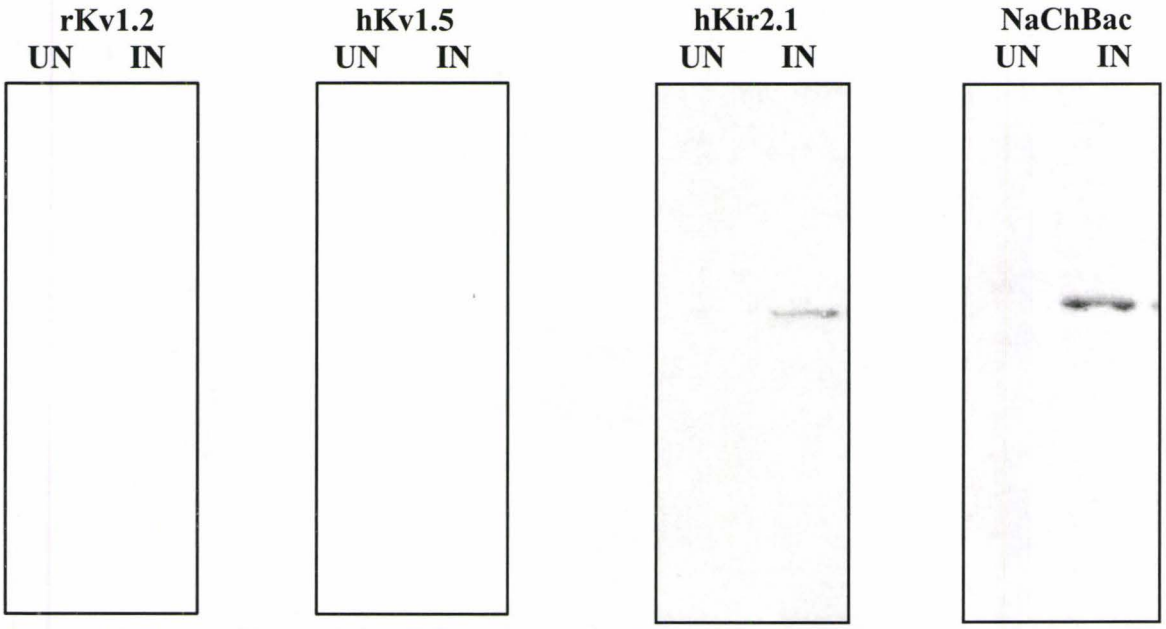

Figure 5.4 Western-blot analysis of direct truncated minimal channels. Same amount of *E.coli* cells (quantified by OD_{600}) expressing different constructs were analyzed by 15% SDS-PAGE. Minimal channels were then identified by immunoblotting using an anti-His-tag antibody. UN: un-induced; IN: induced.

Minimal channels generated by connecting PF of type II and III channels with C-terminal domain of KcsA

From our previous study, we found that the C-terminal domain of KcsA has dual functions as pH-sensor and tetramerization domain (19,20). And it is essential for the expression and stability for the PF domain of KcsA (20). It may also provide similar effect to make expressible and openable channels if the PF domains of other channels are spliced into the KcsA scaffold.

Because there are some known conserved interactions between the N-terminal and C-terminal domains of KcsA (His25 in N-terminus with residues 113-117 in C-terminus) that may assist the stability of PF domain (34), we chose to keep both cytoplasmic domains of KcsA in our scaffold. Similar strategy was used for designing chimeras for all different target channels. In the example of KcsA-rKv1.2, after sequence alignments of the PF domains between KcsA and rKv1.2, we identified conserved residues near N-terminal end of outer helix and C-terminal end of inner helix. And we built chimeric channels by connecting them at these conserved residues. We also identified one region in inner helix near the membrane surface area and tried every residue in this region as a splicing point (Figure 5.3 B, 5.5).

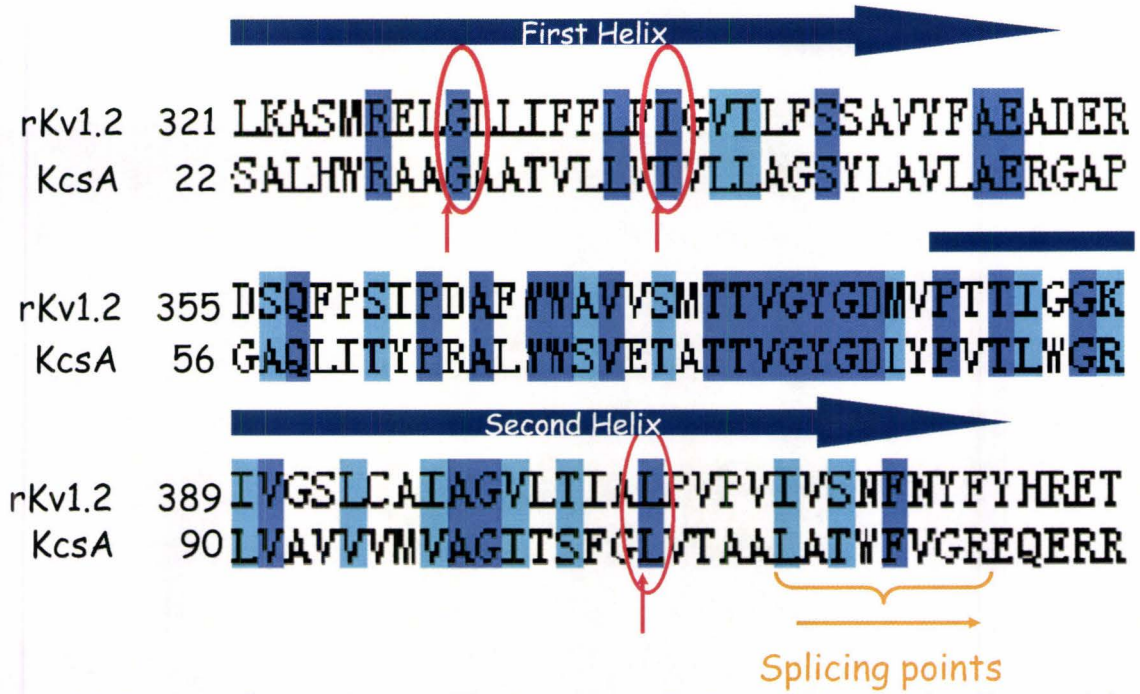

Figure 5.5 Sequence alignment between PF of KcsA and PF of rKv1.2. Conserved residues used for splicing in chimeric channels are circled and indicated by red arrows. The region near membrane surface used for splicing is indicated by yellow arrow.

A number of KcsA-rKv1.2 chimeric channel constructs can be induced with detectable amount by Western-blot. Compared the directly truncated constructs, the expression level of these constructs are much improved. Especially for some of them with relatively high expression level, a dimer band could also be observed (Figure 5.6 A). When the samples with dimer band were heated before running the gel, the dimer band disappeared, which indicated that they are real oligomeric state of expressed channel proteins (Figure 5.6 B). However the solubility of these proteins is still very limited, which may be due to the non-optimal splicing in the design which causes the folding of chimeras into non-native structures (Figure 5.6 C). The results for other target channels are similar to the rKv1.2 case (Figure 5.6 D).

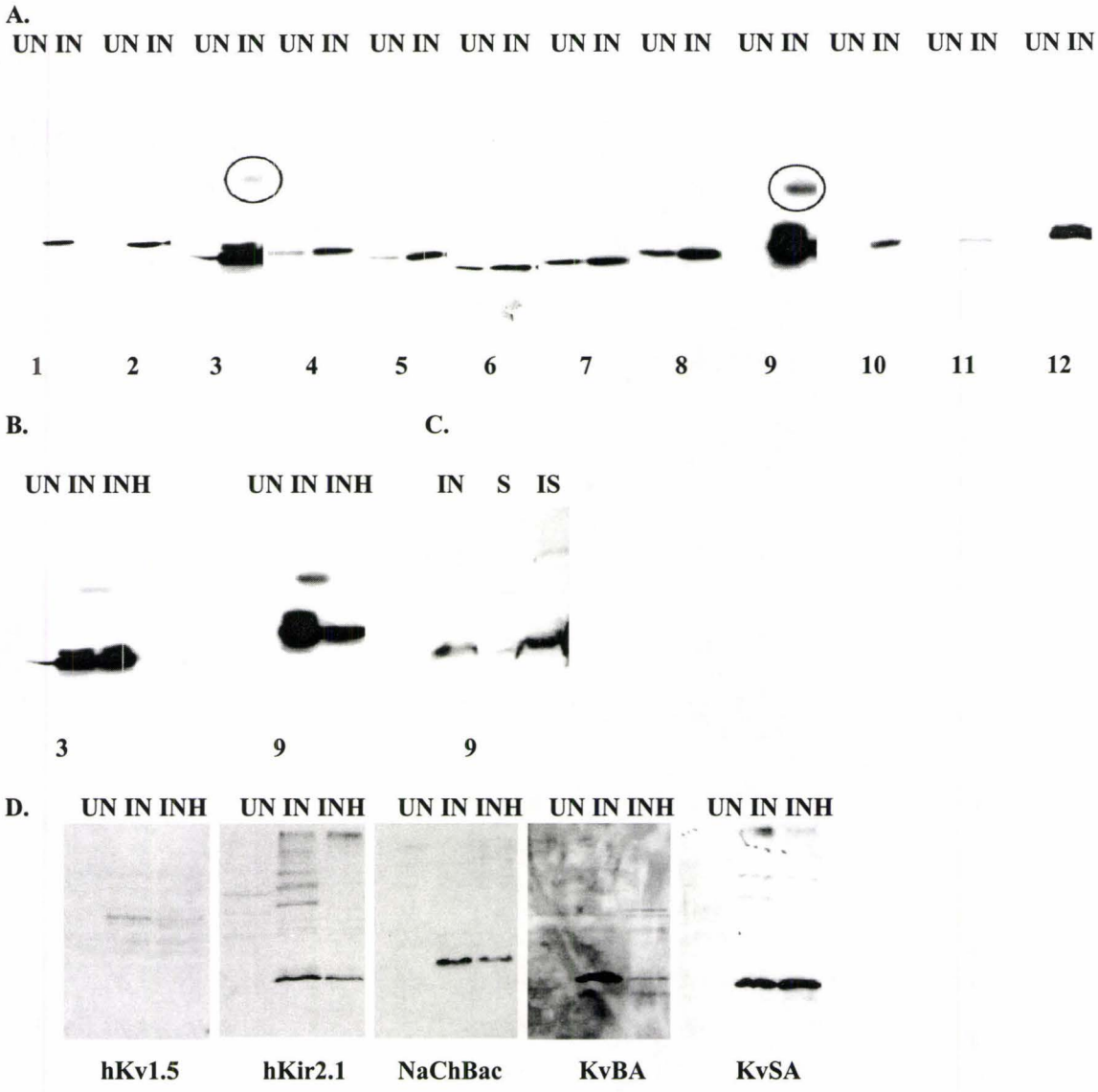

Figure 5.6 Western-blot analysis of chimeric channels between big channels and C-terminal domain of KcsA. (A) Same amount of *E.coli* cells (quantified by OD_{600}) expressing chimeric constructs 1-12 of rKv1.2-KcsA (see supplementary data for detailed sequences) were analyzed by 15% SDS-PAGE. Minimal channels were then identified by immunoblotting using an anti-His-tag antibody. UN: un-induced; IN: induced. (B) Heat treatment of the rKv1.2-KcsA constructs 3 and 9. INH: induced with heating. (C) Solubility test for rKv1.2-KcsA construct 9. S: soluble fraction; IS: insoluble fraction. (D) Induction tests for chimeric channels: hKv1.5-KcsA, hKir2.1-KcsA, NaChBac-KcsA, KvBA-KcsA and KvSA-KcsA (see supplementary data for detailed sequences).

Minimal channels generated by connecting PF of big channels with artificial tetrameric coiled coils

From the study of KcsA, we knew that the function of its wild-type C-terminal domain could be replaced by artificial tetrameric coiled coils (20). We found a correlation between the tetramer stability and the expression level of the PF domain. The location of this tetramerization domain could be either N-terminal end or C-terminal end, but the C-terminal fusion constructs had higher expression level than N-terminal ones. Nevertheless, in the wild type Kv channels, there is an N-terminal cytoplasmic tetramerization domain known as T1 domain. Consequently, to build the chimeric channels between PF of big channels and artificial tetramerization domains, we still tried to put different types of tetrameric coiled coils to either N-terminal or C-terminal end of the PF domains (Figure 5.3 C).

We screened a number of chimeric constructs between different channels and tetrameric coiled coils. Most of them have obvious improvement on expression level compared to PF domains alone and KcsA fusion constructs. Among them, the C-terminal fusion constructs of rKv1.2 with right-handed coiled coil, RHCC, showed higher expression level than others. We sampled constructs with RHCC spliced into different positions of rKv1.2 channel and the best one is the one connected to residue 418 of rKv1.2 channel KcsA (see supplementary data for detailed sequences). It showed highest expression level, promising dimer and tetramer bands on SDS-PAGE, and also very good solubility (Figure 5.7 B & C).

A.

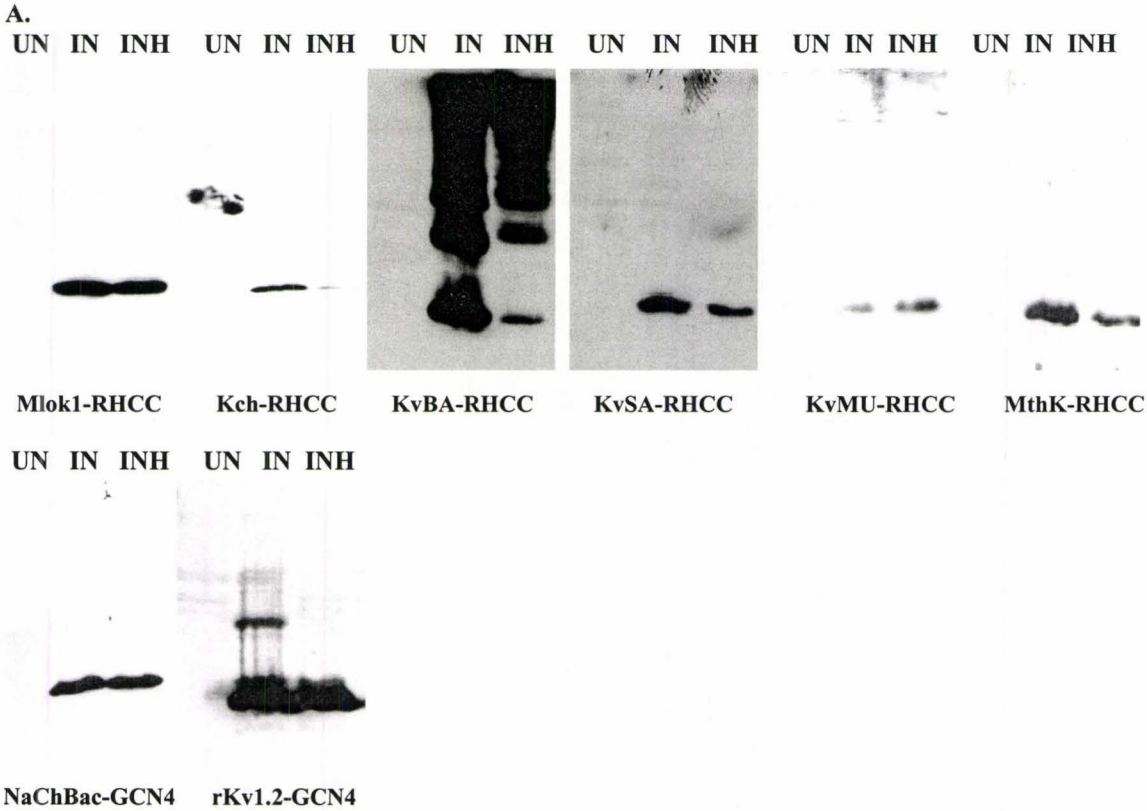
UN IN INH UN IN INH UN IN INH UN IN INH UN IN INH UN IN INH
Mlok1-RHCC
Kch-RHCC
KvBA-RHCC
KvSA-RHCC
KvMU-RHCC
MthK-RHCC
UN IN INH UN IN INH
NaChBac-GCN4
rKv1.2-GCN4

B.

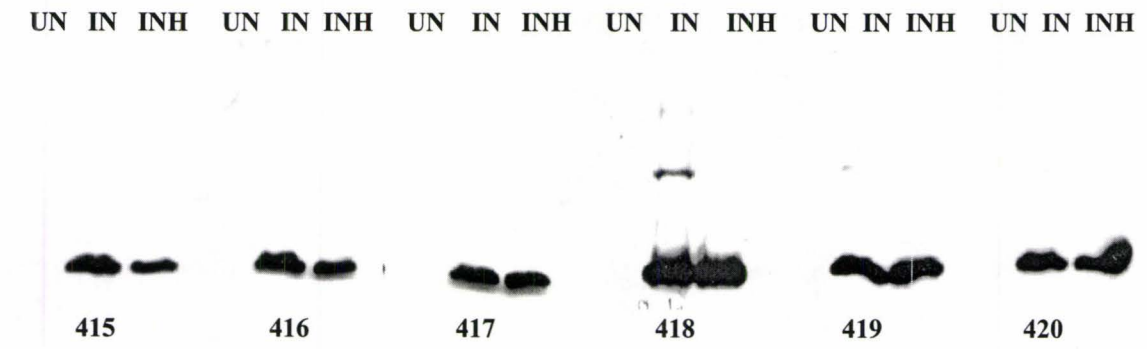
UN IN INH UN IN INH UN IN INH UN IN INH UN IN INH UN IN INH
415
416
417
418
419
420

C.

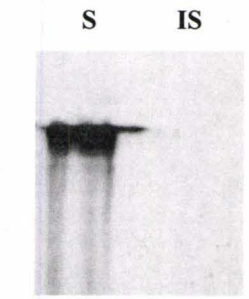
S
IS

D.

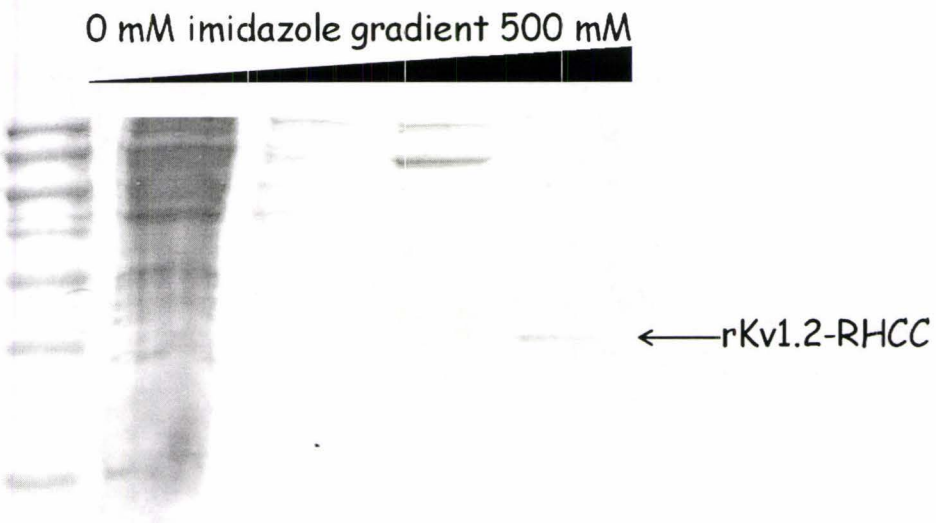

Figure 5.7 (A) Western-blot analysis of chimeric channels between big channels and tetrameric coiled coils. Same amount of *E.coli* cells (quantified by OD_{600}) expressing different constructs were analyzed by 15% SDS-PAGE. Minimal channels were then identified by immunoblotting using an anti-His-tag antibody. UN: un-induced; IN: induced; INH: induced with heating. (B) Western-blot analysis of different chimeric channels between rKv1.2 and RHCC. The numbers below the picture are the residue numbers in rKv1.2 where RHCC was spliced into. (C) Solubility test of rKv1.2-RHCC. S: soluble fraction; IS: insoluble fraction. (D) rKv1.2-RHCC was purified by Ni^{2+} column and analyzed by 15% SDS-PAGE. Amount of imidazole for the elution of His-tagged channel protein is indicated on the gel. The position of purified rKv1.2-RHCC is pointed by the arrow.

We put this construct into large-scale expression. We can purify 0.4 mg of this protein by Ni^{2+}-chelate chromatography from 1 L *E.coli* cell culture (Figure 5.7 D). The biophysical properties of rKv1.2-RHCC were characterized by using CD-spectroscopy and gel-filtration chromatography (Figure 5.8). The secondary structure of this protein is mainly alpha-helical and the majority of the protein is in tetrameric form, proving that most likely the protein is folded correctly. Currently we are searching for crystallization conditions for this construct.

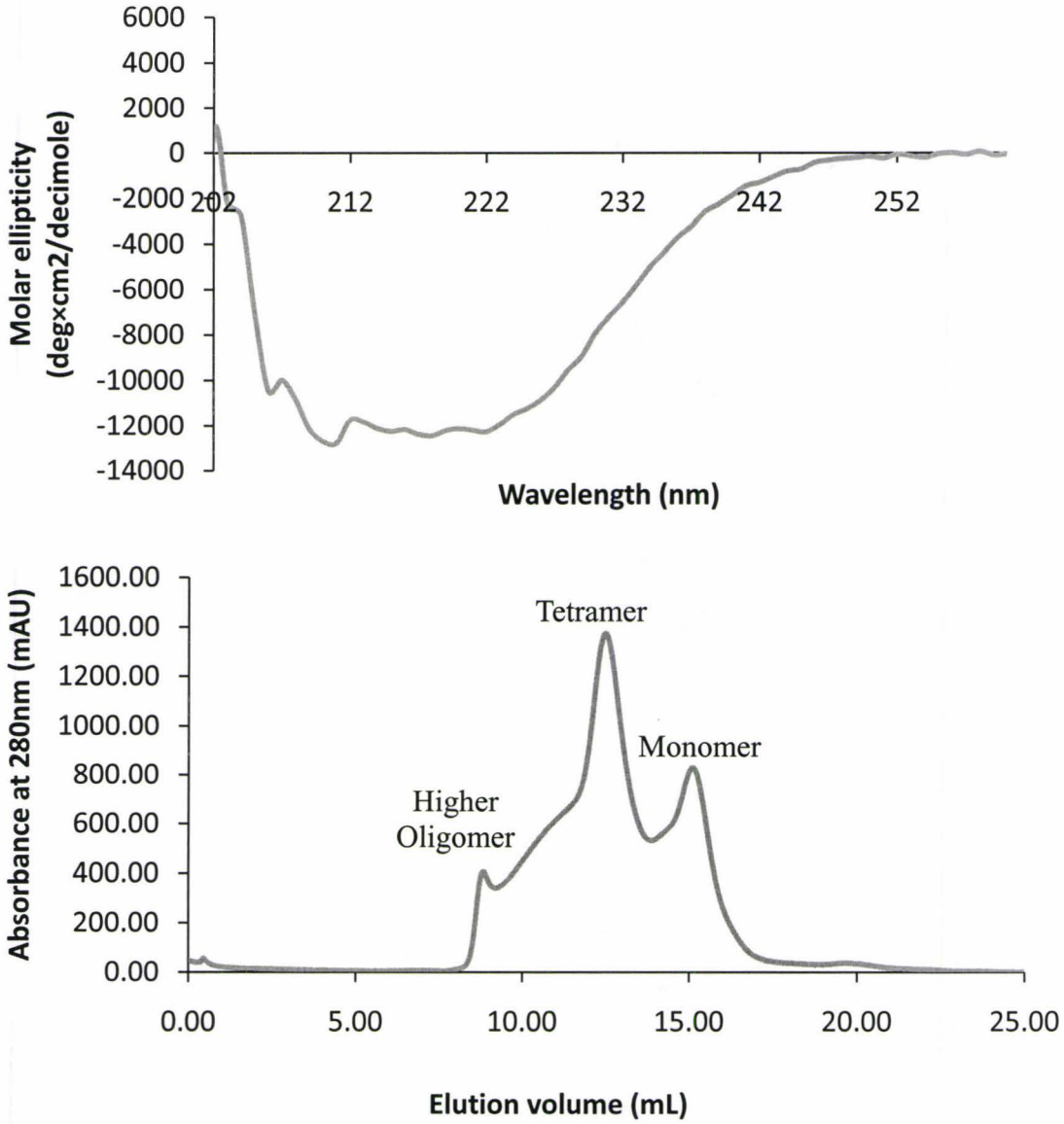

Figure 5.8 Biophysical characterization of rKv1.2-RHCC. (A) CD spectra of tetrameric rKv1.2-RHCC in LDAO. Its estimated α-helical content is 47.2%. (B) Elution profile of rKv1.2-RHCC from gel-filtration chromatography column. The estimated molecular weights of the tetrameric and monomeric LDAO-rKv1.2-RHCC micelles are 221.3 kDa and 54.1 kDa, respectively.

Minimal channels generated by connecting PF of big channels with their native C-terminal domains

One of the major problems in building chimeric channels is to select a proper splicing point. Without the guidance of structural information it is almost impossible to computationally derive a proper splicing point and therefore a large number of splicing variants have to be screened. From the screening of a large number of splicing constructs in this study we indeed obtained a number of properly folded hybrids. However, many more hybrids have to be screened to identify the optimal constructs for structural studies because the current hybrids do form higher oligomers and have non-ideal solubility properties. Before continuing on to generate more hybrids, we attempted to bring back their native C-terminal domains and analysed their effect on the function and assembly of their respective minimal channels.

We added back the wide type C-terminal domains to PF domains of a couple of big channels and used the best N-terminal truncation positions we identified from previous studies of KcsA (see supplementary data for detailed sequences) (Figure 5.3 D). When these constructs were induced, all of them can be induced with considerable amount and especially for mini-rKv1.2C construct, all tetramer, dimer and monomer bands could be observed on SDS-PAGE (Figure 5.9 A & B). When the membrane fraction was separated from soluble fraction by ultra-centrifugation, the tetramer and dimer bands only presented in membrane fraction, but the monomeric protein presented in both soluble and membrane fractions, which indicated that the properly assembled channels only stay in cell membrane but the individual monomeric channel protein will traffick between the membrane and soluble phases. When the sample in membrane fraction was heated up, the

oligomeric bands disappeared, indicating that they were real oligomeric states of our protein (Figure 5.9 C).

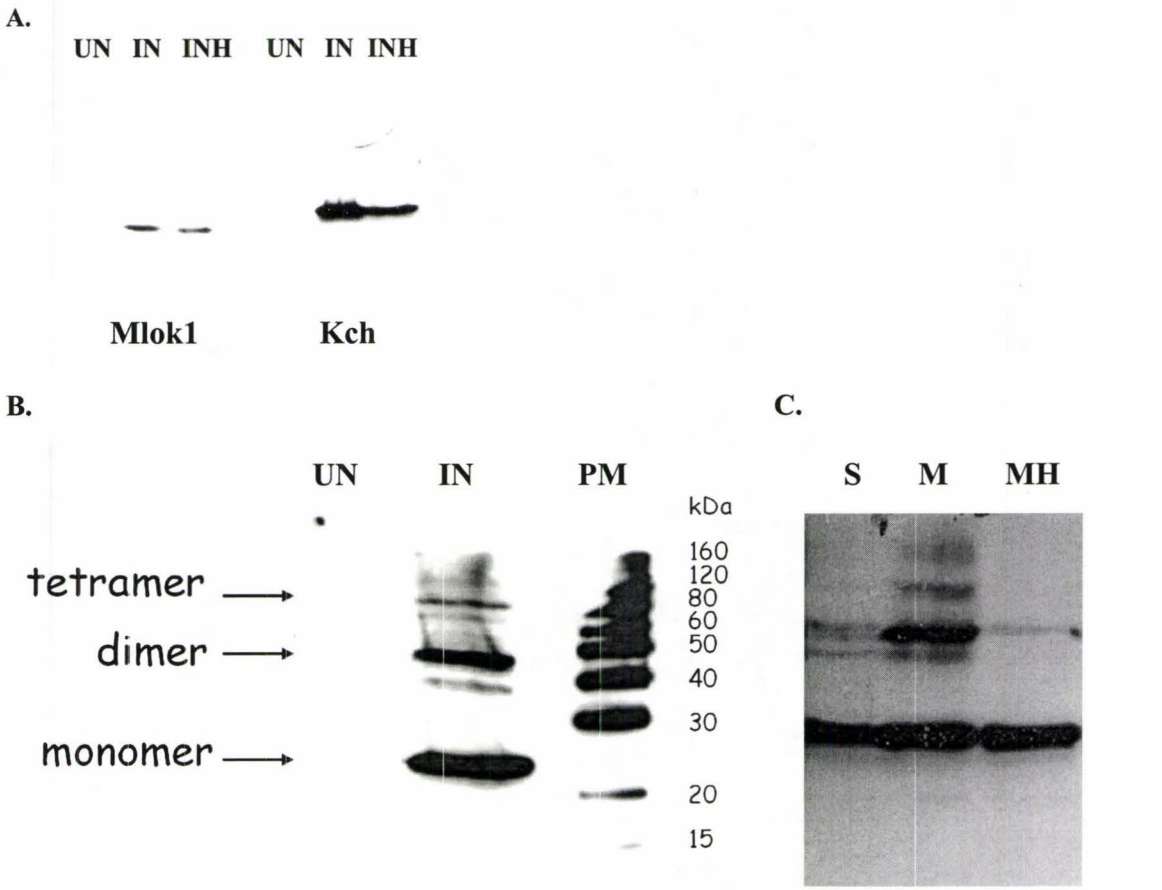

Figure 5.9 Western-blot analysis of minimal channels composed of PF domains of Mlok1, Kch, (A) rKv1.2 (B) and their own C-terminal domains, respectively. *E.coli* cells expressing mini-rKv1.2C was analyzed by 15% SDS-PAGE and then identified by immunoblotting using an anti-His-tag antibody. UN: un-induced; IN: induced; PM: protein marker. (C) Examination of mini-rKv1.2C in different cell fractions and heat treatment of the samples from membrane fraction. S: soluble fraction; M: membrane fraction; MH: membrane fraction with heating.

Plate assays to test the functions of engineered channels

In order to test the functions of many different constructs without tedious electrophysiological experiments, we chose to use the plate assays. In the absence of K^+ in the medium, the electrochemical gradient for K^+ will drive K^+ to leak from the cell if sufficient amount of potassium channels are expressed and open in the cell membrane.

Because the K^+ is one of the major intracellular cations, drastic change in its concentration will affect normal cellular function and stop the growth of the cell. In the example of mini-rKv1.2C, we used empty pET28 vector as negative control, KcsA and KcsA-GCN4 as positive control. Before induction, all cells grew very well (Figure 5.10 A1). But in the presence of 0.1 mM IPTG, only negative control could survive on LB plate. All cells expressing channels did not survive (Figure 5.10 A2). This toxicity can be rescued by adding of extra K^+ in the medium but not by the same amount of Na^+, proving this effect is K^+ channel specific (Figure 5.10 A3 & 4). In this assay, minimal Kv showed similar effect as KcsA channel, indicating it preserved the major property as a normal potassium channel. When we changed the concentration of K^+ in medium gradually, we found the mini-rKv1.2C required less potassium for the rescue compared to KcsA or KcsA-GCN4 (Figure 5.10 B). There are two possibilities for this observation: first, the opening probability of mini-rKv1.2C is lower than that of KcsA; second, the expression level of mini-rKv1.2C is lower than that of KcsA so that it leaks less K^+. The selectivity of the minimal channel was tested by two other ions: rubidium and lithium. Theoretically, the selectivity of a normal potassium channel is: $K^+ \approx Rb^+ >> Na^+ \approx Li^+$. In our plate assay, Rb^+ showed a similar effect as K^+ and Li^+ showed a similar effect as Na^+, indicating the selectivity of our minimal channel is very similar to a normal K^+ channel (Figure 5.10 C). If the toxicity is caused by the leakage of K^+ from expressed K^+ channels, it should be able to be prevented by channel blockers. We tested two K^+ channel blockers, tetraethylammonium (TEA) and Ba^{2+}. Both of them successfully rescued the cells expressing K^+ channels (Figure 5.10 D). Because the binding of TEA depends on the structure of selectivity filter, it demonstrates again the structure of our minimal Kv

channel did not change very much compared to the wild type Kv channel. A number of other channels gave similar results as mini-rKv1.2C in plate assay (data not shown).

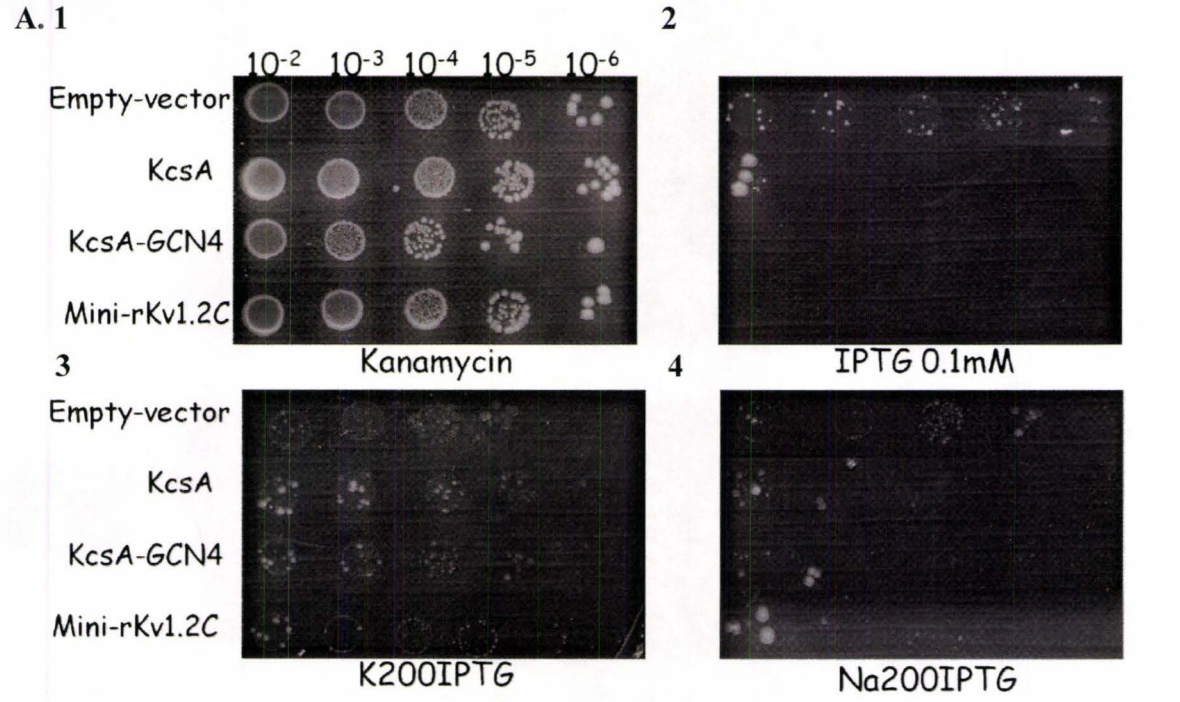

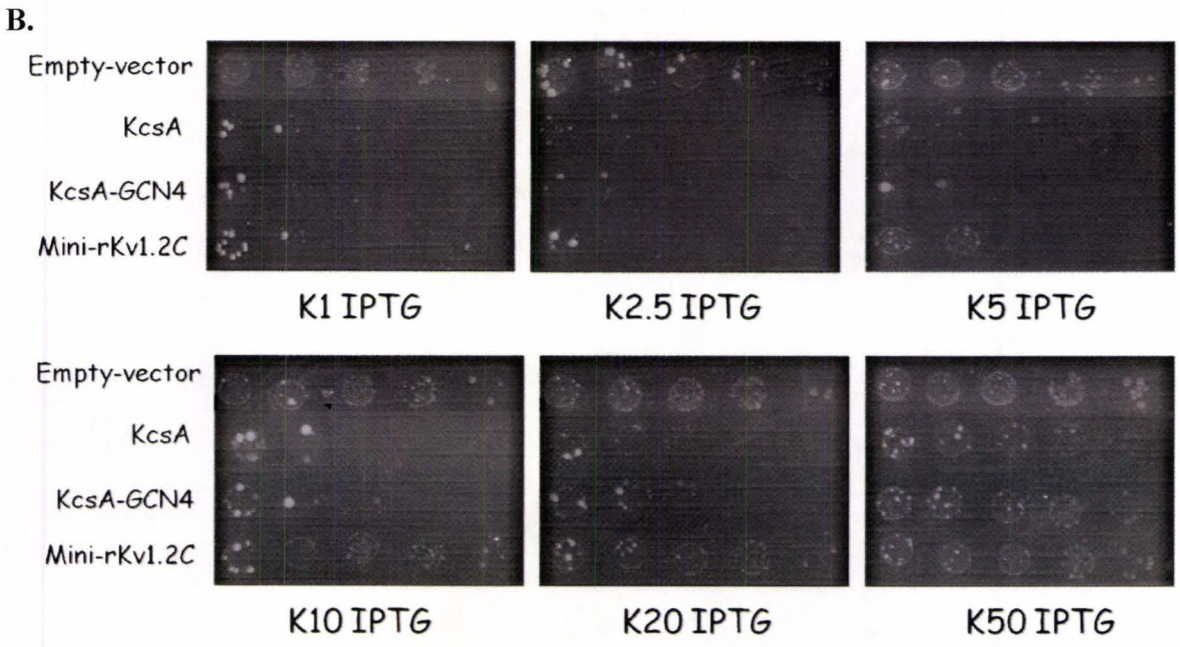

C.

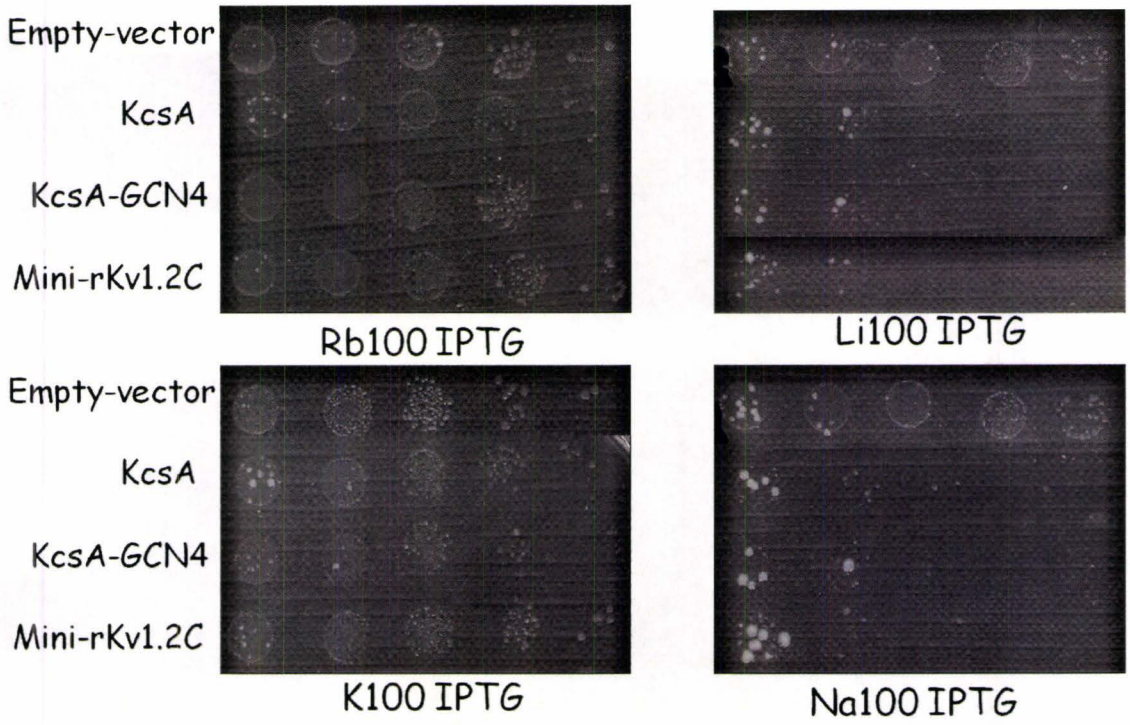

D.

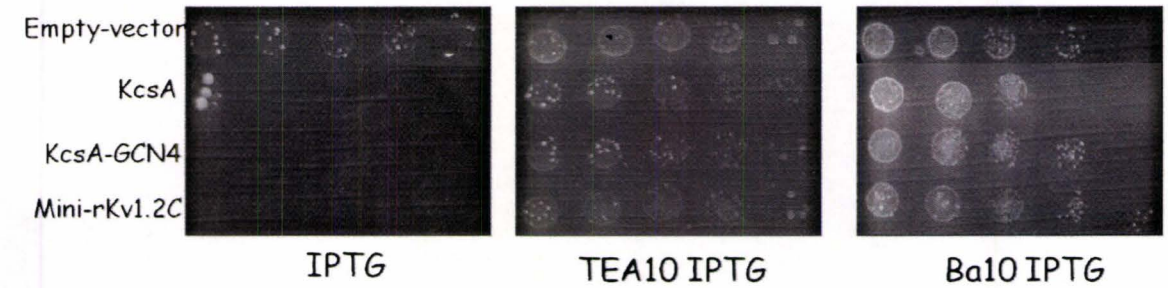

Figure 5.10 Plate assays for testing functions of different potassium channels. The BL21 cells transformed with labeled plasmids (on the left of pictures) were grown to stationary phase and then gradually diluted from 10^2 to 10^6 fold. 5 μL cells from each dilution were inoculated onto LB plate containing ions or drugs as labeled below the pictures. (A) Comparison of cells grown on plates without (upper left) and with (upper right) 1 mM IPTG, with 1mM IPTG and 200 mM K^+ (below left), or with 1mM IPTG and 200 mM Na^+ (below right). (B) Comparison of cells grown on plates with 1 mM IPTG and different concentration of K^+ (from 1 mM to 50 mM). (C) Testing the selectivity of minimal channel by comparing cells grown on plates with 1 mM IPTG and 100 mM Rb^+ or Li^+ or K^+ or Na^+, respectively. (D) Test the effect of potassium channel blockers (10 mM TEA or Ba^{2+}). 1 mM IPTG was present in every plate.

5.4 DISCUSSION

The modular property of potassium channels was proposed by many groups and has been demonstrated by crystal structures, chimeric channel experiments and discovery of channel modules in other distantly related protein families (2-9). However, the trials to express individual modules such as PF and VS are still scarce. There are a few successful examples of PF domain expression, including calcium channel RyR1(35), prokaryotic Kv channel (36) and skeleton muscle sodium channel (37,38). But the systematic expression of a variety of ion channels modules using universal platforms has not been reported yet. In our current study, we identified RHCC as a universal fusion partner to assist the expression and stability of PF domains of ion channels from different families. The minimal chimeric channels we built kept the similar biophysical properties and normal functions as wild type potassium channels. Their high expression level and homogeneity made crystallization trials on these valuable structural entities promising.

There are several advantages to build the minimal ion channels. First, it has advantage in protein expression. Considering the size of minimal Kv channel, PF domain, is only one fifth of the original size, the number of possible folding intermediates and chance of misfolding should be much reduced. Second, it has the advantage in structure determination. One of the major obstacles in protein crystallization is the inter-domain flexibility. By building the minimal channels, we can diminish the intrinsic flexibility in multi-module ion channel proteins and produce well-behaved rigid single modules. At the same time, we can also avoid some glycosylation sites on the channel and increase the homogeneity of the sample. Third, by replacing the big voltage-sensing domain with alternative small sensors, it can facilitate the drug-screening process.

From our previous study on KcsA, we found that without the assistance from cytoplasmic tetramerization domain, the transmembrane domain itself does not have enough force to hold the pore together during *in vivo* channel assembly (19,20). The result of our minimal channel generated by direct truncations agreed with what we observed in KcsA studies, without assistance from cytoplasmic domain, the PF cannot be expressed.

In KcsA study, we also saw a correlation between tetramer stability and protein expression level (20). The continuous coiled coil design of chimeric channel KcsA-RHCC gave extreme thermostability and high expression level. After inspecting of ion channel with known crystal structures, we found that the inner helices of the PF domains from all different ion channels form a right-handed coiled coil structure, which hints that the stable continuous coiled coil structures can always be achieved by adding suitable tetrameric right-handed coiled coil peptides to different PF domains. Because different PF domains have different diameters near membrane surface region, identification of a suitable coiled coil structure become critical. There are three ways to choose the coiled coil and optimal splicing position: computational modeling, screening and selection. In previous study, we used modeling to guide our design for KcsA-RHCC construct. In this study, because the crystal structures for many of our target channels are unavailable, we screened many constructs with different splicing motifs with RHCC, some of which gave us high expression level and homogeneity. In order to increase the efficiency of this system as an expression platform, in the future, we can introduce random mutations near the junction region and use selection to identify the best chimeric constructs. *E.coli* mutant strain LB2003 has opposite effect as our BL21 strain and requires the expression

of functional channels for normal growth of cells, whose function may be useful for the selection of properly spliced chimeric channels.

The *E.coli*-based protein-engineering system developed here is intended for both structural study and functional characterization of variety of ion channels. These studies can assist in solving crystal structures of physiologically important ion channels and indirectly assist structure-based rational drug design, or directly facilitate the screening for novel potent and selective modulators of ion channel function which can combat some of the neuronal, cardiac, and immune channel-mediated diseases.

5.5 MATERIALS AND METHODS

Molecular cloning

The genes encoding pore-forming domains of all selected channels were synthesized with optimal codon usage for *E. coli* (39) (gene synthesized by BioBasic Company, Tonroto, Canada) and PCR amplified. The amplified fragments were joined to selected peptides, C-terminal domain of KcsA, Kv or other tetrameric coiled coil, by fusion PCR (40), digested with the corresponding restriction enzymes and cloned into pET28M, a modified pET28a expression vector (19). The sequences of these constructs were confirmed by dideoxynucleotide sequencing.

Protein Expression and Purification

E.coli BL21(DE3) cells were transformed with pET28M/chimeric channels. Single colony was inoculated and grown in 100 mL LB (Luria Bertani) broth with 100 μg/mL kanamycin (as the final concentration) at 37°C overnight. The culture was then diluted into 1 L LB broth with 100 μg/mL kanamycin and further grown for 100 minutes. Protein

expression was induced by the addition of IPTG to a final concentration of 1 mM. Cells were pelleted after 3 hrs of incubation at 37°C, resuspended in lysis buffer (20 mM Tris, pH 8, 150 mM KCl, and 1 mM PMSF) and subsequently lysed by French Press at 10,000 psi. The cell lysate was centrifuged at 100,000 × g for 1 hr and the pellet was solubilized in 20 mL of 20 mM Tris, pH 8, 150 mM KCl, 1 mM PMSF and 1% v/v LDAO overnight at 4°C. The resuspended mixture was centrifuged at 100,000 × g for 1 hr and the supernatant was loaded onto a HisTrap™ HP column (GE Healthcare). Protein was purified using a FPLC system (Pharmacia) with a linear gradient of 0 - 500 mM imidazole. Purified proteins were analyzed by 15% SDS-PAGE with Coomassie blue staining and Western-blot by using an anti-His-tag antibody (Cell Signaling).

Gel-filtration Chromatography

Gel-filtration chromatography was run on a FPLC system (Amersham Biosciences Corp.) using a Superdex 200 column (Amersham Biosciences Corp.) equilibrated in 50 mM Tris buffer (pH 8), 150 mM KCl and 0.1% v/v LDAO.

Circular Dichroism measurement

Protein samples at a 10 μM monomeric protein concentration were dissolved in 20 mM K_2HPO_4 (pH 8), 150 mm KCl and 0.1% v/v LDAO. The protein concentration was determined by the bicinchoninic acid (BCA) assay (Sigma). CD spectra of the samples were recorded in a 0.1 cm path length cell at 25°C using a 410 CD spectrometer (AVIV Biomedical Inc., Lakewood, NJ, USA). The secondary structure content of each sample

was quantified using the CD spectrum analysis program cdsstr of the cdpro suite (http://lamar.colostate.edu/~sreeram/CDPro /main.html).

Plate assays

BL21 (DE3) cells transformed with different plasmids were grown to stationary phase and then were gradually diluted from 10^2 to 10^6 fold. 5 μL cells from each dilution were inoculated onto LB plates with or without 0.1mM isopropyl-b-thio-galactoside (IPTG). Components were included or omitted as required. The plates were incubated overnight at 37°C before photographs were taken.

5.6 REFREENCE

1. Hille, B. (2001) *Ion Channels of Excitable Membrane*, Sinauer Associates, Inc, Sunderland, MA
2. Jiang, Y., Lee, A., Chen, J., Ruta, V., Cadene, M., Chait, B. T., and MacKinnon, R. (2003) *Nature* **423**, 33-41
3. Long, S. B., Campbell, E. B., and Mackinnon, R. (2005) *Science* **309**, 897-903
4. Lu, Z., Klem, A. M., and Ramu, Y. (2001) *Nature* **413**, 809-813
5. Ohndorf, U. M., and MacKinnon, R. (2005) *J Mol Biol* **350**, 857-865
6. Iwasaki, H., Murata, Y., Kim, Y., Hossain, M. I., Worby, C. A., Dixon, J. E., McCormack, T., Sasaki, T., and Okamura, Y. (2008) *Proc Natl Acad Sci U S A* **105**, 7970-7975
7. Kohout, S. C., Ulbrich, M. H., Bell, S. C., and Isacoff, E. Y. (2008) *Nat Struct Mol Biol* **15**, 106-108
8. Murata, Y., and Okamura, Y. (2007) *J Physiol* **583**, 875-889
9. Murata, Y., Iwasaki, H., Sasaki, M., Inaba, K., and Okamura, Y. (2005) *Nature* **435**, 1239-1243
10. Cooper, E. C., and Jan, L. Y. (1999) *Proc Natl Acad Sci U S A* **96**, 4759-4766
11. Sobey, C. G. (2001) *Arterioscler Thromb Vasc Biol* **21**, 28-38
12. Shieh, C. C., Coghlan, M., Sullivan, J. P., and Gopalakrishnan, M. (2000) *Pharmacol Rev* **52**, 557-594
13. Fernandez, D., Ghanta, A., Kauffman, G. W., and Sanguinetti, M. C. (2004) *J Biol Chem* **279**, 10120-10127

14. Myokai, T., Ryu, S., Shimizu, H., and Oiki, S. (2008) *Mol Pharmacol* **73**, 1643-1651

15. Colatsky, T. J. (1996) *Circ Res* **78**, 1115-1116

16. Bankston, J. R., and Kass, R. S. (2008) *Nature* **456**, 183-185

17. Birch, P. J., Dekker, L. V., James, I. F., Southan, A., and Cronk, D. (2004) *Drug Discov Today* **9**, 410-418

18. Ruta, V., and MacKinnon, R. (2004) *Biochemistry* **43**, 10071-10079

19. Pau, V. P., Zhu, Y., Yuchi, Z., Hoang, Q. Q., and Yang, D. S. (2007) *J Biol Chem* **282**, 29163-29169

20. Yuchi, Z., Pau, V. P., and Yang, D. S. (2008) *FEBS J* **275**, 6228-6236

21. Jenke, M., Sanchez, A., Monje, F., Stuhmer, W., Weseloh, R. M., and Pardo, L. A. (2003) *EMBO J* **22**, 395-403

22. Li, M., Jan, Y. N., and Jan, L. Y. (1992) *Science* **257**, 1225-1230

23. Shen, N. V., Chen, X., Boyer, M. M., and Pfaffinger, P. J. (1993) *Neuron* **11**, 67-76

24. Kreusch, A., Pfaffinger, P. J., Stevens, C. F., and Choe, S. (1998) *Nature* **392**, 945-948

25. Tinker, A., Jan, Y. N., and Jan, L. Y. (1996) *Cell* **87**, 857-868

26. Jiang, Y., Pico, A., Cadene, M., Chait, B. T., and MacKinnon, R. (2001) *Neuron* **29**, 593-601

27. Quirk, J. C., and Reinhart, P. H. (2001) *Neuron* **32**, 13-23

28. Schmalhofer, W. A., Sanchez, M., Dai, G., Dewan, A., Secades, L., Hanner, M., Knaus, H. G., McManus, O. B., Kohler, M., Kaczorowski, G. J., and Garcia, M. L. (2005) *Biochemistry* **44**, 10135-10144

29. Zhou, L., Olivier, N. B., Yao, H., Young, E. C., and Siegelbaum, S. A. (2004) *Neuron* **44**, 823-834

30. Doyle, D. A., Morais Cabral, J., Pfuetzner, R. A., Kuo, A., Gulbis, J. M., Cohen, S. L., Chait, B. T., and MacKinnon, R. (1998) *Science* **280**, 69-77

31. Shi, N., Ye, S., Alam, A., Chen, L., and Jiang, Y. (2006) *Nature* **440**, 570-574

32. Kuo, A., Gulbis, J. M., Antcliff, J. F., Rahman, T., Lowe, E. D., Zimmer, J., Cuthbertson, J., Ashcroft, F. M., Ezaki, T., and Doyle, D. A. (2003) *Science* **300**, 1922-1926

33. Jiang, Y., Lee, A., Chen, J., Cadene, M., Chait, B. T., and MacKinnon, R. (2002) *Nature* **417**, 515-522

34. Takeuchi, K., Takahashi, H., Kawano, S., and Shimada, I. (2007) *J Biol Chem*

35. Kang, G. B., Song, H. E., Song, D. W., Kim, M. K., Rho, S. H., Kim do, H., and Eom, S. H. (2007) *Protein Pept Lett* **14**, 742-746

36. Santos, J. S., Grigoriev, S. M., and Montal, M. (2008) *J Gen Physiol* **132**, 651-666

37. Chen, Z., Alcayaga, C., Suarez-Isla, B. A., O'Rourke, B., Tomaselli, G., and Marban, E. (2002) *J Biol Chem* **277**, 24653-24658

38. Pincin, C., Ferrera, L., and Moran, O. (2005) *Biochem Biophys Res Commun* **334**, 140-144

39. Dong, H., Nilsson, L., and Kurland, C. G. (1996) *Journal of molecular biology* **260**, 649-663

40. Shevchuk, N. A., Bryksin, A. V., Nusinovich, Y. A., Cabello, F. C., Sutherland, M., and Ladisch, S. (2004) *Nucleic Acids Res* **32**, e19

5.7 SUPPLEMENTARY DATA

Protein Sequences used in this study:

Only the fragments involved in this studied are displayed. The starting and ending residue numbers are labeled in sequence.

KcsA:

1mppmlsgllarlvklllgrhgsalhwraagaatvllvivllagsylavlaergapgaqlitypralwwsvetattvgygdlyp
vtlwgrlvavvvmvagitsfglvtaalatwfvgreqerrghfvrhsekaaeeaytrttralherfdrlermlddnrr160

Kch:

1mshwatfkqtatnlwvtlrhdilalavflngllifktiygmsvnlldifhikafseldlsllanaplfmlgvflvlnsigllfrakl
awaisiilllialiytlhfypwlkfsigfciftlvfllilrkdfshssaaagtifafisfttllfystygalylsegfnprieslmtafyfsie
tmstvgygdivpvsesarlftisviisgitvfatsmtsifgplirggfnklvkgnnhtmhrkdhfivcghsilaintilqlnqrgq
nvtvisnlpeddikqleqrlgdnadvipgdsndssvlkkagidrcrailalsdndadnafvvlsakdmssdvktvlavsdsk
nlnkikmvhpdiilspqlfgseilarvlngeeinndmlvsmllnsghgifsdndeletkadskesaqk417

KvSA:

206srrtevwvrgrlgiyvaattvllvlvaslavldaergapdpsitnysdavwwaavtittvgygdfypvttegrlvavglmi
ggigligfvtgslatwivdrvtgr310

KvMU:

102galqkavgnavrgrimlytisgvslliyvtslailnqerghpgatitsfgkavwwaittvttvgygdlypitvtgrviavll
miggisligvvtaslaswivqrvae208

KvBA:

85nrtggmavrgritlytccsvtllmyigalaeldvergvpgasitdfgeaiwwsfvtvttvgygdlspvtwqgrciaiglmit
gvaligivtatlaswivdrvrd188

Rat Kv1.2:

321lkasmrelglliffl figvilfssavyfaeaderdsqfpsipdafwwavvsmttvgygdmvpttiggkivgslcaiagvlt

ialpvpvivsnfnyfyhret421

Human Kv1.5:

435glliffl figvilfssavyfaeadnqgthfssipdafwwavvtmttvgygdmrpitvggkivgslcaiagvltialpvpvi

vs517

MthK:

1mvlvieiirkhlprvlkvpatrilllvlaviiygtagfhfiegeswtvslywtfvtiatvgygdyspstplgmyftvtlivlgigtf

avaverlleflinreqmklmglidvaksrhvvicgwsestleclrelrgsevfvlaedenvrkkvlrsganfvhgdptrvsdle

kanvrgaravivdlesdsetihcilgirkidesvriiaeaeryenieqlrmagadqvispfvisgrlmsrsiddgyeamfvqdv

laeestrrmvevpipegsklegvsvldadihdvtgviiigvgrgdeliidpprdysfragdiilgigkpeeierlknyisa336

Human BK1:

267ilktsnsiklvnllsifistwltaagfihlvensgdpwenfqnnqaltywecvyllmvtmstvgygdvyakttlgrlfmv

ffilgglamfasyvpeiieli gnrkkyggsysavsgrkhivvcghitlesvsnflkdflhkdrddvnveivflhnispnlelealf

krhftqvefyqgsvlnphdlarvkiesadaclilankycadpdaedasnimrvisiknyhpkiriitqmlqyhnkahllnips

wnkegddaiclaelklgfiaqsclaqglstmlanlfsmrsfikieedtwqkyylegvsnemyteylssafvglsfptvcelcfv

klkllmiaieyksanresrilinpgnhlkiqegtlgffiasdakevkraffyckachdditdpkrikkcgckrledeqpstlspk

k686

Human Kir2.1:

82rwmlvifclafvlswlffgcvfwliallhgdldaskegkacvsevnsftaaflfsietqttigygfrcvtdecpiavfmvvfq

sivgciidafiigavmakm183

Mlok1:

1msvlpflriyaplnavlaapgllavaaltipdmsgrsrlalaallaviwgayllqlaatllkrragvvrdrtpkiaidvlavlvpl
aaflldgspdwslycavwllkplrdstffpvlgrvlanearnligvttlfgvvlfavalaayvierdiqpekfgsipqamwwav
vtlsttgygdtipqsfagrvlagavmmsgigifglwagilatgfyqevrrgdfvrnwqlvaavplfqklgpavlveivralrar
tvpagavicrigepgdrmffvvegsvsvatpnpvelgpgaffgemalisgeprsatvsaattvsllslhsadfqmlcssspeia
eifrktalerrgaaasa355

NaChBac:

145gnililmsiffyifavigtmlfqhvspeyfgnlqlslltlfqvvtleswasgvmrpifaevpwswlyfvsfvligtfiifnlfi
gvivnnveake239

RH4:

1aalaqikkeiayllakikaeilaalkkikqeia33

GCN4:

1rmkqiedkleeilsklyhienelarikkllger34

RHCC:

1gsiinetaddivyrltviiddryeslknlitlradrlemiindnvstilasi52

Composition of chimeric channel constructs:

Numbers labeled below are residue numbers in indicated proteins. Protein sequences refer to upper contents. They are all cloned into pET28 vector using BamHI and EcoRI sites to generate N-terminal 6-histidine tag except special notation. TEV cleavage recognition sequence used as linker is ENLYFQGGT.

Direct-truncation constructs:

rKv1.2: 323-419

hKv1.5: 435-517

hKir2.1: 82-183

NaChBac: 145-239

Chimeras with the cytoplasmic domain of KcsA:

rKv1.2-KcsA:

Construct 1: rKv1.2 (323-411) – KcsA (113-160)

Construct 2: rKv1.2 (323-412) – KcsA (114-160)

Construct 3: rKv1.2 (323-413) – KcsA (115-160)

Construct 4: rKv1.2 (323-414) – KcsA (116-160)

Construct 5: rKv1.2 (323-415) – KcsA (117-160)

Construct 6: rKv1.2 (323-416) – KcsA (118-160)

Construct 7: rKv1.2 (323-417) – KcsA (119-160)

Construct 8: KcsA (1-29) - rKv1.2 (329-411) – KcsA (113-160)

Construct 9: KcsA (1-37) - rKv1.2 (337-411) – KcsA (113-160)

Construct 10: KcsA (1-37) - rKv1.2 (337-404) – KcsA (106-160) C-terminal His-tag

Construct 11: KcsA (1-37) - rKv1.2 (337-404) – KcsA (106-160)

Construct 12: KcsA (1-29) - rKv1.2 (329-404) – KcsA (106-160)

hKv1.5-KcsA: KcsA (1-29) - hKv1.5 (435-517) – KcsA (113-160)

hKir2.1-KcsA: KcsA (1-13) – hKir2.1 (82-183) – KcsA (117-160)

NaChBac-KcsA: KcsA (1-27) - NaChBac (147-235) – KcsA (116-160)

KvBA-KcsA: KvBA (91-176) – KcsA (109-160)

KvSA-KcsA: KvSA (207-298) – KcsA (109-160)

Chimeras with coiled coils:

Mlok1-RHCC: Mlok1 (124-215) – RHCC (16-52)

KvBA-RHCC: KvBA (91-181) – RHCC (16-52)

KvSA-RHCC: KvSA (207-302) – RHCC (16-52)

KvMU-RHCC: KvMU (105-201) – RHCC (16-52)

MthK-RHCC: MthK (1-94) – RHCC (16-52)

NaChBac-GCN4: NaChBac (145-239) – TEV - GCN4 (1-34)

rKv1.2-GCN4: rKv1.2 (323-419) – TEV - GCN4 (1-34)

rKV1.2-RHCC:

415: rKv1.2 (322-415) – RHCC (16-52)

416: rKv1.2 (322-416) – RHCC (16-52)

417: rKv1.2 (322-417) – RHCC (16-52)

418: rKv1.2 (322-418) – RHCC (16-52)

419: rKv1.2 (322-419) – RHCC (16-52)

420: rKv1.2 (322-420) – RHCC (16-52)

Chimeras with native C-terminal domains:

Mlok1C: 124-355

KchC: 128-417

rKv1.2C: 318-499

Chapter 6

Perspectives

What is it next? The development of a universal ion channel expression platform using the tetrameric coiled coil RHCC in this work potentially creates an invaluable tool for structural and functional studies on a variety of ion channels. This platform has been tested on several ion channels from different families. Hybrid channels show increased expression levels, higher stability and normal functions. Nevertheless there are still a few issues that need to be addressed in the future in order to optimize this system.

RHCC is a good tetramerization helper. However, it is not compatible with all of the tested channels at the connection between the tetramerization and pore-forming domains. Different pore-forming domains have different diameters at the junction layer and therefore each requires a coiled coil with similar diameter for the formation of a stable continuous coiled coil structure. A set of coiled coils with various diameters is required for the generation of a universal expression platform. On the other hand, since most eukaryotic Na^+ and Ca^{2+} channels are in heterotetrameric arrangement, a symmetric coiled coil like RHCC may mislead the assembly of functional channel. Instead, asymmetric tetrameric coiled coils like SNARE (Soluble NSF Attachment Protein Receptors) complex may be a better candidate because besides being a tetramerization domain it also confers a preset order in channel assembly.

The most difficult part in the application of this platform is the identification of proper spliced positions for the generation of functional chimeras. The scarcity of structural information on ion channels limits the application of computer modeling in the design of chimeric channels with non-native tetramerization domain. In this study we

circumvented this problem by generating a large numbers of constructs and identifying good candidates by screening their expression using Western-blot. However, this is not efficient enough if we were to work on a large number of ion channels. Selection-based strategies may be a better choice for the implementation of this platform. We can generate a library of hybrid channels by varying the spliced positions as well as protein sequences in the splice junction region by fusion PCR and error-prone PCR, respectively. Functional constructs amongst the library can be selected using *E.coli* strains, such as LB2003, that are devoid of ions transport mechanisms. LB2003 cannot grow in a medium with low concentration of K^+ ions unless functional K^+ channels are being introduced and expressed in the cell.

Overexpression of the functional pore-forming modules of ion channels will open the door for understanding the selectivity for different ions and facilitate practical drug-screening application. The maturation of this system will have a tremendous future and the future is ahead of us.